

University of Mississippi

eGrove

Electronic Theses and Dissertations

Graduate School

1-1-2020

Behavioral Chronopharmacology Of Cannabinoids In Young And Aged Mice

Erik Lewis Hodges

Follow this and additional works at: <https://egrove.olemiss.edu/etd>

Recommended Citation

Hodges, Erik Lewis, "Behavioral Chronopharmacology Of Cannabinoids In Young And Aged Mice" (2020). *Electronic Theses and Dissertations*. 1810.
<https://egrove.olemiss.edu/etd/1810>

This Dissertation is brought to you for free and open access by the Graduate School at eGrove. It has been accepted for inclusion in Electronic Theses and Dissertations by an authorized administrator of eGrove. For more information, please contact egrove@olemiss.edu.

BEHAVIORAL CHRONOPHARMACOLOGY OF CANNABINOIDS
IN YOUNG AND AGED MICE

A Dissertation

presented in fulfillment of requirements

for the degree of Doctorate of Philosophy

in the Department of BioMolecular Sciences

Division of Pharmacology

The University of Mississippi

by

ERIK LEWIS HODGES

May 2020

Copyright © Erik L. Hodges 2020

ALL RIGHTS RESERVED

ABSTRACT

The overarching goal of this research is to explore the biological mechanisms of aging and formulate novel therapeutic approaches to mitigate age-related impairments. The presence and pervasiveness of ~24 hour (circadian) rhythms in molecular and behavioral dynamics suggests that the mechanisms regulating these rhythms are integral to biological aging and possibly amenable to therapeutic interventions. Based on evidence presented in this dissertation, we conclude that the endocannabinoid system is a mediator of both central and peripheral circadian physiology. Additionally, the hormetic pharmacological properties of the synthetic cannabinoid CP55940 suggest that bidirectional modulation of circadian rhythms via cannabinoids is possible.

Chapter 1 summarizes seminal work and recent advances in the fields of biological aging, circadian rhythms, cannabinoid pharmacology, and the concept of hormesis. The culmination of this chapter poses the central question: are exogenous cannabinoids capable of bidirectionally restoring age-related changes in circadian rhythms? Chapter 2 describes behavioral pharmacology studies wherein young and aged mice were administered varying doses of CP55940 to determine how exogenous cannabinoids affect locomotion, body temperature, and nociception. Data acquired from these high-powered experiments demonstrate that CP55940 is significantly more potent and efficacious in old mice, and that extremely low doses of this exogenous cannabinoid elicit paradoxical locomotor stimulation in young mice.

In Chapter 3 we quantified the age- and sex-specific characteristics of voluntary wheel running (VWR) in mice housed under constant darkness - a model for age-related circadian rhythm disruption. We then assessed the ability of CP55940 to alter the timing of activity onset, offset, and total locomotion. Our results indicate that higher doses of CP55940 given immediately after waking acutely suppress wheel running behavior but lead to a rebound in activity later in the day. The final chapter summarizes these results and discusses future studies which can expound upon this novel research. Collectively, this work establishes experimental and analytical methods useful for investigating cannabinoid pharmacology and evaluating circadian rhythm-restoring therapeutics in aged rodents. Given the recent surge in cannabinoid use and the lack of preclinical evidence of these compounds in elderly subjects, these results provide a critically needed foundation for future experimental work.

DEDICATION

I dedicate this work to my parents Eliot and Jamelle, for their unwavering love and support, and for inspiring me to follow my dreams. To my sister Lauren, for instilling my insatiable curiosity and joy of learning. And to Noa, for her patience, compassion, and daily demonstration of limitless potential through hard work.

LIST OF ABBREVIATIONS AND SYMBOLS

AALAC	Association for Assessment and Accreditation of Laboratory Animal Care International
ADHD	Attention Deficit Hyperactivity Disorder
2-AG	Arachidonoyl Glycerol
AM	Alexandros Makriyannis
AMP	Adenosine Monophosphate
ANOVA	Analysis of Variance
BL	Black
BMAL	Brain and Muscle ARNT-Like 1
CB	Cannabinoid
CB1	Cannabinoid Receptor 1
CB2	Cannabinoid Receptor 2
CBD	Cannabidiol
CBDV	Cannabidivarin
CBG	Cannabigerol
CBV	Cannabivarin
CLOCK	Circadian Locomotor Output Cycles Kaput
CNS	Central Nervous System

CP	Charles Pfizer
CRY	Cryptochrome
CT	Cycle Time
DAGLα	Diacylglycerol Lipase- α
DD	Dark:Dark, Constant Darkness
DMSO	Dimethyl Sulfoxide
DNA	Deoxyribonucleic Acid
EGF	Epidermal growth factor
ERK	Extracellular Signal-regulated Kinase
FAAH	Fatty acid amide hydrolase
FSH	Follicle-stimulating hormone
GABA	Gamma aminobutyric acid
GAPDH	Glyceraldehyde 3-phosphate dehydrogenase
GH	Growth Hormone
GPCR	G-protein Coupled Receptor
GPR	G-protein Receptor
GTP	Guanosine-5'-triphosphate
HPRT	Hypoxanthine-guanine phosphoribosyltransferase
HSP	Heat Shock Protein
IACUC	Institutional Animal Care and Use Committee

IGF	Insulin-like Growth Factor
IP	Intraperitoneal
IR	Infrared
JPEG	Joint Photographic Experts Group
JWH	John W. Huffman
LC	Liquid Chromatography
LD	Light:Dark, Normal Lighting Conditions
LH	Luteinizing Hormone
MGL	Monoacylglycerol Lipase
MS	Mass Spectrometry
NAPE	N-acyl phosphatidylethanolamine phospholipase D
NIDA	National Institute on Drug Abuse
NWOSU	Northwestern Oklahoma State University
OF	Old Female
EtOH	Ethanol
OM	Old Male
PAS	Photobeam Activity System
PCR	Polymerase Chain Reaction
PDF	Portable Document Format
PER	Period

PET	Positron Emission Tomography
PLD	Phospholipase-D
PNG	Portable Network Graphics
REM	Rapid Eye Movement
RNA	Ribonucleic Acid
ROA	Route of Administration
RPM	Rotations Per Minute
RT-PCR	Reverse Transcription - Polymerase Chain Reaction
SCN	Suprachiasmatic Nuclei
SVG	Scalable Vector Graphic
THC	Tetrahydrocannabinol
THCV	Tetrahydrocannabivarin
TIFF	Tagged Image File Format
TRP	Transient Receptor Potential
TRPV	Transient Receptor Potential Vanilloid
VEGFR	Vascular Endothelial Growth Factor
WIN	Winthrop
YF	Young Female
YM	Young Male
ZT	Zeitgeber Time

ACKNOWLEDGEMENTS

I am eternally grateful for my academic advisor, Nicole Ashpole, who gave me a second chance and pushed me to pursue my passion. This work would not have been possible without her guidance, trust, and understanding. I thank my committee members: Kristie Willett, Jason Paris, and Alberto Jose Del Arco Gonzalez for their reassurance, constructive criticism, and patience - this project and my career have greatly benefitted from you all.

TABLE OF CONTENTS

ABSTRACT	II
DEDICATION	IV
LIST OF ABBREVIATIONS AND SYMBOLS	V
ACKNOWLEDGEMENTS	IX
LIST OF FIGURES.....	XIV
LIST OF TABLES.....	XVI
CHAPTER 1: AGING, CIRCADIAN RHYTHMS, AND CANNABINOIDS	1
ABSTRACT.....	1
BIOLOGICAL AGING.....	2
CIRCADIAN RHYTHMS AND AGING	3
THE ENDOCANNABINOID SYSTEM IN ADVANCED AGE.....	7
CANNABINOID BEHAVIORAL PHARMACOLOGY.....	9
HORMESIS AND CANNABINOID CHRONOPHARMACOLOGY	12
CONCLUSIONS.....	16
FIGURES.....	17
CHAPTER 2: AGE-DEPENDENT HORMESIS-LIKE EFFECTS OF THE SYNTHETIC CANNABINOID CP55940 IN C57BL/6 MICE.....	24

ABSTRACT	24
INTRODUCTION	24
RESULTS	26
<i>Acclimation to Vehicle Injection and Baseline</i>	26
<i>Behavioral and Physiological Responses to CP55940</i>	27
<i>Responses to CP55940 and CB1 or CB2 Antagonism</i>	29
<i>Pharmacokinetics of CP55940 and Endocannabinoid Gene Expression in the Brain</i>	31
DISCUSSION:.....	31
METHODS.....	37
<i>Animals</i>	37
<i>Blinding</i>	38
<i>Drugs, Dosing, and Administration</i>	38
<i>Acclimation</i>	39
<i>Body Weight</i>	39
<i>Rectal and Pelage/Surface Temperature</i>	39
<i>Locomotion - Open Field</i>	40
<i>Nociception - Hot Plate</i>	41
<i>Nociception - Hot Water Tail Withdrawal</i>	41
<i>Gene Expression - qPCR</i>	42
<i>Experimental Timeline</i>	42
<i>Data Analysis, Statistics, and Exclusions</i>	43
FIGURES.....	44
CHAPTER 3: CANNABINOIDS AS CHRONOBOTICS IN AGING MICE.....	54
ABSTRACT.....	54
INTRODUCTION:	55

RESULTS:	58
DISCUSSION.....	65
METHODS.....	69
<i>Animals</i>	69
<i>Recording Spontaneous Wheel Running</i>	70
<i>Experimental Timeline</i>	70
<i>Drugs, Dosing, and Administration</i>	71
<i>Body Weight</i>	71
<i>Data Acquisition, Quantification of Rhythms, and Statistical Analysis</i>	72
<i>Data and Code Availability</i>	74
FIGURES.....	75
CHAPTER 4: CONCLUSIONS, LIMITATIONS, AND FUTURE DIRECTIONS	91
GRAPHICAL ABSTRACT:	91
SUMMARY OF FINDINGS:	91
<i>Aging Circadian Rhythms and Cannabinoids</i>	91
<i>Cannabinoid Hormesis</i>	93
<i>Cannabinoids as Chronobiotics</i>	94
LIMITATIONS AND FUTURE DIRECTIONS:	95
<i>Existing Data and Tools</i>	96
<i>Mice as a Model for Circadian Rhythm Disruption</i>	96
<i>Mitigation of Circadian Confounds</i>	97
<i>Vehicle, Drug, and Route of Administration</i>	98
<i>Experimental Design of Hormesis Study</i>	99
BIOLOGICAL AGING AND CIRCADIAN RHYTHMS AS DYNAMICAL SYSTEMS	100
FIGURES.....	103
LIST OF REFERENCES	106

APPENDIX	137
MATLAB CODE	138
<i>Step 1 - Import Merged CSV Counts</i>	138
<i>Step 2 - Add Metadata</i>	145
<i>Step 3 - Add Light Schedule</i>	158
<i>Step 4 - Mark Noise and Cleanup Data</i>	164
<i>Step 5 - Select and Splice Data</i>	176
<i>Step 6 - Create Surface Plots</i>	180
CURRICULUM VITAE	191

LIST OF FIGURES

Figure 1.1: The relationship between lifespan, healthspan, cognition, disease burden, and survival.....	17
Figure 1.2: Environmental inputs and physiological outputs of mammalian circadian rhythms.	18
Figure 1.3: Molecular components of cellular circadian rhythms.....	20
Figure 1.4: Hormesis and the chronobiotic potential of THC in aged subjects.	22
Figure 1.5: Hypothetical model of cannabinoid hormesis in the restoration of age-related circadian rhythm disruption.	23
Figure 2.1: Experimental timeline.....	44
Figure 2.2: Baseline measures during vehicle acclimation.....	45
Figure 2.3: Effects of CP55940 on locomotion, thermoregulation, and nociception in young-adult (4m) and old (22m) C57BL6 mice.	46
Figure 2.4: Behavioral and physiological effects of CP55940 co-administered with the CB1 inverse agonist AM251 in young-adult (4m) and old (22m) male C57BL6 Mice.	48
Figure 2.5: Effects of CP55940 and AM630 coadministration in young males.....	50
Figure 2.6: Effects of CP55940 on peripheral locomotion in the open field.....	51
Figure 2.7: Animal cohorts and experiments.....	52
Figure 2.8: Sample sizes.....	53

Figure 3.1: Experimental timeline of baseline wheel running and treatment with CP55940.....	75
Figure 3.2: Circadian locomotion of C57BL6 mice housed under normal lighting (12:12, LD) and constant darkness (00:24, DD).....	78
Figure 3.3: Quantification of changes in average activity onset, activity offset, duration of activity, and total activity during normal lighting and constant darkness.	79
Figure 3.4: Treatment with varying doses of the synthetic cannabinoid CP55940 in young and old male mice.	82
Figure 3.5: Treatment with varying doses of the synthetic cannabinoid CP55940 in young and old female mice.	84
Figure 3.6: Voluntary wheel running of young and old male and female C57BL6 mice on the day before, during, and after injection with varying doses of CP55940.	86
Figure 3.7: Quantification of total wheel running 1, 1-6, and 6-12 hours after injection of the synthetic cannabinoid CP55940.....	87
Figure 3.8: Quantification of changes in average activity onset, activity offset, duration of activity following injection of the synthetic cannabinoid CP55940.....	89
Figure 4.1: Frequency of word-cluster combinations present in a systematic literature search.....	103
Figure 4.2: Time-of-day effect on thermoregulatory response to vehicle injection during acclimation trials.	104
Figure 4.3: Time-of-year effect on housing room humidity.	105

LIST OF TABLES

Table 2.1: Quantitative-PCR analysis of gene-expression in regions of brain tissue from young-adult (4m) and old (22m) male mice.....	49
Table 3.1: Proportion of animals whose activity onset and offset shifted greater than 15 minutes from normal lighting to constant darkness.	81

CHAPTER 1:
AGING, CIRCADIAN RHYTHMS, AND CANNABINOIDS

ABSTRACT

Numerous aspects of mammalian physiology exhibit cyclic daily patterns, known as circadian rhythms. However, studies in aged humans and animals indicate that these physiological rhythms are not consistent throughout the life span. The simultaneous development of disrupted circadian rhythms and age-related impairments suggests a shared mechanism which may be amenable to therapeutic intervention. Recently, the endocannabinoid system has emerged as a complex signaling network which regulates numerous aspects of circadian physiology relevant to the neurobiology of aging. Agonists of cannabinoid receptor-1 (CB1) have consistently decrease neuronal activity, core body temperature, locomotion, and cognitive function. Paradoxically, several lines of evidence now suggest that very low doses of cannabinoids are beneficial in advanced age. One potential explanation for this phenomenon is that these drugs exhibit hormesis - a biphasic dose-response wherein low doses produce the opposite effects of higher doses. Therefore, it is important to determine the dose-, age-, and time-dependent effects of these substances on the regulation of circadian rhythms and other processes dysregulated in aging. This review highlights three fields - biological aging, circadian rhythms, and endocannabinoid signaling - to critically assess the therapeutic potential of endocannabinoid modulation in aged individuals. If the hormetic properties of exogenous cannabinoids are confirmed, we conclude that precise

administration of these compounds may bidirectionally entrain central and peripheral circadian clocks and benefit multiple aspects of aging physiology.

BIOLOGICAL AGING

In humans, it is well accepted that the end of life is wrought with numerous concomitant disease states which impose immense personal and social burden. As such, the study of core biological processes involved in aging has become an increasingly prominent topic. Interestingly, there is a clear dichotomy among individuals regarding measures of age-related performance ¹. This phenotypic heterogeneity is particularly important when considering cognitive ability, since the deterioration of mental functions can greatly influence a person's quality of life. Though many aspects of cognition decline with age, spatial orientation and speed of processing appear particularly susceptible to age-related dysfunction ². Physiologically, the loss of neuronal synapses, chronic inflammation, oxidative stress, and impaired neurovascular coupling all contribute to declining cognitive performance with age ³⁻⁵. Fortunately, several studies indicate age-related cognitive impairment can be partially prevented or delayed using targeted pharmacological or hormonal interventions ⁶⁻¹⁰.

One of the earliest reported symptoms of aging is disturbed sleep ^{11,12}. Sleep/wake cycles are one example of the biologic phenomenon known as circadian rhythms. Though sleep requirements change throughout the lifespan, sleep quality and consistency are known to markedly deteriorate with age (**Figure 1.1**) ¹³. This is relevant to cognitive decline since sleep is an integral factor in the consolidation of memory, and age-related sleep disruptions are often concomitant with cognitive impairment and/or neurodegenerative diseases ¹⁴⁻¹⁹. Despite the necessity of sleep for survival, defining

the physiological *purpose* of sleep has been exceedingly difficult. However, relatively recent discovery of the glymphatic system and the sleep-dependent regulation of metabolite clearance from the brain indicates that sleep is vital to the maintenance of proteostasis in the central nervous system²⁰. Since proteostatic dysfunction is common in many pathologies of aging, disturbed sleep may play a causal role in age-related cognitive disorders. Although it remains unclear how age-dependent changes in the physiologic regulation of sleep are controlled, the maintenance of healthy sleep patterns in advanced age seems undeniably important to cognitive function.

CIRCADIAN RHYTHMS AND AGING

Circadian rhythms are scale-invariant biological patterns that correlate to the cyclic relationship of the Sun and Earth^{21,22}. Extrinsic cues such as light and environmental temperature are known as *zeitgebers* (time-givers) which entrain organisms' behaviors to particular times of day and improve evolutionary fitness (**Figure 1.2**)^{23,24}. Though it has long been observed that animals behave in a manner inherently tied to the time of day, only recently have the molecular and physiological underpinnings of these processes been elucidated²⁵⁻²⁷. Importantly, changes in these *clock genes* are attributed to both the process of aging and the pathogenesis of age-related diseases^{11,28,29}.

Seminal work in hamsters and mice revealed that when aged animals are housed in complete darkness, their *free-running* (intrinsic) circadian rhythms of locomotion are significantly different from younger animals³⁰⁻³². Additionally, studies of molecular clocks indicate that both rhythm amplitude and regularity deteriorate with age³³. More recent studies have confirmed these age-related changes in circadian rhythm

amplitude and period are exacerbated in the absence of environmental cues³⁴. Though these findings suggest deteriorating rhythms can be masked or compensated by environmental cues, aberrant sleep/wake cycles have also been observed in several species of aged subjects under normal lighting conditions^{13,17,19,35}.

In addition to impaired sleep, the amplitude of circadian locomotor activity and body temperature are known to decline in aging humans and rodents³⁶⁻³⁸. The circadian range of rectal temperature in mice is ~2.0°C, which declines to 0.5-1.0°C in advanced age; a similar reduction in range has been reported in humans³⁹⁻⁴¹. Daily locomotion also goes down in mice, with average daily running wheel counts declining by ~50%⁴². Furthermore, sleep-dependent production of the pleiotropic humoral factor Growth Hormone declines with age, and it is reported that these disruptions precede or are comorbid with cognitive dysfunction^{43,44}. A recent study suggests that age-related changes in the epigenetic regulation of the clock gene *Per1* underlies some aspects of cognitive decline⁴⁵. Whether circadian dysfunction is causal in age-related cognitive decline remains to be known, however the striking overlap of these observations warrants further investigation. Taken together, these observations suggest that both molecular and behavioral circadian rhythms might be responsive to- and responsible for- many aspects of biological aging.

Within the brain, the suprachiasmatic nuclei (SCN) of the mammalian hypothalamus are believed to be the primary neural sites of circadian integration⁴⁶. The SCN as a whole, through unknown mechanisms, integrates the oscillatory rhythm of each constituent neuron and collectively adopts a unified tone^{27,47,48}. Neuronal projections from the SCN transmit this coordinated rhythm to surrounding hypothalamic

and brainstem structures responsible for basic physiological functions such as the sleep/wake cycle, locomotor activity, regulation of body temperature, and hormone production^{49,50}. At the molecular level, cellular circadian clocks consist of transcription-translation feedback loops which exhibit tightly coupled daily rhythms (**Figure 1.3**). When exposed to a normal 24-hour light cycle, neurons of the SCN rhythmically express these clock genes that oscillate with periods of roughly 24 hours^{49,51}. Light, temperature, food, and pharmaceuticals can all act as zeitgebers, which modulate endogenous clock gene activity by extending or shortening the period of oscillation^{52,53}. Such drugs, known as *chronobiotics*, influence circadian physiology by either directly impinging on core clock molecules or altering entrainment systems. Therapeutically, chronobiotics are used to shift or amplify endogenous circadian rhythms and reduce dissonance with environmental conditions⁵⁴. Though circadian dysregulation is reported with chronic or uncontrolled use of exogenous substances such as caffeine, cannabis, and stimulant medications⁵⁵⁻⁵⁸. Promising ongoing research suggests that chronobiotics may be beneficial in cases of jet-lag, shift-work, and potentially aging,^{59,60}.

The SCN is often considered the primary regulator of mammalian circadian rhythms, although cell-autonomous molecular feedback loops have been observed in nearly all tissues throughout the body^{61,62}. In peripheral tissues, the period of each cell's rhythm is very near to 24 hours, although their exact rates are determined by body temperature, humoral factors, and nutritional state^{23,47,53,63-65}. Critically, in contrast to the clock gene rhythms of peripheral tissues, neurons of the SCN appear resistant to entrainment by body temperature^{66,67}. Since the SCN is directly responsible for the rhythm of body temperature, this presents a potential mechanism through which the

SCN can regulate clocks in peripheral tissues^{62,68}. Core body temperature - a vital physiological output which exhibits circadian rhythmicity - declines with age, and older subjects exhibit impaired thermogenesis⁶⁹⁻⁷¹. If the circadian rhythms of peripheral tissues are functionally entrained by body temperature, then age-related impairments of thermoregulatory capacity could explain why the rhythms of some peripheral tissues are unable to be properly maintained. Furthermore, since neuronal activity in the SCN determines central clock rhythms, and peripheral cellular clocks are entrained by thermic signals, pharmacological interventions which influence both neuronal activity and body temperature are of particular interest.

Declining circadian function with age is not associated with changes in overall SCN volume, however several studies report altered physiological properties in this brain region^{72,73}. In vivo electrophysiological recordings of the SCN show reduced amplitude and “noisy” signals as animals age, suggesting that neuronal function is compromised³². Additionally, increases in reactive astrocytes have been observed in the SCN of aged rodents^{72,73}. This is further emphasized by the concomitant age-related reduction in neural excitability within one downstream region of the hypothalamus innervated by the SCN, the subparaventricular zone. Mechanistically, reductions in several forms of potassium conductance have been shown to contribute to age-related alterations in SCN neural activity^{74,75}. More work is needed to understand the molecular mechanisms that precipitate these functional changes in the SCN and to determine their specific role age-related circadian dysfunction.

Even if targeting the SCN is not currently feasible, several studies demonstrate pharmacological manipulation of the peripheral clock network is possible^{61,76}. One of

the most profound regulators of lifespan across species is caloric intake, and evidence in flies suggests that this effect on lifespan is mediated via peripheral circadian clock gene expression ⁷⁷. Pharmacologically, dexamethasone was shown to alter clock gene expression in the liver, kidney, and heart via hormonal glucocorticoid signaling ⁷⁸. Peripheral circadian rhythms have also been modulated by drug-induced increases in cAMP levels ⁶¹. These findings show that although some aged tissues are arrhythmic they can still be pharmacologically induced to oscillate. Such reports are promising, since they suggest the machinery governing clock gene expression in the periphery remains intact even when the system is desynchronized. Targeting cAMP receptors is particularly exciting, as G-protein coupled receptors (GPCRs) are often regulators of cAMP. GPCRs are commonly successful drug targets, and over 35% of currently approved drugs act on these receptors ⁷⁹. Collectively, this implies that a large number of proteins may be amenable to therapeutically regulating circadian signaling. Future studies aimed at restoring circadian function within the SCN or preventing peripheral dysregulation may simultaneously benefit multiple pathologies of aging.

THE ENDOCANNABINOID SYSTEM IN ADVANCED AGE

One potential target for the pharmacological manipulation of circadian rhythms in advanced age is the endocannabinoid system ⁸⁰. Discovery of the endocannabinoid system occurred when searching for the receptors responsible for the psychotropic effects of plants from the genus *Cannabis* ⁸¹⁻⁸³. Multiple cannabinoid receptors have been identified in mammals, including the canonical CB1 and CB2 as well as more-recently identified receptors like GPR55 and GPR18 ^{80,84-86}. These cannabinoid receptors are GPCRs which exhibit distinct binding affinities for various endogenous

and exogenous ligands ^{80,86,87}. Radiographic localization of these receptors revealed profound expression of CB1 in the brain and central nervous tissue, while CB2 is primarily located in peripheral immune cells ⁸⁸⁻⁹⁰. The term *cannabinoid* refers to any compound which binds to these receptors, while the term *endocannabinoid* specifically refers to endogenously produced ligands ⁸⁰. The endocannabinoid system consists of these receptors and their endogenous ligands, which include N-arachidonylethanolamine (Anandamide) and 2-Arachidonoyl glycerol (2-AG) among others ^{91,92}. Numerous studies of the endocannabinoid system demonstrate that these ligands and receptors collectively regulate sleep, hunger, body temperature, and cognition – several of the circadian behaviors disrupted in advanced age ⁹³⁻⁹⁶.

As with many other physiological processes, the endocannabinoid system varies markedly with age ⁹⁷. There have been conflicting reports regarding age-related changes of CB1 in the brain. Some reports in rodents suggest that CB1 mRNA expression is reduced in advanced age ^{98,99}, while others indicate there is no change or even region-specific increases in CB1 ¹⁰⁰⁻¹⁰³. These discrepancies are also observed in humans, with post-mortem analyses showing reductions in CB1 radiolabeling in some studies, while newer PET scans of living individuals showing sex-specific increases in CB1 reactivity within aged females ¹⁰⁴⁻¹⁰⁶. Despite the various reported changes in expression, studies have shown a reduction in CB1-stimulated GTPγS functional activity in rodents and humans ^{98,103,104}. In addition to potential changes in receptor expression and function, reductions in the endocannabinoid ligand 2-AG have been observed in advanced age ¹⁰⁷. Considering the importance of this brain region to learning, memory, and pathologies of aging, it is likely that the changing endocannabinoid system impacts

cognitive behaviors. In support of this idea, studies using CB1-deficient mice show that reducing these signals leads to the development of unique age-related behavioral disturbances earlier than wildtype mice ¹⁰⁸. Curiously, young CB1-deficient mice outperform wildtype controls in social and object recognition tasks as well as operant learning paradigms, suggesting that the effects of the endocannabinoid system are influenced by the developmental age of the animals ¹⁰⁸⁻¹¹⁰. Although the exact mechanisms of these fluctuations are still under investigation, it appears that the preservation of endocannabinoid system function is vital to the aging brain.

Given the extensive activity of endocannabinoids throughout the central nervous system, there appears to be a substantial link between the endocannabinoid system and those physiological processes subject to age-related dysfunction. Additional evidence suggests that the endocannabinoid system plays a key role in circadian physiology. Several circadian behaviors are intricately linked to endocannabinoid signaling, namely: thermoregulation, nociception, locomotion, and food-intake ⁹³⁻⁹⁶. Centrally, neurons of the SCN express CB1 and alter their rates of firing in the presence of synthetic cannabinoid agonists and antagonists ^{111,112}. A recent primate study also revealed a circadian rhythm of cannabinoid receptor transcription in both the central nervous system and peripheral tissues ¹¹³. Moreover, cannabinoids are powerful regulators of body temperature - indicating that these compounds indirectly entrain peripheral cellular clocks. Taken together, these findings demonstrate a connection between the behavioral impairments observed in advanced age, disrupted circadian rhythms, and alterations in the endocannabinoid system.

CANNABINOID BEHAVIORAL PHARMACOLOGY

Although the endocannabinoid system is regulated by endogenous molecules like 2-AG and anandamide, exogenous cannabinoids such as those found in *Cannabis* are also known to modulate this system. Rigorous pharmacological study of *Cannabis* (also known as Marijuana, Marihuana) has a long and complex history ¹¹⁴. Historical records of *Cannabis*-use have been documented for millennia, but the structures and potential functions of the chemicals synthesized within *Cannabis* are still being elucidated ^{81,82,115,116}. Two of the most-studied *phytocannabinoids* (plant-derived cannabinoids), are Δ -9-tetrahydrocannabinol (THC) and cannabidiol (CBD), although growing bodies of literature exist for cannabigerol (CBG), cannabivarin (CBV), and many others ⁹². THC is considered to be the primary psychoactive compound in *Cannabis* and is an agonist of both CB1 and CB2 ¹¹⁶. The mechanism by which CBD exerts its physiological effects is unknown and widely disputed, as the K_i for CB1 and CB2 is over 100 fold lower than that of THC on these receptors ¹¹⁷. Though most of the focus is on phytocannabinoids like THC, it is important to also note that *Cannabis* produces a wide variety of monoterpenoids and sesquiterpenoids - which may also act directly on cannabinoid receptors ^{118,119}. Extensive reviews of *Cannabis*, phytocannabinoids ⁹², cannabinoid receptors ⁸⁰, and endocannabinoid pharmacology ¹²⁰, have previously been published.

Human empirical and anecdotal evidence demonstrates that exogenous cannabinoids profoundly impact cognition and physiology ^{114,115,121,122}. However, studies of phytocannabinoids are somewhat difficult to interpret given the extreme diversity of compounds present in raw plant-matter or extracts. As such, knowledge of each cannabinoid's specific pharmacological profile is crucial to consider any potential

therapeutic applications for these substances. Receptor-subtype-specific compounds have been vital to delineating the shared and specific effects of CB1 and CB2 on physiological functions ^{123,124}. Many synthetic cannabinoids have been identified using the Tetrad Assay – a battery of behavioral tasks for assessing CB1 function in rodents ^{80,125}. These tests measure locomotion, catalepsy, thermoregulation, and analgesia as endpoints of CB1 receptor activity ¹²⁵. Though the Tetrad Assay has proven useful as a drug screening mechanism, its relatively limited scope does not permit full characterization of an animal's behavioral status, especially when one considers the behaviors altered in advanced age. In addition to nociception, locomotion, and thermoregulation, CB1 activity regulates learning and memory, sleep/wake activity, food-intake, anxiety, attention, and cardiovascular function ¹²⁶⁻¹³³.

In both animals and humans, memory impairment following acute or chronic administration of CB1 agonists has been repeatedly reported ¹³⁴⁻¹³⁸. However, alternative studies indicate that these memory-impairing effects are dose- and age-dependent ¹³⁹⁻¹⁴⁴. Recent evidence in rodents suggest that some these effects can be partially blocked by co-administration with CBD, a finding which may explain why anecdotes of whole-plant *Cannabis*-use often disagree with the receptor-specific effects seen in animal studies ^{145,146}. The diverse behavioral phenotypes elicited from modulation of the endocannabinoid system emphasize the importance of understanding this integral physiological system.

Despite the large volume of studies conducted on exogenously administered cannabinoids, synthesis of this data is difficult due to inconsistent compositions of phytocannabinoids, doses, and routes of administration (ROAs) ¹⁴⁷⁻¹⁵⁰. Additionally,

there is a significant disparity between preclinical dosing regimens and those currently accepted for human consumption. Regarding THC, many rodent experiments use intraperitoneal doses ranging from 1mg/kg to 30mg/kg, however, current recreational and clinical amounts for humans are closer to 0.15mg/kg orally ¹⁵¹⁻¹⁵⁴. While the pharmacokinetic profiles vary markedly between rodents and humans ¹⁵⁵, several studies now show that injections of THC can alter animal behavior and molecular signaling at doses as low as 0.002mg/kg ^{140,156}. Recent attempts have been made to more adequately model the routes of administration used by humans ^{126,127,157-160}. The results of these studies indicate that cannabinoids administered orally have a delayed onset and longer duration of action than when they are inhaled ^{127,158,161}. These route of administration-dependent effects are to be expected; however, preliminary evidence suggests that chronic *Cannabis*-use may also alter the gut microbiome ¹⁶². Given that recreational and medicinal cannabinoids are often administered orally, future studies of microbiome-mediated cannabinoid metabolism are of particular importance. Taken together, it is imperative that these discrepancies in dosing and route of administration are carefully considered and discussed in future studies.

HORMESIS AND CANNABINOID CHRONOPHARMACOLOGY

There is little debate regarding the deleterious effects of cannabinoids in high doses, however the reported effects of more modest amounts are somewhat conflicting. High doses of THC (≥ 3 mg/kg in rodents, ≥ 0.15 mg/kg in humans) are consistently reported to disrupt cognitive function in rodents and produce psychoactive effects in humans ^{136,138,142,163-165}. Despite the consistent inhibitory or soporific effects of cannabinoids at higher doses, studies which have examined lower amounts often report

stimulatory effects at the lowest doses tested ^{143,166-172}. Though exogenous cannabinoids are known to induce hypothermia and hypolocomotion, several investigations have reported increased body temperature and locomotion following treatment at low doses ^{171,173,174}. A similar biphasic effect of THC on intracranial self-stimulation was reported in rats treated with 0.1 or 1.0mg/kg ¹⁶⁷. Based on this study, the authors concluded that an acute intraperitoneal injection of 0.1mg/kg THC induced reward-seeking behavior while the higher dose elicited anhedonia. Mechanistically, the effects of higher doses appear to be mediated in-part by CB1 signaling in GABAergic neurons ¹⁶⁸. A growing body of literature now suggests that low doses (≤ 3 mg/kg) of THC and other synthetic cannabinoids may prevent certain aspects of age-related cognitive decline in rodents ^{139,143,156,175}.

Within the context of exogenously administered cannabinoids and cognition, the hormetic dose-response of this compound may rectify these disparate reports ¹⁷⁶. *Hormesis* describes a biphasic dose-response where low amounts of a substance produce opposite effects of higher doses ¹⁷⁷. Great efforts have been made in recent years to catalog and characterize reports of dose-response experiments which cannot be explained by traditional, linear models ¹⁷⁸. Continued work in this field now suggests that one explanation for this biphasic response is through *preconditioning* ¹⁷⁹⁻¹⁸¹. This is in line with work previously presented by Sarne et al. which indicates that exposure to low doses of exogenous cannabinoids blunt the negative impacts of subsequent insults ^{180,182}. These findings have intriguing implications for the study of aging, since preconditioning biological systems during critical developmental windows may bolster resilience to age-related dysfunction ^{183,184}.

Interestingly, the hormetic dose-response of THC on body temperature has been reported for many years (**Figure 1.4A**)^{171,173,180}. Additionally, exogenous cannabinoids alter anxiety-related behaviors in dose-dependent, bidirectional manner - although the nature of this relationship is poorly understood¹⁸⁵⁻¹⁸⁸. Early observations regarding the time- and temperature-dependence of THC's effects may also shed light on these seemingly incongruent findings. A classic study by Ernest Abel revealed that the time of day in which THC is administered drastically affects the physiological response, a phenomenon now referred to as *chronopharmacology*¹⁸⁹. Similarly, an elegant study by Pertwee and Tavendale in 1977 revealed that the ambient temperature markedly altered rates of oxygen consumption and body temperature changes induced by THC administration¹⁹⁰. Furthermore, sex-specific responses to cannabinoids may present a confounding factor when interpreting these results, as previous reports have indicated that doses of THC that impaired cognition in males actually improved measures in females^{191,192}.

Given the current evidence, it is difficult to discern whether the cognitive-enhancing effects of low-dose cannabinoids are due to 'true' hormesis, age-dependent changes in endocannabinoid function, or both. The work by Sarne and colleagues demonstrates that exceptionally small amounts of THC (0.002mg/kg) are sufficient to influence neurobiology. These studies reported that a single dose of 0.002mg/kg, IP produced neuroprotection in young male mice and lasting cognitive enhancement in old females^{140,156,174,193}. Critically, pilot studies at this dose were reported to increase body temperature and stimulate locomotion - a finding which supports the hormetic stimulatory response¹⁸⁰. While the evidence presented by Suliman also supports that

the effects of cannabinoids are age-dependent, the data from this study indicate that there is a 'window' in which cannabinoids may improve function ¹⁴³. Although there are not enough doses in these studies to clearly demonstrate hormesis, we feel that this evidence is supportive nonetheless.

The range of doses studied by Sarne et al. indicate that doses which improve cognitive performance in old animals (0.002mg/kg) cause impairments in young animals, and the studies by Bilkei Gorzo et al. (3mg/kg THC) in old animals also support this. These findings, and others, indicate a clear effect of aging on response to exogenous cannabinoid administration. The possibility remains, however, that the lowest dose of THC reported by Sarne et al. (0.0005mg/kg THC, IP) in young animals, may still lie above the stimulatory hormetic range for this age group. This hypothesis is supported by their biochemical studies which report the highest activation of P-ERK in the cerebella of young animals at this dose (0.0005mg/kg) (Amal 2010).

To date, we are unaware of a modern study specifically designed to determine if cannabinoids exhibit hormesis, and whether this hormetic dose-range is altered with age. Even if preliminary evidence suggests there is cannabinoid hormesis in young animals, it remains to be seen if this same hormetic curve persists with age or if the stimulatory range might change. Though there are several potential mechanistic explanations for these age-dependent effects, recent studies support a desensitization of endocannabinoid machinery with age. Ultimately, additional studies testing multiple doses in young and old animals are required to directly compare the hormetic range of exogenous cannabinoids.

Despite the importance of these pharmacological considerations across different compounds and systems, hormesis and chronopharmacology remain understudied components of many biomedical studies - particularly those in aged animals ¹⁹⁴. These two distinct properties have intriguing implications for the potential use of cannabinoids as therapeutics. Namely, that it may be possible to attain opposing physiological effects based solely on the dose- and time-of-administration. To this end, application of these pharmacological properties to a highly dynamic and heterogenous condition such as age-dependent circadian dysfunction, may provide a wide range of therapeutic potential **(Figure 1.4B)**.

CONCLUSIONS

Taken together, the findings discussed here suggest that altered circadian rhythms are a potential biomarker of aging, and restoration or preservation of these rhythms in aged individuals might benefit certain age-related pathologies. The endocannabinoid system is a promising target in the treatment of age-related disease, given the diverse physiological processes it regulates. Centrally, modulation of SCN activity by cannabinoids supports their classification as a chronobiotics, and careful, therapeutic application use of these compounds may serve to restore abnormal behavioral rhythms in aged subjects. Moreover, the biphasic effects of cannabinoids on body temperature may allow for the “tuning” of peripheral molecular clocks **(Figure 1.5)**. Many additional experiments are necessary to fully characterize the hormetic dose-response of exogenous cannabinoids such as THC and examine their potential efficacy in the amelioration of age-related circadian dysfunction. As societal opinions of ‘aging

as a disease' and 'cannabinoids as medicine' shift, further inquiry of these previously intractable topics may prove greatly beneficial to human health.

FIGURES

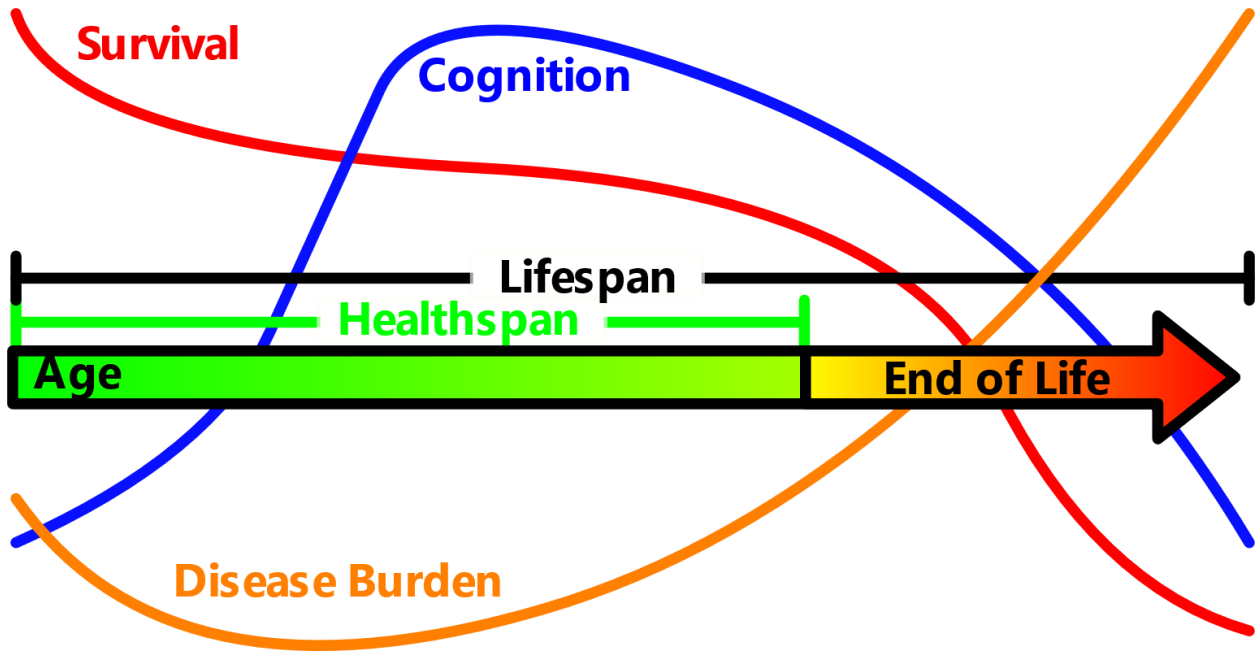


Figure 1.1: The relationship between lifespan, healthspan, cognition, disease burden, and survival.

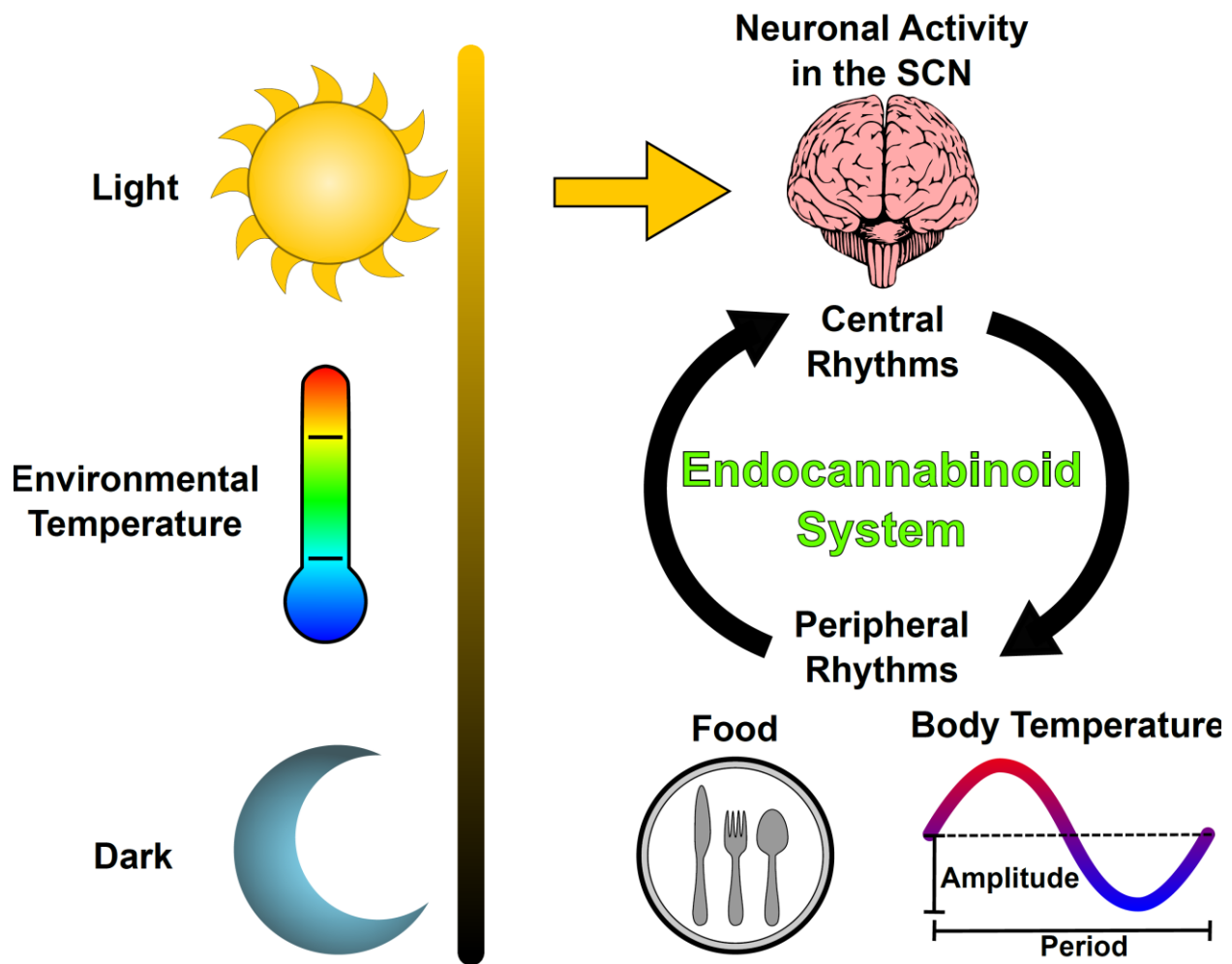


Figure 1.2: Environmental inputs and physiological outputs of mammalian circadian rhythms.

Routine daily exposure to light entrains the SCN to a 24-hour period via the retinohypothalamic tract. Neurons of the SCN rhythmically alter their rates of firing in response to changing environmental conditions and humoral signals. Outputs from SCN neurons drive central rhythms in hormone production, locomotor activity, feeding behavior, and body temperature. Peripherally, cellular rhythms are entrained by the daily oscillation of body temperature and food-intake. Since endocannabinoid activity is

known to regulate SCN neurons, body temperature, and food-intake, evidence suggests that the endocannabinoid system is a key component of physiological circadian rhythms.

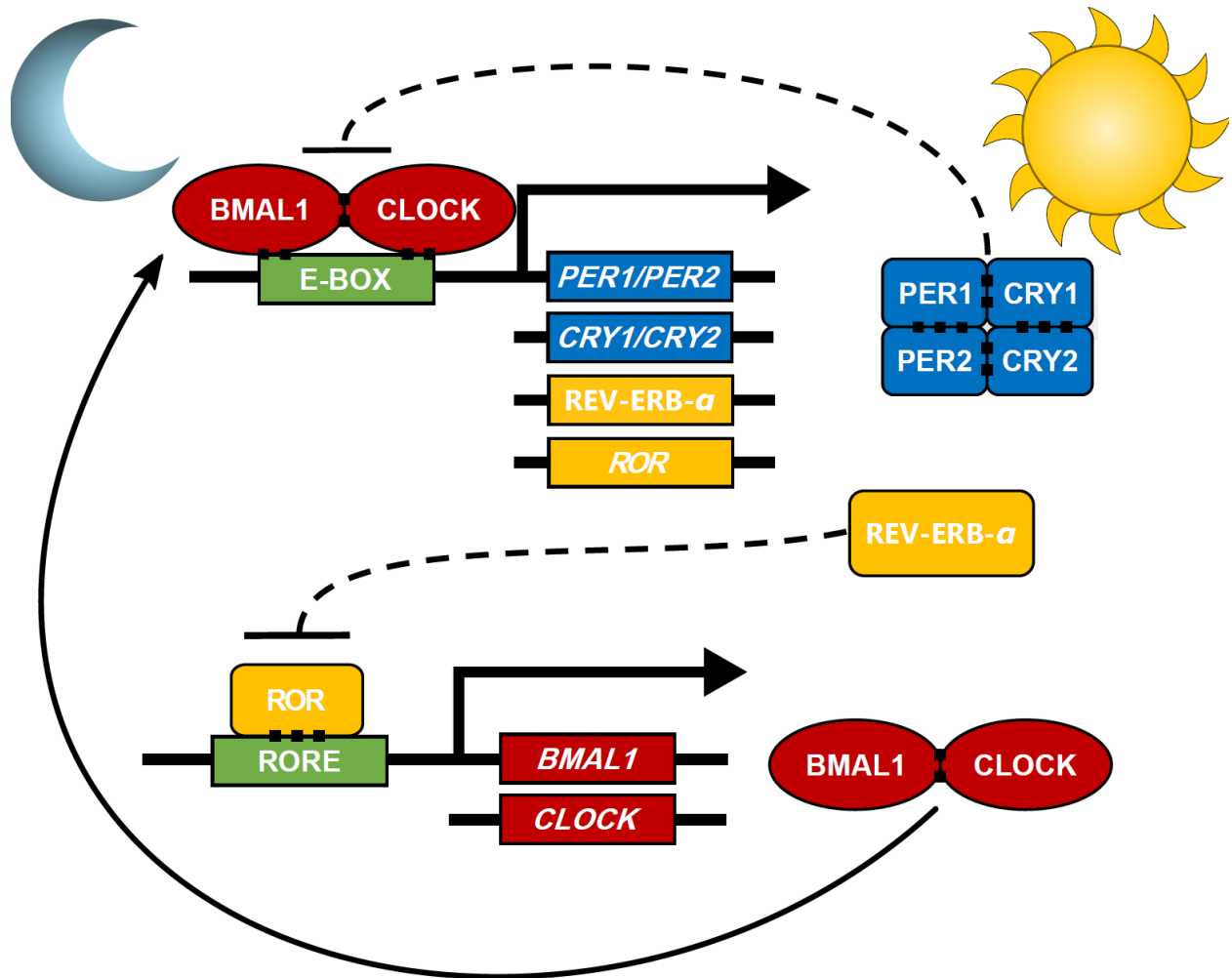
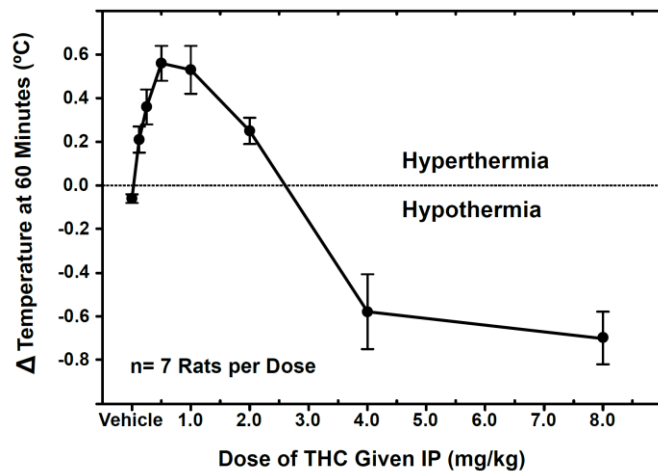


Figure 1.3: Molecular components of cellular circadian rhythms.

The core circadian molecular loop consists of two proteins, Brain and muscle arnt-like 1 (BMAL1) and Circadian Locomotor Output Cycles Kaput (CLOCK), which interact to form a transcriptional activator complex that stimulates transcription of the Period and Cryptochrome genes (PER1, PER2, CRY1, and CRY2). The Per and Cry proteins accumulate in the cytoplasm throughout the day and ultimately bind to the BMAL1:CLOCK complex. Sufficient binding of the PER:CRY complex to the BMAL1:CLOCK complex prohibits transcription of PER and CRY mRNA. As protein

levels of PER and CRY diminish, the BMAL1:CLOCK complex is allowed to stimulate transcription once more.

A) Hormetic Dose-Response of THC on Rectal Temperature



B) Young Old Old + THC

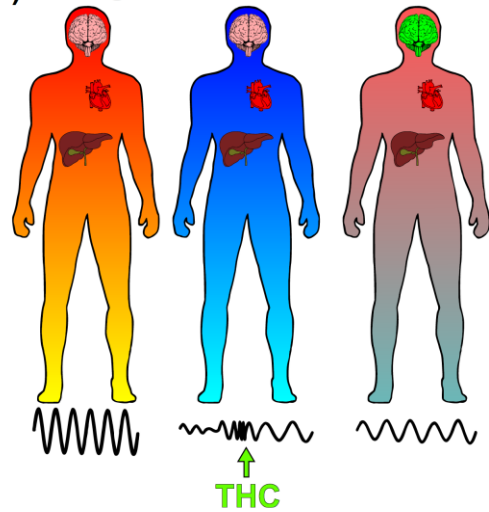


Figure 1.4: Hormesis and the chronobiotic potential of THC in aged subjects.

Panel A) Hormetic dose-response of THC on rectal temperature in rats. Data redrawn from: Sofia, R.D., 1972. A paradoxical effect for 1-tetrahydrocannabinol on rectal temperature in rats. Research communications in chemical pathology and pharmacology, 4(2), pp.281-288.

Panel B) Declining amplitude and increasing lability of central and peripheral rhythms with age may be amenable to therapeutics which simultaneously alter neuronal activity in the SCN and body temperature. Using the chronopharmacological properties and hormetic dose-response of THC, low-dose exposure may help to rescue dysfunctional clocks in aging systems.

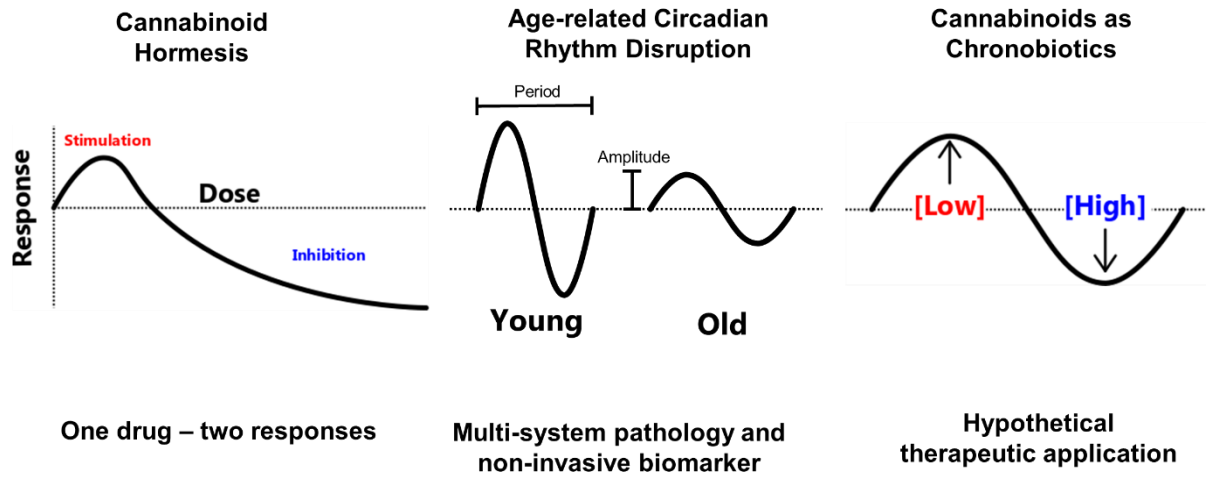


Figure 1.5: Hypothetical model of cannabinoid hormesis in the restoration of age-related circadian rhythm disruption.

CHAPTER 2:
AGE-DEPENDENT HORMESIS-LIKE EFFECTS OF THE
SYNTHETIC CANNABINOID CP55940 IN C57BL/6 MICE.

ABSTRACT

Use of cannabis and cannabinoid-containing substances is increasing among geriatric patients, despite relatively sparse preclinical evidence in aged models. To better understand the effects of exogenous cannabinoids on aging male and females, we compared the age- and dose-dependent physiological and behavioral effects of the synthetic cannabinoid CP55940 in adult and aged C57BL/6 mice. Locomotion, body temperature, thermal nociception, and fecal output were measured following CP55940 administration. Our findings indicate that CP55940 is more potent and efficacious in older mice, evidenced by exaggerated antinociceptive and soporific responses when compared to younger adult mice. Additionally, we report that low doses of CP55940 paradoxically stimulate locomotion in young mice, however this hormesis-like response is not as evident in aged animals. These bidirectional effects appear to be mediated via the endocannabinoid CB1 and CB2 receptors.

INTRODUCTION

Collectively, the canonical receptors (CB1 and CB2), endogenous ligands (anandamide and 2-arachidonoylglycerol), biosynthetic regulators (N-acyl phosphatidylethanolamine phospholipase D [NAPE-PLD] and diacylglycerol lipase- α

[DAGL α]), and metabolizing enzymes (fatty acid amide hydrolase [FAAH] and monoacylglycerol lipase [MGL]) of the endocannabinoid system are known to dynamically regulate numerous aspects of mammalian physiology. Though extensive work has been conducted on the behavioral and developmental effects of exogenous cannabinoids early in life, substantially less is known regarding the physiological effects of these substances in advanced age^{92,195}. This lack of information, coupled with rapidly shifting trends in cannabis- and cannabinoid-use worldwide puts elderly patients particularly at-risk. Furthermore, emerging evidence suggests that the endocannabinoid system may play a fundamental role in the biological processes of aging. This is exemplified by transgenic mice that are genetically deficient in CB1, which exhibit progeroid cognitive and physiological phenotypes¹⁰⁸. However, pharmacological manipulation of endocannabinoid signaling does not appear to produce consistent effects across the lifespan. This is evidenced in studies where chronic infusion of the phytocannabinoid Δ -9-tetrahydrocannabinol (THC) was shown to enhance cognition in aged mice at doses which impair younger animals' performance¹³⁹.

Cannabis and cannabinoid-containing substances have been used therapeutically for millennia, but rigorous evaluation of their medical value is still ongoing¹¹⁵. In preclinical rodent models, the effects of CB1-acting compounds are traditionally measured using the "Tetrad Assay" - a battery of tests that measure locomotion (open field), body temperature (rectal probe), catalepsy (ring-immobility), and nociception (hot plate or tail withdrawal)^{196,197}. The synthetic cannabinoid CP55940 is a well-documented, high-affinity CB1/CB2 mixed agonist which elicits the hallmark phenotypes observed in these behavioral assays. Studies have demonstrated that the

phenotypes produced by CP55940 are similar to those produced by high doses of the phytocannabinoid THC - hypolocomotion, hypothermia, and antinociception - though CP55940 is substantially more potent and efficacious than THC in these assays^{198,199}.

While there is consensus regarding the soporific, aversive, and antinociceptive effects of CB1 agonists at high doses, several studies report contradictory stimulation of locomotion, body temperature, and cognitive behaviors at low or ultralow doses^{173,176,195,200}. One explanation for these biphasic dose-responses is the biological adaptive response known as *hormesis*¹⁸³. Though hormesis, preconditioning, and bidirectional dose-responses are widely evident in numerous biological systems, systematic reporting of these low-dose effects is exceedingly difficult and often overlooked. Such findings are critical, however, as the stimulatory hormesis-like effects observed with low doses of cannabinoids in young animals may underlie the differential cognitive effects reported in aged animals^{140,176,182}. To date, we are unaware of a study which specifically permits the comparison of young vs aged animals' responses to low doses of cannabinoids. To determine whether this biphasic response to cannabinoids is age-dependent, we experimentally assessed the dose-dependent physiological and behavioral effects of CP55940 at multiple doses in young and aged, male and female mice.

RESULTS

Acclimation to Vehicle Injection and Baseline

In order to adequately capture potential biphasic behavioral and physiological responses elicited by the synthetic CB1/CB2 agonist CP55940, we administered this compound via intraperitoneal (IP) injection at the following weight-adjusted doses:

0.001, 0.01, 0.1, 0.4, and 0.8mg/kg. Prior to treatment with CP55940, animals underwent a 6-day acclimation period consisting of 3 days of handling and temperature measurement, followed by 3 additional days of temperature recordings before and after vehicle injection (1:1:18, EtOH:Kolliphor:Saline) (**Figure 2.1**). During the acclimation period, baseline temperature was measured immediately before and 60 minutes after injection using both a rectal probe and a non-contact infrared (IR) thermometer. During acclimation recordings, both age groups showed a slight but consistent average reduction in rectal and IR temperatures 60 minutes after injection of the vehicle solution (**Figure 2.2**). Additionally, old mice weighed more while having lower baseline rectal and skin/pelage temperatures than young mice (**Figure 2.2**).

Behavioral and Physiological Responses to CP55940

On the day of behavioral testing, male and female mice were injected with varying doses of CP55940 or vehicle then assessed for locomotor, thermoregulatory, or nociceptive responses. No sex-specific differences were observed throughout the study, thus data from both males and females was combined. Activity measurements recorded in the open field 30-60 minutes after injection indicate that treatment with CP55940 displays a significant Age:Dose interaction effect on total locomotion (Locomotion~Age*Dose, $H(5,351) = 11.451, p=0.043$). Interestingly, young mice treated with the lowest dose of CP55940 tested (0.001mg/kg) exhibit significantly increased locomotion compared to age-matched vehicle-treated control animals ($p<0.05$, **Fig. 2.3A**). However, old animals administered this same dose did not significantly differ from age-matched vehicle-treated controls. As expected, higher doses of CP55940 significantly reduced locomotion in both young and aged animals though this

suppression was evident in aged animals at a dose of 0.1mg/kg, which was not soporific in young animals (**Fig. 2.3A**). In both age groups, doses of CP55940 ≥ 0.4 mg/kg induced severe catalepsy (**Fig. 2.3A**). Though no effect of Age was detected on fecal output during the open field task (Feces~Age, $H(1,297) = 1.57$, $p=0.210$), young vehicle-treated animals produced significantly more fecal pellets during the open field task than old control animals ($p=0.004$). Additionally, at doses of CP55940 ≥ 0.01 mg/kg fecal output was significantly reduced in both age groups (**Fig. 2.3B**).

Immediately following the 60-minute temperature recordings, nociception was quantified by placing each mouse onto a 52°C heated plate and recording the latency to lick its hind-paw or jump. Significant simple main effects of Dose (Latency~Dose, $H(5,353) = 149.41$, $p<0.001$) and Age (Latency~Age, $H(1,353) = 9.21$, $p=0.002$) were detected in this assay, though no interaction between these factors was observed (**Fig. 2.3C**). Among vehicle-treated animals, young mice were significantly quicker to respond than older mice ($p=0.005$). The antinociceptive effects of CP55940 were highly significant in both age-groups at doses of 0.4 and 0.8mg/kg, though aged animals were significantly slower to respond than young animals at both of these doses. In later cohorts of animals, nociception was also assessed via tail-immersion in a hot water bath (46°C). The results from these tests were similar to the hot-plate, although no main effect of Age was detected (**Fig. 2.3D**). Intriguingly, a significant reduction in latency to withdraw tail was observed in old animals treated with the intermediate dose of 0.01mg/kg ($p=0.049$). In agreement with the hot plate recordings, age groups showed highly significant antinociception at doses of CP55940 ≥ 0.4 mg/kg.

Rectal and skin/pelage temperatures were measured 60 minutes post-injection via rectal probe and infrared thermography. Both of these measures displayed a significant main effect of Dose during behavioral testing (Δ Rectal~Dose $H(5,349) = 182.01$, $p < 0.001$ and Δ Skin ~Dose, $H(5,340) = 146.06$, $p < 0.001$). In vehicle-treated animals, rectal and skin/pelage temperatures were significantly elevated from baseline in young and old mice (**Fig. 2.3E-F**). When compared to vehicle-injected animals, high doses of CP55940 (0.4 and 0.8mg/kg, IP) significantly reduced rectal temperature in both age groups. Importantly, this decline in rectal temperature was more pronounced in aged mice, which exhibited reductions in rectal temperature at the dose of 0.1mg/kg which had no effect in younger animals.

Responses to CP55940 and CB1 or CB2 Antagonism

To determine whether the biphasic effects of CP55940 could be accounted for by activity at canonical cannabinoid receptors, we coadministered CP55940 with the CB1 or CB2 inverse agonists - AM251 or AM630, respectively. Based on previous literature, doses of 3mg/kg AM251 or AM630 were administered to modulate CB1- and CB2-mediated signaling and behavior^{201,202}. Two doses of CP55940 shown to stimulate locomotion in young males (0.001 and 0.01mg/kg,IP) were administered alone or in the presence of AM251 or AM630; additionally, a high dose (0.8mg/kg) that significantly reduces locomotion in both young and old animals was coadministered with AM251(3mg/kg). AM251 alone significantly reduced locomotion (**Fig. 2.4A**) and attenuated both the stimulatory and inhibitory effects of CP55940 on locomotion in young males (**Fig. 2.4A**). In contrast, AM630 coadministration in young males significantly attenuated the psychomotor stimulation elicited by CP55940 but did not

block the reduction in fecal output produced by CP55940 at a dose of 0.01mg/kg (**Fig. 2.5**).

The CB1 inverse agonist AM251 also blocked the inhibitory effects of 0.01mg/kg CP55940 on fecal output in young males (**Fig. 2.4B**). Fecal output was significantly increased with coadministration of 0.8mg/kg CP55940 with AM251 compared to 0.8mg/kg CP55940 alone; although this was a partial rescue by AM251, as a significant decrease from vehicle control was still observed with the coadministration of drugs (**Fig 2.4B**). Similar to the rescue of catalepsy, the antinociceptive and hypothermic effects of 0.8mg/kg CP55940 were abrogated by 3mg/kg AM251 (**Fig. 2.4C-D**), suggesting CB1 mediates many responses following high dose synthetic cannabinoid administration.

While aged animals did not show significant stimulatory locomotor effects with low doses of CP55940, we verified that the mechanism responsible for the changes observed with high doses of CP55940 was unchanged in advanced age. Coadministration of AM251 significantly attenuated the hypolocomotor, antinociceptive, and hypothermic effects of CP55940 in aged males (**Fig. 2.4E-H**). Similar to the effects in young males, changes in fecal output were partially rescued by coadministration of AM251 with CP55940 in aged males (**Fig. 2.4F**), although it is important to note that AM251 alone significantly increased fecal output (**Fig. 2.4F**). 3mg/kg of AM251 also reduced locomotor activity and significantly reduced body temperature in the aged mice (**Fig. 2.4E and H**), similar to the changes seen with AM251 alone in the young males (**Fig. 2.4 A and D**).

Pharmacokinetics of CP55940 and Endocannabinoid Gene Expression in the Brain

To determine the mechanism for the enhanced potency of CP55940 seen in aged animals, pharmacokinetic distribution of CP55940 in the blood and brain was quantified following both 0.1 and 0.8mg/kg injections. Unfortunately, both of these efficacious doses fell below the LC-MS/MS detection limits in these samples (data not shown). Gene expression in brain tissue was also analyzed to determine whether the expression of endocannabinoid receptors or their regulatory proteins was increased in the aged animals that showed enhanced responses to CP55940. Significant reductions in CB1 gene expression were observed in both cortical and hypothalamic tissue samples from aged animals, ($p=0.04$ and 0.02 , respectively) (**Table 2.1**). Fatty acid amide hydrolase expression was also significantly reduced in the cortex of aged mice (**Table 2.1**). No changes significant changes in CB2 were noted.

DISCUSSION:

Taken together, these findings reveal that the effects of CP55940 on thermoregulation and behavior are highly age- and dose-dependent. Importantly, CP55940 given to aged mice is significantly more efficacious than equivalent doses administered to young mice, and the dose of 0.1mg/kg appears to be a key inflection point in this differential response. In young mice, our data indicate that low (<0.01 mg/kg, IP) and high (>0.1 mg/kg, IP) doses of CP55940 bidirectionally regulate measures of locomotion, and these increases in total locomotion are not associated with thigmotactic aversive behavior (**Figure 2.6**)²⁰³. However, under the present conditions we did not detect significant CP55940-induced stimulation of locomotor activity in aged mice at any dose of CP55940 tested. The distinct locomotor responses observed in both age groups

at doses of 0.1mg/kg CP55940 indicate that continued characterization of this specific dosing window may help to clarify these differing effects^{176,182}.

In contrast to antinociceptive effects of CP55940 at doses ≥ 0.4 mg/kg, significantly enhanced nociception was observed in aged but not young mice tested using the hot-water tail withdrawal task (**Fig. 2.3D**). As this task is less reliant on gross locomotor activity than the hind-paw licking measured in the hot plate assay, the ability to detect this effect highlights the importance of tasks with wide detection ranges and sensitivity when studying hormesis. Additionally, the age-dependent responses seen in these assays of nociception further highlight the importance of using multiple endpoints when studying aged animals. Given the high prevalence of elderly patients seeking cannabinoid-based therapeutics for chronic pain, additional studies in this model are greatly needed.

During extensive vehicle acclimation recordings, both young and old mice exhibited slight reductions in core-body and skin/pelage temperatures 60 minutes post-injection (**Figure 2.2**). However, on the day of behavioral testing, vehicle treated animals consistently showed increases in rectal and IR temperatures (**Fig. 2.3D and E**). One explanation for this differential response is that during behavioral testing, post-injection temperatures were taken immediately after animals completed open field locomotor assessment. Therefore, it is possible that the hyperthermia observed following vehicle-treatment in this context is confounded by locomotion in the open field. Additionally, the high rectal temperatures recorded in young vehicle-treated mice following open field testing may represent a ceiling-effect, precluding the replication of previously-observed hyperthermia induced by low doses of cannabinoids¹⁷³. The

effects of cannabinoids on thermoregulation may not be limited to brain-stem mediated mechanisms and may also be influenced by peripheral vasodilation, as previously reported²⁰⁴. Thus, we chose to measure skin temperature in addition to core body temperature. A reduction in temperature of both measures was noted with high doses of CP55940 in all groups tested.

Consistent with previous studies, no significant differences in locomotion were observed with AM630 alone in this study (**Figure 2.5**). However, we were surprised that the psychomotor stimulation with low doses of CP55940 was blocked by either AM251 or AM630. This suggests that both CB1 and CB2 mediate, at least in part, the hormetic-like response. Future studies comparing the effects of CB1 and CB2 antagonists using cognitive assays where ultralow doses of cannabinoids have demonstrated protective effects might further delineate whether the observed blockade of hormesis is unique to locomotion or extends to other behaviors in rodents¹⁵⁶.

It is not currently clear what the mechanism is which increases responsiveness to this cannabinoid in the aged mice. In the present study, we observed significantly decreased CB1 gene expression in aged mouse cortex and hypothalamus. This is similar to previous research which demonstrated CB1 levels vary throughout the lifespan, although these age-related changes appear to be region-specific^{99,103}. A reduction in receptor-expression by aged animals that show enhanced CB1-dependent physiological phenotypes is perplexing, although a similar phenomenon was observed in dopaminergic GPCRS. Following chronic receptor blockade, production of DA receptor declines yet results in chemical “supersensitivity”²⁰⁵. While CB1 expression was decreased, there was also a significant reduction in the expression of FAAH1 in the

aged cortex, suggesting potential elevations of endocannabinoid levels within our aged mice. Future studies of cannabinoid receptor heterodimerization and biased agonism, which have yet to be assessed in aged mammals, may also yield beneficial insight on this matter. An alternative hypothesis is that cannabinoids may have increased access to the central nervous system due to declining blood brain barrier function in aged animals. During the course of this study we attempted to assess the pharmacokinetic distribution of CP55940 in two independent cohorts of young and aged mice following an injection of 0.1mg/kg and 0.8mg/kg. Despite the fact that these doses consistently elicited behavioral phenotypes, this amount of CP55940 ultimately proved to be below our detection limits in serum, liver, and whole-brain tissue samples.

Mechanistically, our studies with the CB1 and CB2 inverse agonists suggest that the psychomotor, thermoregulatory, and antinociceptive effects of CP55940 at doses of 0.001 and 0.01mg/kg, IP are independently mediated by both receptors. Treatment with AM251 alone produced simultaneous reductions in locomotion and rectal temperature, while greatly increasing fecal output, suggesting that AM251 at a dose of 3mg/kg,IP is aversive in young male mice. The notable observation that CP55940 at 0.01mg/kg abrogates the antinociceptive effects of AM251 in young males (**Fig. 2.4C**) suggests that this dose of CP55940 in combination with AM251 may restore tonic endocannabinoid activity to baseline levels. The importance of maintaining tonic endocannabinoid signaling has been discussed in detail previously, and the limited effect of AM251 administration, by itself, suggests that the age-dependent responses we observed may be due to elevated endocannabinoid tone²⁰⁶. As discussed, our aged animals exhibited significant decreases in FAAH1, which could lead to increased

anandamide levels in the aged cortex. It is possible that increased anandamide, or other endocannabinoids, may contribute to the baseline difference in nociception between age groups (**Fig. 2.3C**). Regardless, CB1 antagonism rescues many of the phenotypic changes observed with high doses of CP55940 in both the young and old mice. However, the failure of AM251 coadministration to rescue the reduction in fecal output seen at the highest dose (0.8mg/kg,IP) of CP55940 tested (**Fig. 2.4B**) suggests a CB1-independent mechanism, and may be due to interactions with the TRPV1 receptor as recently reported ²⁰⁷.

We were surprised that the effects of CP55940 were not sex-specific, as aging rodent studies are often marked by pronounced sex-dependent phenotypes²⁰⁸⁻²¹¹. Moreover, studies of nociception and pain responses also commonly show sex-dependent effects^{212,213}, as well as known sex- and gender-specific differences in cannabis abuse and physiological responses following cannabis consumption in humans^{214,215}. These studies often denote that such changes are driven in part by differences in muscle mass and fat tissue distribution. In the current study, we did not control for changes in body composition, estrous state, or the stage of reproductive senescence within our young or aged cohorts but weight was consistently recorded and all drugs were administered at weight-adjusted doses (**Figure 2.2**). Our data suggest that the psychostimulatory effects observed at low doses and the robust inhibitory effects seen at high doses are more strongly influenced by age than sex in mice.

The present study offers substantial evidence that the behavioral and physiological effects of CP55940 are highly age-dependent, though several additional considerations remain to be addressed. Specifically, the current experiments utilized a

highly potent synthetic cannabinoid known to agonize both CB1 and CB2. Despite its high affinity for these receptors, high doses of CP55940 modulate additional receptors and influence physiological functions in cells that lack CB1 or CB2²¹⁶. The expansive endocannabinoidome presents numerous additional targets, such as the previously mentioned TRPs or biosynthetic/metabolizing enzymes, which are also likely involved in mediating the diverse effects of CP55940²¹⁷. Additionally, though the consumption of synthetic cannabinoids is increasing²¹⁸, the use of cannabis and isolated phytocannabinoids is far more common. Many phytocannabinoids exhibit unique pharmacological profiles that target both canonical CB1 and CB2 endocannabinoid receptors as well as other nonclassical endocannabinoid targets²¹⁷. Accordingly, expanded studies on the age-dependent effects of cannabis-derived compounds such as THC and non-psychoactive constituents like CBD and terpenes are now greatly needed.

Rising healthcare costs coupled with the increased availability of cannabinoid-based substances marketed as therapeutics have put elderly patients in a particularly vulnerable position. Although aging phenotypes in humans and rodents are multifaceted and exceedingly diverse, reduced physical activity, sleep disturbance, and chronic pain are some of the most commonly reported conditions reported in advanced age. The present study indicates that in mice, the synthetic cannabinoid CP55940 exhibits bidirectional and behavior-specific effects that are greatly influenced by the age of the subject. Therefore, additional studies are required to discern the mechanistic basis for this increased responsiveness in aged rodents and to determine whether these age-dependent effects are species and/or compound-specific. In the wake of rapidly shifting

policies affecting access to cannabinoids worldwide, additional preclinical evidence in aged models will be vital to anticipate potential effects these substances may have on aging populations.

METHODS

Animals

All procedures were approved by the University of Mississippi Institutional Animal Care and Use Committee (IACUC). Experimental cohorts consisted of two age groups: 2-4 months (young) and 21-24 months (old) of age. Experiments were performed on male and female C57BL/6NHsd mice acquired from Envigo (Cat.#: 044) or C57BL/6 mice from the National Institutes of Aging Aged Rodent Colony. A priori power analysis indicated that statistically significant differences based on a medium effect (Cohen's $f > 0.25$) could be detected with group sizes $n \geq 10$. The total number of animals used for this study is listed in **Figure 2.8**. All animals were housed in the AALAC-accredited University of Mississippi Animal Facility and given access to food (Cat.#: 7001, Envigo Teklad 4% Fat Rodent Diet) and tap-water ad libitum for the duration of experiments. Mice were group-housed (4 mice/cage) in climate-controlled rooms (30-40% relative humidity, 21-23°C) under a 12:12 'reverse' light cycle (lights OFF at 8:00am and ON at 8pm). Upon arrival into the facility, animals were immediately group-housed in 75 in² clear polycarbonate cages (Cat.#: AN76, Ancare) with 1/8" corn cob bedding and environmental enrichment (Cotton Nestlets, Ancare, and Crink'l Nest, The Andersons Lab Bedding) then allowed to acclimate to the facility for 7 days before experimentation. Following this week of acclimation animals were weighed, fitted with a metal ear-tag (Cat.#: INS1005-1LSZ, Kent Scientific) and randomized into balanced experimental

treatment groups based on body weight. Mice were checked daily, and clean cages were replaced every week. All experiments and procedures were performed under dim red light (<1lux) during the animals' active cycle.

Blinding

The experimenter was blinded to all treatment groups during drug-administration and experimentation through the use of arbitrarily coded drug-containers.

Drugs, Dosing, and Administration

The synthetic cannabinoid CP55940 (Cat.#:0949, Tocris) was initially diluted in 100% ethanol (Cat.#:2701, Decon Labs) to a stock concentration of 10mg/mL and kept at -20°C. The CB1 antagonist, AM251 (Cat.#:1117, Tocris) was initially diluted in 100% ethanol (Cat.#:2701, Decon Labs) to a stock concentration of 10mg/mL and kept at -20°C. The CB2 antagonist, AM630 (Cat.#:1120, Tocris) was initially diluted in 66.6% ethanol (Cat.#:2701, Decon Labs) and 33.3% Dimethyl sulfoxide (DMSO, Cat.#: 276855, Sigma-Aldrich) to a stock concentration of 6.66mg/mL and kept at -20°C. On the day of each experiment, fresh vehicle solution was prepared by first dissolving Kolliphor EL (formerly known as Cremophor EL, Cat.#: C5135-500G, Sigma Life Science) in 100% ethanol, then adding sterile 0.9% HSP pH 7.4 saline (Cat.#: 00409488810, Hospira) in a ratio of (1:1:18). Experiments using AM251 or AM630 were performed by pre-mixing either AM251 or AM630 with respective doses of CP55940 prior to injection. All drug mixtures were administered at a volume of 1mL/100g body weight.

During testing, the animal's temperature and weight were recorded then a body weight-adjusted dose of vehicle or CP55940 was administered via intraperitoneal (IP)

injection using a 1mL syringe (Cat.# 309602, Becton, Dickinson and Company[BD]) and a 25 gauge needle (0.5 x 16mm, Cat.# 305122, BD).

Acclimation

On the day of behavioral testing, all animal cages were placed onto a plastic or metal cart and relocated to the testing room where they were allowed to acclimate for 3 hours prior to testing. Throughout the acclimation and testing periods, the room remained dark and white noise was continuously played at a volume of ~60db.

Body Weight

Body weight was measured at the start of every experimental procedure to ensure accurate drug administration and as an endpoint for exclusion in the event that an animal's mass decreased >10% in a week. Animals were gently removed from their cages by lightly gripping the base of their tail and placed into a lidless pipette-tip box on top of the balance. Once the animal ceased moving the mass was recorded. In between recordings, the pipette-tip box was wiped clean with ethanol, dried with a paper towel, and the balance was tared.

Rectal and Pelage/Surface Temperature

Rectal temperature was measured using a Digi-Sense Advanced Precalibrated Thermocouple Thermometer (Cat.#: EW-20250-91, Kent Scientific) which was connected to a 1.9cm x 0.165cm rectal probe (Cat.#: RET-3, Kent Scientific). Before measurement, the rectal probe was cleaned using 70% ethanol, dried, and lightly lubricated with petroleum jelly. Animals were briefly immobilized on the top of a metal cage lid, and then securely restrained by gripping the scruff (nape of the neck). After confirming the animal's identification/ear tag, the rectal probe was gently inserted 1.9cm

into the animal's rectum. Once a stable measurement was achieved (~3-5 seconds) the temperature was recorded.

Skin/pelage temperature was measured via infrared thermography at the dorsal pelvis using a FLIR Non-Contact Infrared Spot Thermal Camera (Cat.#: TG165, FLIR). Emissivity was set to 0.85, as suggested previous research²¹⁹. Immediately after weighing, while the animal was standing still and upright in an empty pipette-tip box, the thermal camera was held directly above the animal exactly 10cm away from the animal's skin. Once a stable measurement was achieved (~3-5 seconds) the temperature was recorded.

Locomotion - Open Field

Locomotor activity was measured by placing a single mouse into a lidless clear-plastic open field arena (41x41x38cm), which was surrounded by a 16x16 photobeam array (Photobeam Activity System, San Diego Instruments) or recorded using a ceiling-mounted camera. Locomotion in the X and Y directions were quantified using beam breaks or software-based tracking (Ethovision XT-13, Noldus). During recording four open field arenas were used simultaneously, and each arena was shielded on three sides by 60cm black plastic dividers so that animals could not see each other. When administered at high doses, the psychoactive effects of CP55940 are pronounced from 10-120 minutes. Thus, locomotor activity was measured continuously for 30 minutes, beginning 30 minutes after drug or vehicle injection. Beam breaks in the X and Y directions were sampled every 5 seconds for 30 minutes and then exported to spreadsheets at the conclusion of testing. Peripheral locomotion was defined as any locomotion which occurred in the outermost 50% of the open field arena. After removal

from the open field, animals were briefly (1-5 minutes) placed into temporary cages before testing on the hot plate.

Nociception - Hot Plate

Nociception was measured by placing a single mouse on top of a preheated 52°C thermal block (Cat.#: PE34, IITC Life Sciences), and recording the latency to withdraw and/or lick their hind-paws. During testing, a hollow clear-plastic cylinder 25cm in diameter by 35cm high was placed on top of the heated thermal block to prevent animals from leaving the hot plate. Animals were placed in the cavity of the plastic cylinder directly in contact with the hot plate and closely monitored for phenotypic responses of nociception. Based on preliminary experiments, we concluded that the latency to lick the hind paws was the most reliable indicator of nociception. Immediately after licking their hind-paws, the timer was stopped and the animal was removed from the hot plate and placed back into a temporary cage. If an animal failed to respond to the thermal stimulus in 45 seconds, the timer was stopped and the animal was rapidly removed from the hot plate to prevent tissue damage.

Nociception - Hot Water Tail Withdrawal

Several cohorts of male and female mice were also tested using a hot-water bath preheated to 46°C. After testing on the hot plate, animals were allowed a 90s recovery period, then gently scruffed by the nape of the neck and their tails were dipped 1/3 from the tip into heated water. The latency to withdraw the tail was manually recorded using a stopwatch.

Gene Expression - qPCR

Cortical, hippocampal, and hypothalamic RNA was isolated using the RNA-easy mini kit (Qiagen) and converted to cDNA using High-Capacity RNA-to-cDNA kit (Applied Biosystems). RT-PCR was performed using TaqMan Universal PCR Master mix (Life Technologies) and TaqMan validated primers (Mm01212171_s1 (Cnr1), Mm02620087_s1 (Cnr2), Mm01187898_m1 (Cnrip1), Mm00515684_m1 (FAAH), Mm03024075_m1 (HPRT), Mm99999915_g1 (GAPDH)) on the CFX Connect Real time PCR detection system (Bio-Rad). Results were normalized to the housekeeping gene HPRT. The experimenter was unaware of age group during testing and was unblinded during delta-delta CT analysis.

Experimental Timeline

After ear-tagging and enrollment into treatment groups, a 6-day acclimation period was begun. Initially, animals were acclimated for 3 days to handling, weighing, and temperature measurement with the rectal probe and IR camera. Next, the animals were acclimated for 3 days to all of the previous procedures, as well as IP injection of vehicle (1:1:18, Ethanol:Kolliphor EL:Saline) and a follow-up 60m temperature recording after the initial injection. Drug administration and behavioral experiments were performed on the 7th day. In the event of repeated testing such as the AM251 and AM630 studies (**Figure 2.7**), animals were left undisturbed for 7 days between rounds of testing. Subsequent rounds of testing used only a 3-day acclimation period, wherein the animals receive vehicle injections and 60m follow-up temperature recordings.

Data Analysis, Statistics, and Exclusions

Data analysis was performed, collected, and analyzed using a combination of Microsoft Excel (v2016, Microsoft), RStudio (v.1.1.456, RStudio Team), MATLAB (r2019a, MathWorks), PAS (v2.0.3, San Diego Instruments), PAS Data Reporter (v1.0.1.0, San Diego Instruments), Ethovision XT (v13, Noldus), and G*Power (v3.1,²²⁰).

Prior to omnibus testing, all data for a given measurement was tested for outliers, which was defined as those points that were greater or less than three interquartile ranges above or below the 3rd and first interquartile ranges within a single treatment group. After exclusion of these points, data from each measurement were assessed for a normal distribution (Shapiro-Wilk test) and equal variance (Levene test). Since all measures observed failed these tests, simple main effects and interactions were assessed using the non-parametric Scheirer-Ray-Hare (S-R-H) test. A priori significance was set at $\alpha=0.05$. Significant main-effects detected in S-R-H tests were followed by additional post-hoc testing using Dunn's many-to-one method, which is ideal for comparing multiple dose-responses to vehicle/control treatments. The false discovery rate was corrected for using the Benjamini, Hochberg, and Yekutieli method. Additionally, notes regarding injection performance (by the experimenter) were kept during all procedures and were the primary determinant for other exclusions. To mitigate the effects of repeated testing, such as in the case of animals presented in Figure 2, data in this figure have been normalized to the responses of vehicle-treated animals that were tested at the same time.

FIGURES

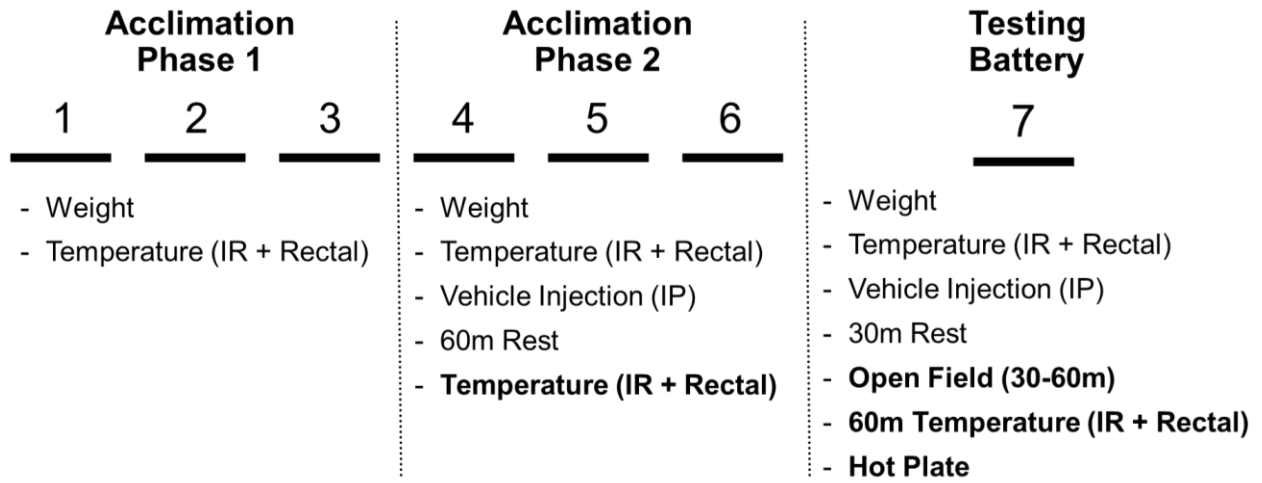


Figure 2.1: Experimental timeline.

Measure	Baseline Weight				Baseline Rectal Temperature				Change in Rectal Temperature				Baseline Skin/Pelage (IR) Temperature				Change in Skin/Pelage (IR) Temperature			
	Male		Female		Male		Female		Male		Female		Male		Female		Male		Female	
	Young	Old	Young	Old	Young	Old	Young	Old	Young	Old	Young	Old	Young	Old	Young	Old	Young	Old	Young	Old
Mean	27.77	32.81	22.62	27.81	37.24	36.86	37.49	36.88	-0.17	-0.28	-0.18	-0.11	30.43	29.94	30.75	29.54	-0.30	-0.12	-0.34	-0.03
S.E.M.	0.06	0.12	0.10	0.21	0.02	0.03	0.04	0.04	0.02	0.04	0.04	0.06	0.03	0.06	0.06	0.06	0.03	0.04	0.06	0.07
n=	655	510	144	144	655	510	144	144	655	510	144	144	655	510	144	144	654	510	144	144

Figure 2.2: Baseline measures during vehicle acclimation.

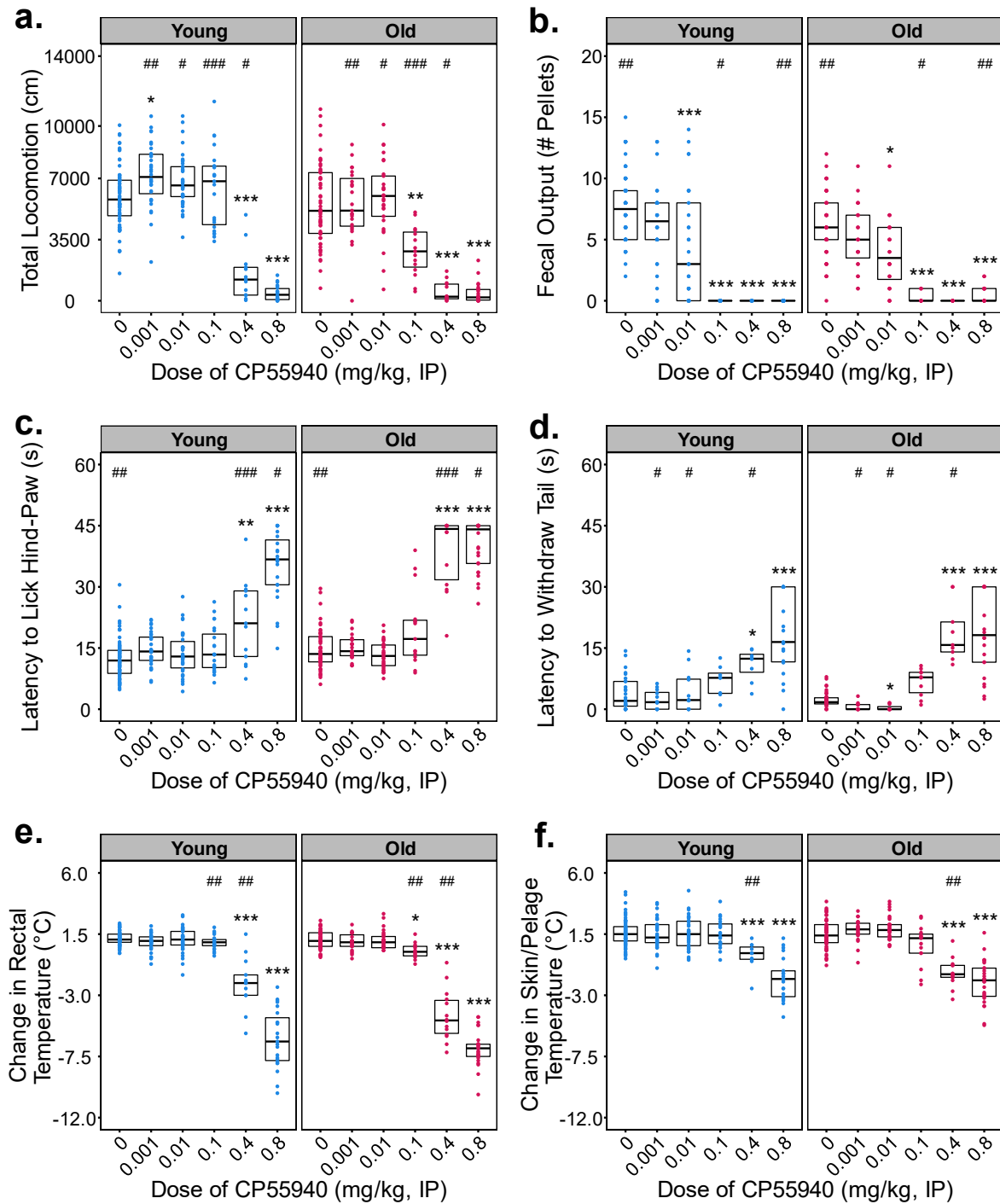


Figure 2.3: Effects of CP55940 on locomotion, thermoregulation, and nociception in young-adult (4m) and old (22m) C57BL6 mice.

CP55940 was administered via intraperitoneal injection at doses ranging from 0.001-0.8 mg/kg to young and old male and female mice. Individual data points for each testing group are overlaid on Tukey-style boxplots. The lower and upper edges of each box represent the first and third quartiles, respectively. The middle horizontal line in each box depicts the median of that dose/age group. Sample sizes for every treatment group and figure panel are listed in **Figure 2.8**. Statistical comparisons of Age, Dose, and Age:Dose interactions were made using the non-parametric Scheirer-Ray-Hare test. Significant omnibus results were followed by planned post-hoc contrasts of each dose vs. vehicle-treated control groups using Dunn's method. The false discovery rate was corrected for using the Benjamini, Hochberg, and Yekutieli method. Within an age group, significant differences ($p < 0.05$) between a given dose and the vehicle response (0 dose) are indicated using asterisks (*). Differences between age groups at a given dose are indicated by pound signs (#).

Panels A-B) Total locomotion and fecal output during Open Field testing, 30-60 minutes after injection of CP55940 or vehicle.

Panel C) Latency to exhibit nociceptive behavior when placed on a 52°C Hot Plate.

Panel D) Latency to withdraw the tail from 46°C water.

Panel E) Change in rectal temperature 60m after injection of drug.

Panel F) Change in infrared recording of skin/pelage temperature 60m after injection of drug.

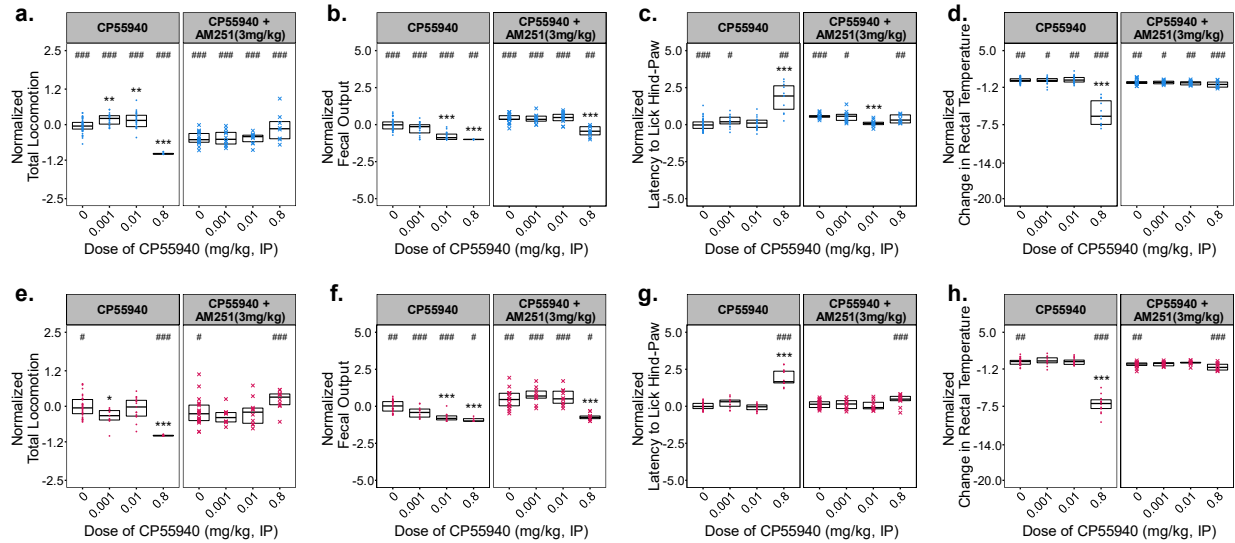


Figure 2.4: Behavioral and physiological effects of CP55940 co-administered with the CB1 inverse agonist AM251 in young-adult (4m) and old (22m) male C57BL6 Mice. Varying doses of CP55940 were administered alone or in a pre-mixed solution with 3mg/kg of AM251 Individual data points for each testing group are overlaid on Tukey-style boxplots. The lower and upper edges of each box represent the first and third quartiles, respectively. The middle horizontal line in each box depicts the median of that dose/age group. Sample sizes for every treatment group and figure panel are listed in **Figure 2.8**. Significant omnibus results were followed by planned post-hoc contrasts of each dose vs. vehicle treated control-groups using Dunn's method. The false discovery rate was corrected for using the Benjamini, Hochberg, and Yekutieli method. Within an age group, significant differences ($p < 0.05$) between a given dose and the vehicle treated response (0 dose) are indicated using asterisks (*). Differences between CP55940 alone and CP55940+AM251 at a given dose are indicated by pound signs (#). **Panels A-D)** Behavioral and physiological responses of young adult (4m) male mice. **Panels E-H)** Responses of old (22m) male mice.

Cortex	n	CB1 ± SE	CB2 ± SE	CRIP1 ± SE	FAAH1 ± SE
Young	6	1.01 ± 0.06	1.03 ± 0.09	1.07 ± 0.18	1.02 ± 0.10
Aged	5	0.81 ± 0.05	0.82 ± 0.12	0.65 ± 0.08	0.59 ± 0.04
		*p=0.04	p=0.19	p=0.08	*p=0.004

Hypothalamus	n	CB1 ± SE	CB2 ± SE	CRIP1 ± SE	FAAH1 ± SE
Young	6	1.01 ± 0.06	1.4 ± 0.64	1.01 ± 0.06	1.00 ± 0.03
Aged	5	0.60 ± 0.15	3.13 ± 1.12	1.11 ± 0.12	0.78 ± 0.11
		*p=0.02	p=0.19	p=0.44	p=0.07

*p ≤ 0.05 t-test, Young vs Aged

Table 2.1: Quantitative-PCR analysis of gene-expression in regions of brain tissue from young-adult (4m) and old (22m) male mice.

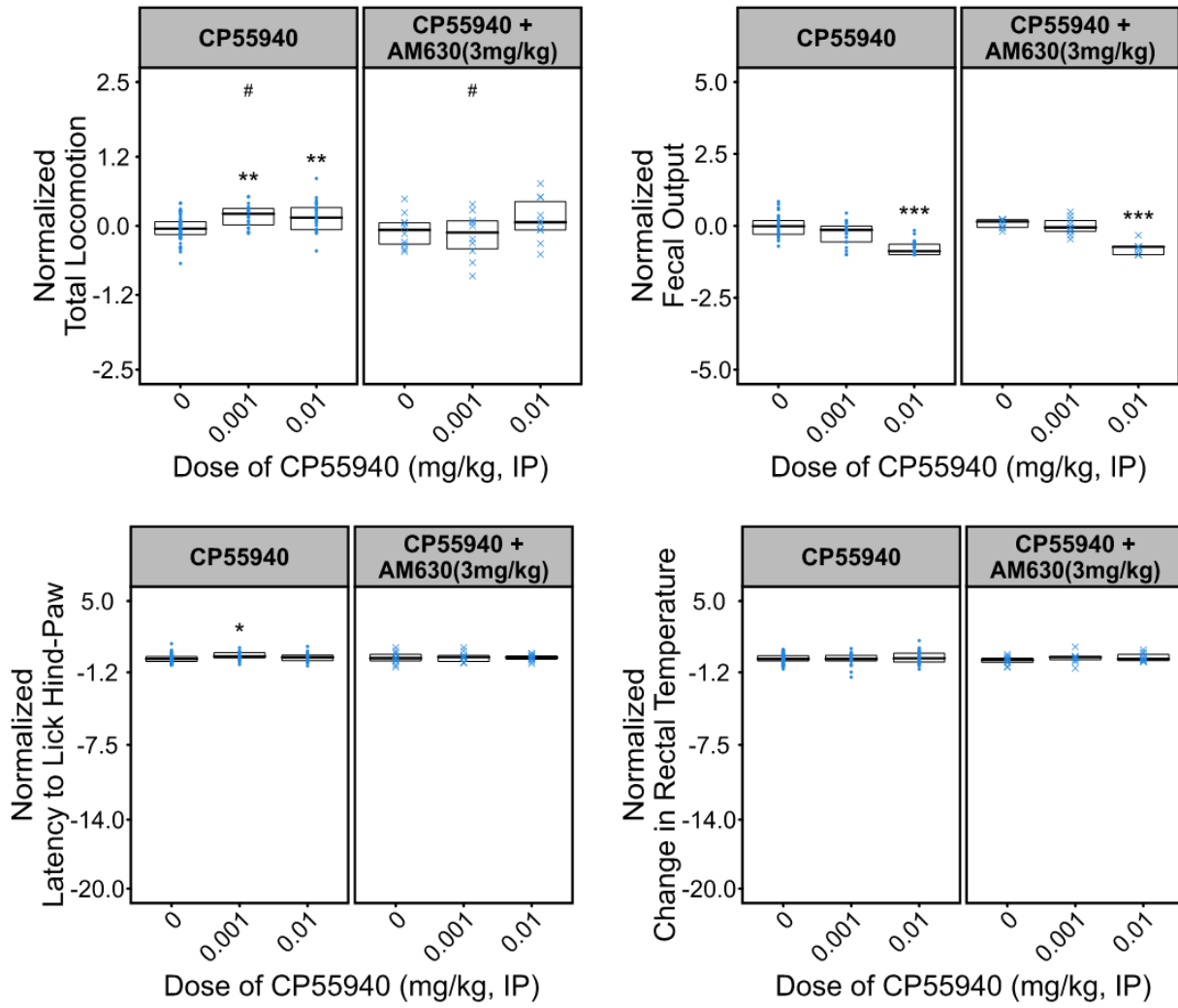
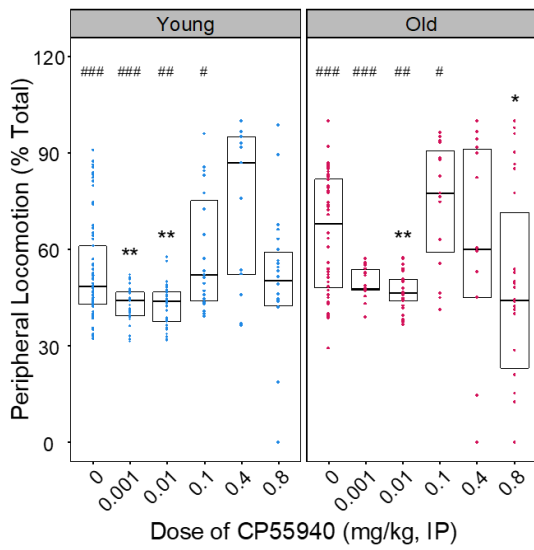


Figure 2.5: Effects of CP55940 and AM630 coadministration in young males.

Young and Old Male and Female



Young Males

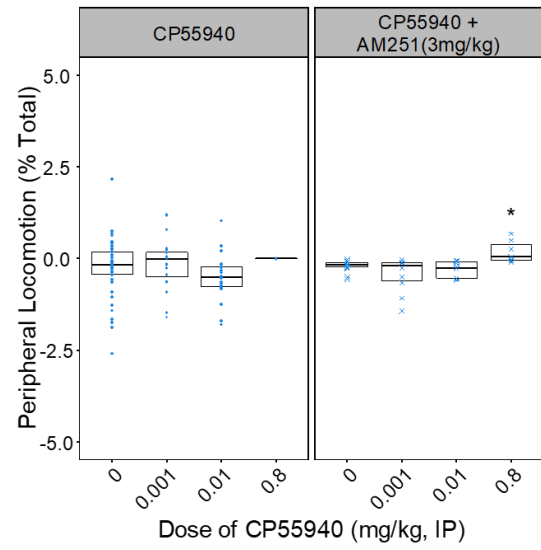


Figure 2.6: Effects of CP55940 on peripheral locomotion in the open field.

Total Animals for All Experiments		
Age	Sex	n=
Young	Male	125
Young	Female	28
Old	Male	60
Old	Female	21

Data in Figure 2 is expressed as % of vehicle treated control (tested on same day)

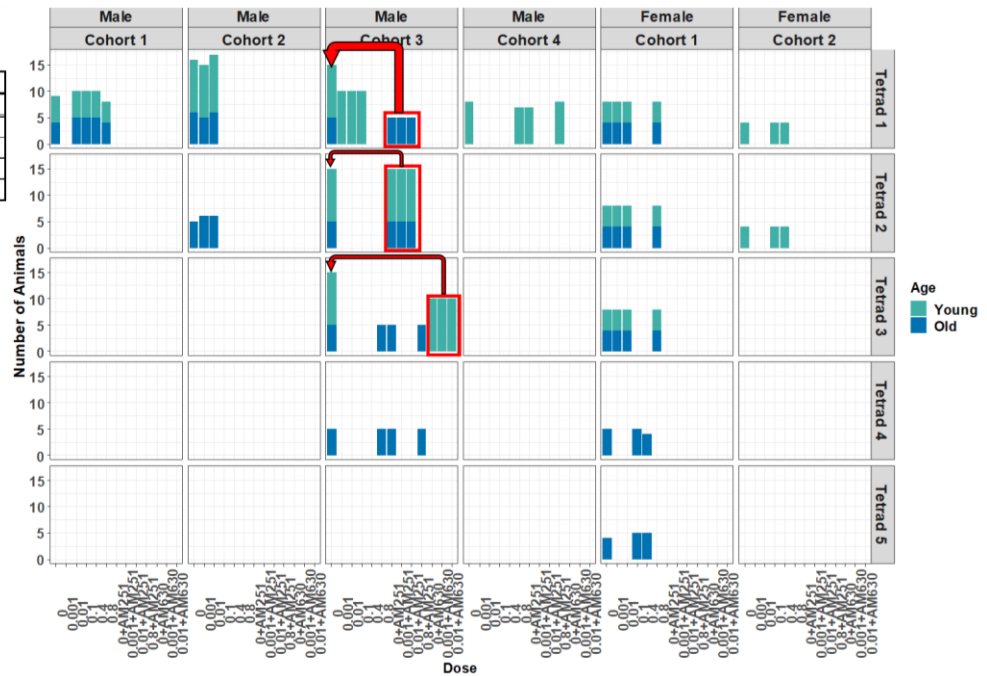


Figure 2.7: Animal cohorts and experiments

Sample Sizes in Figure 2.3													
Dose	Sex	Distance_30m_Total		Fecal_Output		Pain_Latency_Hot_Plate		Pain_Latency_Tail_Water		Temp_Rectal_Change		Temp_IR_Change	
		Young	Old	Young	Old	Young	Old	Young	Old	Young	Old	Young	Old
0	All	73	56	68	52	73	56	28	40	73	56	71	56
0.001	All	32	23	32	23	32	23	12	12	32	23	32	22
0.01	All	38	29	33	24	38	29	12	11	38	28	35	29
0.1	All	23	15	15	9	23	15	8	10	23	13	20	15
0.4	All	13	13	8	7	13	14	8	9	13	14	11	14
0.8	All	22	26	17	21	23	26	19	22	23	25	21	26

Sample Sizes in Figure 2.4																	
Measure		Distance_30m_Total				Fecal_Output				Pain_Latency_Hot_Plate				Temp_Rectal_Change			
Dose Group	Sex	CP55940 Alone	CP55940+ AM251	CP55940 Alone	CP55940+ AM251	CP55940 Alone	CP55940+ AM251	CP55940 Alone	CP55940+ AM251	CP55940 Alone	CP55940+ AM251	CP55940 Alone	CP55940+ AM251	CP55940 Alone	CP55940+ AM251	CP55940 Alone	CP55940+ AM251
		Young	Young	Old	Old	Young	Young	Old	Old	Young	Young	Old	Old	Young	Young	Old	Old
Male	0	51	17	35	20	48	17	31	20	53	14	35	20	53	17	35	18
Male	0.001	20	10	11	10	20	10	11	10	20	10	11	10	20	10	11	10
Male	0.01	26	10	17	10	21	10	12	10	26	10	17	10	26	10	17	9
Male	0.8	10	8	12	10	7	8	10	10	11	8	14	10	11	8	14	10

Figure 2.8: Sample sizes.

CHAPTER 3:
CANNABINOIDS AS CHRONOBOTICS IN AGING MICE

ABSTRACT

A growing number of geriatric patients are seeking cannabinoid-based substances for relief from age-related ailments such as poor sleep, low energy, and chronic pain. Despite this increased demand for cannabinoid-based therapeutics, preclinical evidence of these compounds' efficacy safety in aged subjects is limited. The current lack of preclinical studies in aged models and rapidly growing access to cannabinoid-containing substances has placed elderly patients particularly at-risk. Furthermore, a growing body of evidence suggests that the dose-response to exogenous cannabinoids is bidirectional in young animals but not in aged subjects. A critical limitation of previous studies is their relatively short duration, which precludes the ability to assess multi-day effects of these compounds. To address these gaps in knowledge, the present study examined the effects of age, sex, and treatment with varying doses of the synthetic cannabinoid CP55940 on circadian rhythms of locomotion in mice. Voluntary free wheel running behavior was monitored under normal lighting (12:12, LD), constant darkness, and also with doses of CP55940 ranging from 0.001mg/kg to 0.1mg/kg, IP. Significant effects of both age, sex, and dose of CP55940, as well as interactions among these variables were observed. Dose-dependent changes in running behavior were observed on the day of cannabinoid treatment, as well as

Age:Sex and Dose:Sex in the time of activity onset on the day after treatment.

Together, these data reinforce our previous findings that cannabinoids exert age-dependent effects and establish a strong baseline for future studies aimed at testing potential chronobiotics in young and aged animals.

INTRODUCTION:

The cyclic pattern of Earth's rotation on its axis and revolution around the sun has intimately shaped many aspects of biology. Though many of these biological rhythms are now known to be regulated by the daily light cycle, those physiological rhythms which persist in the absence of light are known as circadian rhythms. Throughout much of the mammalian lifespan these ~24-hour physiological rhythms are widely present and readily observable at numerous observational scales (molecular, cellular, behavioral, etc.). At the biomolecular level, circadian rhythms of body temperature dictate system enthalpy and, as a consequence, nearly all thermodynamically reliant biochemical reactions. At the genetic level, the well-characterized circadian transcription and translation of 'clock' genes intricately regulates numerous aspects of cellular physiology. In mammalian organs and tissues, consistent rhythmic production of growth hormone, cortisol, and other endocrine modulators is vital for proper growth, development, and function. Circadian patterns of behavioral activity integrally shape organisms' adaptation and evolutionary fitness within an ecosystem. Collectively, these biologically pervasive rhythms are critical determinants of organisms' survival.

The causal regulation of lifespan by circadian physiological rhythms is intuitive but the quantification and assessment of this relationship remains elusive. Though the

study of these two intricately related processes predates modern science, technical limitations have historically hindered scientists to making only qualitative descriptions of their relationship. *Mus musculus* (house mouse) is the most widely utilized mammalian model in aging research, and our rich understanding of this species' circadian genetic, physiological, and behavioral characteristics is ideal for assessing pharmacological interventions. This established wealth of knowledge is vitally important to intellectually frame the observed outputs from these complex and dynamic biological systems. Recent technological advances now permit the acquisition and analysis of such high-dimensional (multivariate) data which may help to describe the organization and behavior of many previously intractable biological processes.

Measures of circadian physiology such as locomotor activity, sleep/wakefulness, and core body temperature are all regulated by rhythmic neuronal activity generated by cells in the suprachiasmatic nucleus of the hypothalamus (SCN)^{37,38,74}. The amplitude of these neuronal rhythms, as well as measures of behavioral and physiological outputs, are reduced in advanced age⁷⁵. Older subjects also exhibit impaired thermogenesis which may explain why peripheral tissues, whose rhythms are determined by changes in body temperature, display impaired synchronization with age^{66,69}. Voluntary wheel running (VWR), also known as spontaneous wheel running, is a well-established and commonly reported measure of circadian locomotion in rodents^{21,30}. When presented with a running wheel, mice, rats, hamsters, and many other species of animals will voluntarily run. In the laboratory setting, quantification of this activity reveals circadian patterns which correlate to the animal's sleep/wake cycle and can be used as a

surrogate measurement for the intrinsic physiological processes now known to regulate this behavior.

Therapeutically, drugs which influence circadian physiology are known as chronobiotics (e.g. melatonin) and are used to shift or amplify endogenous circadian rhythms and reduce dissonance with environmental conditions⁵⁴. Both cannabinoid receptor-1 (CB1) transcript and protein are present in the SCN, and direct application of CB1 agonists alters the activity of these neurons. Given that sleep, body temperature, locomotion, and other daily physiological rhythms are primarily generated by neuronal activity in the suprachiasmatic nucleus, the presence of CB1 in these cells supports a role for endocannabinoids in circadian rhythm regulation¹¹². Although preclinical and human studies overwhelmingly report deleterious outcomes on cognitive performance resulting from chronic high levels of cannabinoid-exposure early in life, several studies indicate that these memory-impairing effects are dose-, age-, and sex-dependent^{97,128,134,141,143,191,192}.

CB1 agonists induce profound hypothermia and hypolocomotion at high doses in preclinical rodent models, though several investigations have reported increased body temperature and locomotion following treatment with much lower doses^{171,173,174}. One explanation for these disparate reports is that exogenous cannabinoids exhibit hormesis; that is, low-doses of these compounds produce the opposite effects of high-doses. Mechanistically, the effects of higher doses appear to be mediated in-part by CB1 signaling in GABAergic neurons, although this may not be the case for all behaviors¹⁶⁸. Since neuronal activity in the SCN determines central clock rhythms, and peripheral cellular clocks are entrained by thermic signals, pharmacological

interventions like cannabinoids may provide a wide range of therapeutic potential due to their known influence on both neuronal activity and body temperature.

CP55940 bidirectionally modulates locomotion in mice (Chapter 2), however it remains to be shown whether this compound can dose-dependently increase and decrease VWR in mice. Additionally, previous studies of hyper- and hypo-locomotion caused by synthetic cannabinoid agonists have been limited to short periods of time (<6 hours) immediately following drug exposure. To address this, the current study permits the measurement of potentially multi-day behavioral effects resulting from a single exposure to CP55940.

The fundamental hypothesis of this work is that circadian locomotion is a macroscopic readout of intrinsic physiological function, and the pharmacologic restoration of age-dependent changes of behavioral endpoints will correspondingly mitigate the onset of age-related pathology. To this end, the goal of this study was to explore a computationally-intense, quantitative approach to extract defined features that characterize circadian locomotion across the lifespan in mice. Our initial goal was to establish baseline measures of circadian locomotion by quantifying the age- and sex-dependent characteristics of rhythmic VWR in C57BL6 mice under normal lighting conditions and in constant darkness. Once these age- and sex- specific rhythms were quantified, separate cohorts of mice were administered varying doses of the synthetic cannabinoid CP55940, and the efficacy of this compound to influence measures of circadian locomotion was assessed.

RESULTS:

In order to test the hypothesis that cannabinoid agonists can modulate behavioral rhythms of spontaneous wheel running, we first sought to quantify baseline locomotor rhythms in young and aged male and female mice housed under normal (12:12, LD) lighting and constant darkness (00:24, DD). The use of these two lighting conditions was used to understand potential baseline differences among the age and sex groups which may only be present in the absence of light entrainment. Light is a profound regulator of mammalian locomotor rhythms; therefore, the presence of light can mask intrinsic 'free-running' locomotor rhythms³⁴. Mice were group housed prior to wheel running and kept in a dedicated room with 'reverse' lighting - 12 hours of darkness, beginning at 8am (ZT hour 12), followed by 12 hours of light beginning at 8pm (ZT hour 0). On the first day of testing during the animals' active (dark) cycle, mice of a single age/sex group (n=11-12) were weighed then individually housed in cages containing remotely monitored running wheels. Mice were then left undisturbed for 7 days under normal lighting conditions (**Fig. 3.1A**) and wheel rotations per minute were recorded.

At the end of 7 complete days, a customized light-proof breathable cage-rack cover was placed over all cages. Mice were then left undisturbed, in constant darkness, for an additional seven days of recording. Running wheel activity of each age and sex group during normal lighting and constant darkness has been summarized in **Figure 3.2**. Under normal lighting conditions, all mice exhibited a clear entrainment to the lights, as evidenced by their consistent waking time shortly after lights-off (Zeitgeber Time [ZT Minute 720, ZT Hour 12]) and periods of activity very near to 24 hours (**Fig. 3.2E-H**). During normal (12:12) lighting, there were no significant differences between the Lomb-Scargle computed periods of any age/sex groups. However, under constant darkness a

significant interaction of Age:Sex was detected (2-way ANOVA, DD_Period ~ Age * Sex, Age:Sex, $p < 0.001$). Interestingly, post hoc analysis revealed that young males' (YM) circadian periods were not different from those of old males (OM), but the periods of YM were significantly shorter than those of young females ($p < 0.001$). Additionally, the circadian periods of young females (YF) were significantly longer than those of old females (OF, $p < 0.001$); though no sex specific differences were observed in aged male and female circadian periods.

In addition to quantifying the period, we also quantified total locomotion as well as the timing of activity onset and offset. Quantification of this baseline activity revealed that YM and YF mice exhibited sustained activity while the lights remained off, though male mice at both age groups had substantially lower RPMs than age-matched females. OM mice exhibited the lowest average daily activity, totaling only 11,925 ($\pm 1,301$) total rotations compared to 42,7681 ($\pm 1,259$) total rotations by YF under normal lighting conditions (**Fig. 3.3J**). YM averaged more daily activity than OM ($p < 0.001$) under normal lighting and in constant darkness (**Fig. 3.3J-I**, $p < 0.001$). Similarly, YF averaged more daily wheel rotations than OF in normal lighting as well as constant darkness (**Fig. 3.3J-I**, $p < 0.001$). All age groups averaged more activity during constant darkness; however, the change in activity from normal lighting to constant darkness was significantly higher in old females (OF) compared to OM (**Fig. 3.3L**, $p < 0.01$).

The timing of activity onset and offset were defined as the first 10-minute period of average wheel running that exceeded 20% of that age/sex group's daily maximum. Using this threshold, we observed that under normal lighting conditions YM, YF, and OF all had prompt activity onset following lights off, but OM were significantly slower to

reach the activity onset threshold (**Fig. 3.3A**). Under constant darkness, we observed a significant Age:Sex interaction, wherein YM, OM, and OF mice all began to advance their circadian phases and began running earlier in the day than when housed under normal lighting (2-way ANOVA, Age:Sex, $p=0.001$). In contrast, YF mice remained remarkably consistent following the transition from normal lighting to constant darkness and were significantly different than young males ($p<0.01$, **Fig. 3.3C**). Substantially greater variability across all groups was seen in the timing of activity offset, even under normal lighting conditions (mean onset LD [730±6.0 minutes], mean offset DD [1286±24.8 minutes], **Fig. 3.3D**). Young male and female mice had significantly later offsets of activity than older mice during normal lighting (**Fig. 3.3D**). Nevertheless, a profound effect of age was observed when we quantified the timing of activity offset during LD and DD, with older animals ceasing activity significantly earlier than young mice ($p<0.001$, **Fig. 3.3D-E**). On average, YF had the latest activity offsets and were significantly later to stop activity in DD than young males ($p<0.05$, **Fig. 3.3E**).

To account for the varying shifts in both onset and offset, we quantified overall duration of activity by subtracting the time of activity onset from the time of activity offset (**Fig. 3.3G**). Under both normal lighting and constant darkness, YM and YF groups had longer durations of activity than OM and OF groups ($p<0.01$) though there were no significant differences between the sexes in either age group (**Fig. 3.3G-H**). Despite this, the change in duration of activity from normal lighting to constant darkness was greater in young mice compared to old mice. To our surprise, substantial heterogeneity in onset and offset timing was observed among animals of the same age/sex when transitioning from LD to DD. **Table 3.1** qualitatively categorizes these differences, based

on whether individual animals advanced or delayed their respective time of onset or offset by ± 15 minutes. In DD, the majority of YM and OM advanced their phases. In contrast, while all of the OF mice were phase advanced, YF tended to onset and offset activity later (Fisher's Exact Test, YF:OF, $p = 0.006$, **Table 3.1**).

After completing the baseline recordings, cohorts of naïve young and old male and female mice were used to assess the ability of the synthetic cannabinoid CP55940 to alter locomotor rhythms (**Fig. 3.1B**). In these experiments, mice were exclusively housed under normal lighting (12:12, LD) and allowed to acclimate to single-housing and wheel-running for 14 days prior to drug treatment. Beginning 30-60 minutes after lights off on the 15th day (8:30-9:00am, ZT hour 12.5-13), animals were administered a single intraperitoneal injection of either vehicle (1:1:18, ethanol:Kolliphor:saline) or one of three doses of the synthetic CB1/CB2 agonist, CP55940 (0.001mg/kg [Low], 0.01mg/kg [Med], 0.1mg/kg [High]). Following injections of the synthetic CB1/CB2 agonist, animals were returned to their cages and allowed to freely run for 72 hours before receiving the next of the 3 remaining doses. Ordering of the dose-administrations was randomized based on a Latin-square experimental design.

3D and 2D representations of each age/sex/dose group's average activity on the days before, during, and after each injection are shown in **Figures 3.4, 3.5, and 3.6**. In **Figures 3.4 and 3.5**, "Day of Running 1" was the day before drug injection, "Day of Running 2" is the day of drug administration, and "Day of Running 3" is the day after drug injection. Obvious depressions in locomotor activity can be visually observed with these 3D representations when the mice are treated with 0.1mg/kg CP55940. Additionally, the middle row of **Figure 3.6** clearly depicts the sustained locomotor

effects of CP55940 at different doses on the day of injection. Since most behavioral assays of cannabinoid-mediated effects do not assess behavioral changes beyond 1-2 hours following drug administration, we quantified CP55940-induced changes in locomotion at three different time scales: 1-hour post injection, 1-6 hours post injection, and 6-12 hours post injection (**Figure 3.7**).

Figure 3.7A summarizes total voluntary wheel running during the hour immediately following drug administration. In this short time-period, we observed significant simple main effects of Dose, Age, and Sex ($p=0.023$, $p<0.001$, $p=0.003$, respectively). When compared to vehicle-treated control mice, the highest dose of CP55940 tested (0.1mg/kg, IP) uniquely suppressed wheel-running in the aged mice (**Fig. 3.7A**). However, when activity throughout the first 6 hours after injection were summed, we also observed significant hypolocomotion in YM as well as both sexes of older mice (**Fig. 3.7B**). We also examined wheel running from 6-12 hours post injection to determine whether the hypolocomotion experienced early in the animals' subjective day would be compensated for by additional running in the subjective evening. We observed significant main effects of Age, Sex, and Dose on wheel counts from this time frame (**Fig. 3.7C**). Post hoc analysis of the 3-way ANOVA indicated that the high dose of CP55940 (0.1mg/kg) significantly increased wheel running 6-12 hours post injection across both ages and sexes compared to vehicle treated mice, though no significant interactions between Age, Sex, and Dose were detected ($p=0.009$, **Fig. 3.7C**). This suggests that while 0.1mg/kg CP55940 leads to hypolocomotion in the first few hours following administration, the animals compensate with increased activity later in the day.

Indeed, when the entire 24-hour day was analyzed, no differences in total wheel rotations were observed.

To test whether the short-term reductions in locomotion immediately following CP55940 administration were compensated by higher levels of total running during the animals' subjective evening or if this hypolocomotion persisted to the next day, we quantified the time of activity offset on the day of injection and the animals' time of activity onset on the following morning (**Fig. 3.8**). Significant main effects of Age and Sex were detected in both the time of activity offset on injection day, revealing that young mice are active later than old mice and male mice are active later than female mice ($p < 0.01$, $p < 0.001$, **Fig. 3.8A**). However, when we compared the time of activity offset on injection day to the time of offset on the prior day, this significance was not dependent on Age, only Sex ($p < 0.05$, **Fig. 3.8B**). Similarly, overall running duration on the day of injection was longer in young mice, and male mice had longer running durations than females ($p < 0.001$, $p < 0.01$, **Fig. 3.8C**). Again, when running duration was compared to activity on the day before injection, only a significant effect of Sex was detected ($p < 0.05$, **Fig. 3.8D**).

Finally, we wanted to know whether the effects of CP55940 administered during the animals' subjective morning had measurable effects on the following morning's time of activity onset. We observed a significant effect of Sex on the time of activity onset the day after injection, with female mice becoming active later than male mice ($p < 0.01$, **Fig. 3.8E**). When we compared the timing of activity onset to the day before injection, we observed significant Age:Sex and Dose:Sex interaction ($p = 0.003$, $p = 0.042$, **Fig. 3.8F**). OM had the largest shift in activity onset compared to the day before injection,

becoming active significantly earlier than all other age and sex groups ($p < 0.001$, **Fig. 3.8F**). However, the medium dose of CP55940 (0.01mg/kg, IP) significantly delayed activity onset in both young and old males.

DISCUSSION:

The experiments described here rigorously assessed the age-, sex-, and dose-dependent effects of the synthetic cannabinoid CP55940 on voluntary wheel running in mice. While much work has focused on understanding circadian biology and its influence on aging pathologies, few studies specifically seek to pharmacologically rescue these age- and sex-specific changes using wheel running as a read-out. As biological aging is marked by pronounced sex-specific phenotypes, the quantification of baseline age- and sex-differences in voluntary wheel running was a critical first step to determine the efficacy of our cannabinoid-based interventions. Both aged males and females showed similar reductions in total activity under “normal” 12:12 LD lighting compared to their younger counterparts. This is consistent with previous studies in humans and animal models showing that reduced locomotor activity is a common phenotype of advanced age^{34,221}. Mechanistically, the reduction in locomotor output with age is primarily attributed to decreased dopamine metabolism - rather than decreased levels in total dopamine²²². This is further supported by the finding that levodopa, a dopaminergic and adrenergic neurotransmitter precursor, is capable of restoring some age-related motor deficits in C57BL6 mice; though the effects of levodopa on VWR in the context of circadian locomotion are currently unknown²²³.

Although, under circadian-disrupting housing conditions (constant darkness), sex- and age-specific differences were observed. Young male, young female, and (to a

lesser extent) old male mice exhibit a truncated running duration (active period, α) when housed in constant darkness (**Fig. 3.3I**). In comparison, the remarkably consistent timing of activity onset and offset in young female mice suggests that this group is uniquely resilient to the phase-disrupting effects of constant darkness (**Figs. 3.2-3**). One possible explanation for the consistency observed in these young female mice is their intact estrous cycle. Female mice undergo estropause by 12 months of age, and the loss of these temporally consistent circulating hormones may serve to further disrupt central pacemakers in aged females. The extent of activity onset/offset shifting seen in the aged females (**Table 3.1**), coupled with significantly increased total activity in this group indicates that aging in female mice is associated with a loss of temporal pacemaker regulation, rather than a loss of overall pacemaker amplitude - as has been suggested in general models of circadian-aging^{42,74,224,225}.

Regarding the synthetic cannabinoid CP55940, short-term behavioral assays have demonstrated that this drug is capable of eliciting both stimulatory and inhibitory effects in a dose- and age-dependent manner. Similarly, both the phytocannabinoid THC and the synthetic cannabinoid WIN55212-2 acutely increase DA levels in the locomotion-regulating nucleus accumbens²²⁶. It is currently unclear whether cannabinoid-induced acute stimulation of dopaminergic neurons is sufficient to chronically alter circadian rhythms, since the actions of synthetic cannabinoids on neurons of the SCN are sensitive to GABA-A blockade¹¹². In addition to modulating the excitatory/inhibitory balance of neuronal activity in the SCN, cannabinoids may directly alter the rates of clock gene transcription via epigenetic modification. Though this putative effect has not been directly tested in neurons of the SCN, the chronobiotic

effects of cannabinoids might involve the long-term regulation of histone deacetylases (HDAC) such as HDAC3⁴⁵.

Here, we confirmed that not only are the effects of CP55940 bidirectional, our data also support the notion that high doses produce biphasic actions, such that when a high dose is given early during the subjective daytime there is a modest increase in activity during the subjective evening (**Fig. 3.7C**). It is not clear whether the evening rebound in locomotion is due to a prolonged increase in locomotor drive, or rather just the result of a delayed activity onset due to moderate-high doses of CP55940. To this end, it is vital that the duration of exposure be taken into consideration, and that extreme care is taken when extrapolating the behavioral effects of this compound beyond the initial day of treatment in subjects of different ages/sexes (**Fig. 3.8E-F**). The importance of tempering these extrapolations is perhaps most exemplified by the exacerbated effects seen in older, but not younger mice, at the dose of 0.1mg/kg, IP. Ultimately, the aforementioned effects of this cannabinoid on activity offset/onset following exposure offer additional testable hypotheses that can be explored in the context of the currently unexplained paradoxical effects induced by chronic low-dose cannabinoid treatment in aged animals^{176,182}.

The establishment of repeatable and rigorously defined thresholds for circadian locomotor rhythm quantification, as evidenced in the baseline LD:DD experiments, is a prerequisite to evaluating any potential chronotherapeutic. The use of a threshold based off of animals' maximum daily performance has been previously reported⁴². However, thresholding activity without considering the respective age and sex of the observed subject can hinder interpretation. Based on this, we set our threshold of 20% of animals'

daily maximum across all days in the running wheels. Daily variations in amounts of activity were observed across all animals throughout the experimental observation period. Therefore, it is possible that an individual mouse's activity was simply altered on the three-day analysis period independent of the treatment. We tried to control for this limitation by presenting the data both as the observed values and normalized to the day prior to drug administration. Although computationally intense, this method as well as thresholding based on each animal's daily performance may provide more repeatable, stringent quantification. Another potential limitation of this study is that a Latin Square design was used for the repeated CP55940 injections. While this approach allows all animals to receive all doses, it introduces a potential confound of molecular adaptations in response to previous cannabinoid exposure - as repeated exposure to high doses of cannabinoids can lead to changes in endocannabinoid machinery. To try and limit this, only 'low' doses of CP55940 were administered; the high dose of 0.1mg/kg falls well below the typical dosing of 0.5mg/kg CP55940 commonly used in the tetrad assay. Additionally, treatments were given three days apart to allow for drug wash-out.

Given that in the present study our measures of activity onset and offset resulting from either constant darkness or cannabinoid exposure were highly influenced by both age and sex. Future studies of chronotherapeutics must take these factors into consideration. Additionally, future studies of chronobiotics or other chronotherapeutics should consider employing analyses of both between-group differences as well as interindividual variability. Such analyses would not only clarify the immediate studies being presented, but also assist in the development of relevant preclinical models for personalized therapeutics. Taken together, these data indicate that aged mice are more

sensitive to the synthetic cannabinoid CP55940 than young mice, and additional studies clarifying these age- and sex-dependent mechanisms are warranted. Furthermore, these findings present an experimental framework for testing and evaluating the potential of chronobiotic, rhythm-restoring therapeutics.

METHODS:

Animals

All procedures were approved by the University of Mississippi Institutional Animal Care and Use Committee (IACUC). Experimental cohorts consisted of two age groups: 2-4 months (young) and 19-24 months (old). Experiments were performed on male and female C57BL/6NHsd mice acquired from Envigo (Cat.#: 044) or C57BL/6 mice from the National Institutes of Aging Aged Rodent Colony. All animals were housed in the AALAC-accredited University of Mississippi Animal Facility and given access to food (Cat.#: 7001, Envigo Teklad 4% Fat Rodent Diet) and tap-water ad libitum for the duration of experiments. Cohorts of mice were maintained in climate-controlled rooms (30-40% relative humidity, 21-23°C) using a 12:12 'reverse' light cycle (lights OFF at 8:00am [ZT hour 12, ZT minute 720] and ON at 8pm [ZT hour 0, ZT Minute 0]). Upon arrival into the facility, animals were immediately group-housed (4 mice/cage) in 75 in² clear polycarbonate cages (Cat.#: AN76, Ancare) with 1/8" corn cob bedding and environmental enrichment (Cotton Nestlets, Ancare, and Crink'l Nest, The Andersons Lab Bedding) then allowed to acclimate to the facility for 7 days before experimentation. Following this week of acclimation, animals were weighed, fitted with a metal ear-tag (Cat.#: INS1005-1LSZ, Kent Scientific) and randomized into balanced experimental treatment groups based on body weight.

Recording Spontaneous Wheel Running

During experimentation, mice were singly-housed in 33x15x13 cm clear polycarbonate cages (Cat.# 1144B001, Tecniplast) fitted with electronically monitored running wheels (PT2-MCR1, Actimetrics). Photoelectric sensors attached to each cage recorded wheel rotations and transmitted the data to a nearby desktop computer which was remotely monitored to limit unnecessary entries into the room. For the duration of each experiment (28 days, maximum) each wheel's rotations per minute were recorded using the ClockLab software (Actimetrics). Prior to beginning the experiment, each wheel was lubricated using a food-grade silicone spray (03040, CRC) and calibrated to ensure even resistance between wheels. Mice were checked daily, and clean cages were replaced every week. All experimental handling and procedures were performed under very dim red light (<1lux) during the animals' active period (lights OFF, ZT hour 12 through ZT hour 24/0).

Experimental Timeline

During baseline quantification of age- and sex- specific behaviors, mice were placed into the prepared running wheel cages and allowed to freely run for 7 days. Shortly before lights-on at the end of day 7, a custom-fabricated breathable light-proof fabric was used to cover the entire cage rack and eliminate light-associated cues. Mice were remotely monitored for seven additional days under constant darkness before being removed and returned with their original cage mates. Separate cohorts of animals were used to assess the chronobiotic potential of CP55940 and were tested only under normal lighting conditions (12:12, LD). For the CP55940 experiments, animals were allowed to freely run on the wheels for 14 days prior to drug administration. At the start

of the 15th day of running, immediately after the onset of animals' subjective active period (30-60 minutes after lights OFF, 8:30-9:00am, ZT hour 12.5-13) animals were briefly removed from their cages and administered one of four doses of vehicle or CP55940 via intraperitoneal injection before being immediately returned to their running wheel cages. Following the initial dose, animals were administered a new unique dose of vehicle or CP55940 every 72 hours until each animal had received all 4 doses.

Drugs, Dosing, and Administration

The synthetic cannabinoid CP55940 (Cat.#:0949, Tocris) was initially diluted in 100% ethanol (Cat.#:2701, Decon Labs) to a stock concentration of 10mg/mL and kept at -20°C. On the day of each experiment, fresh vehicle solution was prepared by first dissolving Kolliphor EL (formerly known as Cremophor EL, Cat.#: C5135-500G, Sigma Life Science) in 100% ethanol, then adding sterile 0.9% HSP pH 7.4 saline (Cat.#: 00409488810, Hospira) in a ratio of (1:1:18, ethanol:Kolliphor:saline). All drug concentrations were administered at a volume of 1mL/100g body weight. On the day of testing, immediately after the onset of animals' subjective active period (30-60 minutes after lights OFF, 8:30-9:00am, ZT hour 12.5-13) the animals' weights were recorded, then a body weight-adjusted dose of vehicle or CP55940 was administered via intraperitoneal (IP) injection. All injections were performed under very dim red light using a 1mL syringe (Cat.# 309602, Becton, Dickinson and Company[BD]) and a 25 gauge needle (0.5 x 16mm, Cat.# 305122, BD).

Body Weight

Body weight was measured at the start of every experimental procedure to ensure accurate drug administration and as an endpoint for exclusion in the event that

an animal's mass decreased >10% in a week. Animals were gently removed from their cages by lightly gripping the base of their tail and placed into a lidless pipette-tip box on top of the balance. Once the animal ceased moving the mass was recorded. In between recordings, the pipette-tip box was wiped clean with 70% ethanol, dried with a paper towel, and the balance was tared.

Data Acquisition, Quantification of Rhythms, and Statistical Analysis

Data were collected, processed, analyzed, and visualized using a combination of ClockLab (v3.60, Actimetrics), Microsoft Excel (v2016, Microsoft), RStudio (v.1.1.456, RStudio Team) and numerous R-packages²²⁷⁻²³⁹, MATLAB (r2019a, MathWorks), and Inkscape (v0.92.3). After the completion of all experiments, raw wheel counts were exported from ClockLab to comma-delimited files and imported to MATLAB for annotation and inspection. All wheel counts were annotated with the animal's age, sex, date and time of acquisition, and experimental treatment. In cases where spurious data points were identified due to sensor failures, pre-processing of the data was performed prior to analysis. In such cases, pre-processing involved identifying the timepoints of clearly spurious values (e.g. sustained wheel RPMs of >300 for several hours) were noted, and data values were replaced with 3-minute averages from exactly 24 hours before and after the noisy sections. All experiments began with n=12 running wheels, and recordings which contained spurious values in excess of 10% of the total recording were excluded from further analysis. During baseline (LD/DD) testing, one young male and one old males' recordings were excluded due to sensor failures. During CP55940 testing, three young male, 6 young female, 4 old male, and 4 old female recordings were excluded due to sensor failures.

After pre-processing of the data, surface plots of daily locomotion were produced in MATLAB for visualization of transitions from normal lighting to constant darkness (**Fig. 3.2-3.8**) as well as responses to CP55940 treatment (**Fig. 3.4-3.8**). Quantification of rhythm properties was accomplished using a combination of MATLAB and R, consisting of the following steps. First, a 10-minute moving-average was applied to each animal's raw wheel counts. Next, each animals' average daily rotations per minute (RPMs) were calculated. The minute-by-minute daily averages were then used to compute the Activity Onset and Activity Offset, which were defined as the first 10-minute period of time whose average values were greater or less than 20% of that animal's average daily maximum. Calculation of running period was accomplished by first generating Lomb-Scargle periodograms of each animal's wheel counts within a given lighting condition, then selecting the most prominent peak present in the periodogram. The corresponding value of each peak was used for comparative period lengthening and shortening in constant darkness.

Finally, statistical comparisons between treatment groups were performed. The independent variables for baseline recordings were: age, sex, and light schedule. In the second set of experiments using CP55940, the independent variables were: age, sex, and dose of CP55940 with day of injection as a blocking variable. Prior to omnibus testing, all data for a given measurement was tested for outliers, which was defined as those points that were greater or less than three interquartile ranges above or below the 3rd and first interquartile ranges within a single treatment group. After exclusion of these points, data from each measurement were assessed for a normal distribution (Shapiro-Wilk test) and equal variance (Levene test). A 3-way ANOVA was used to assess

differences between treatment groups. A priori significance was set at $\alpha=0.05$. Significant main-effects and interactions detected in omnibus tests were followed by additional planned contrasts. In the preliminary experiments, the ANOVA model used was Age:Sex:Lighting_Conditions. In the experiments using CP55940, the ANOVA model used was Age:Sex:Dose_CP55940. Additionally, 1-way ANOVA testing was performed on total wheel rotations measured in experiment two to assess dose-dependent changes within a single age/sex group. To determine the proportion of animals which were classified as early-, consistent-, or later risers, Fisher's Exact Test followed by pairwise nominal independence post hoc tests were used. The false discovery rate was corrected for using the Benjamini, Hochberg, and Yekutieli method.

Data and Code Availability

All original data and code used for analysis are available upon reasonable request to the corresponding author, Nicole M. Ashpole (nmashpol@olemiss.edu).

FIGURES

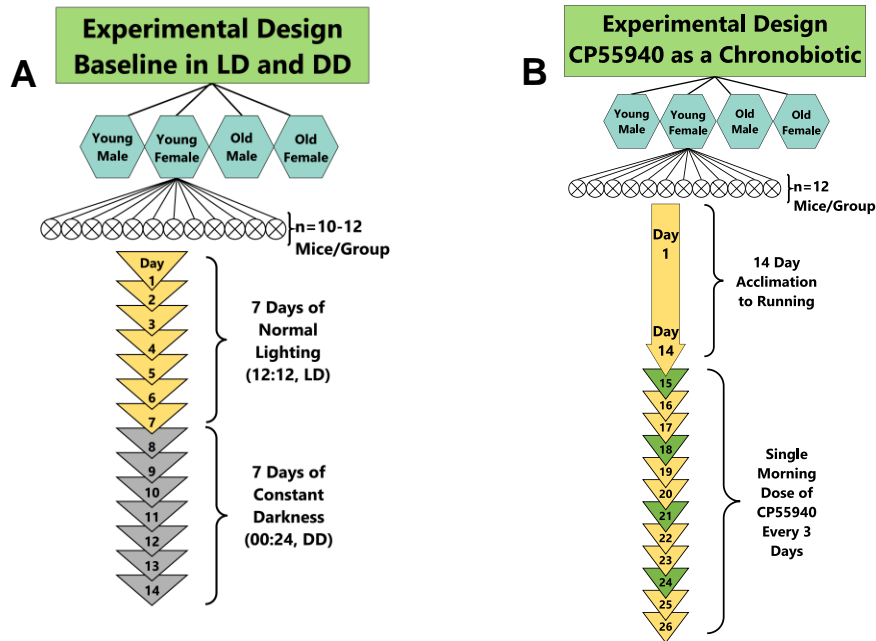


Figure 3.1: Experimental timeline of baseline wheel running and treatment with CP55940.

Panel A) Cohorts of young and old male and female mice were singly housed in cages with remotely monitored running wheels for a total of 14 days. During the first 7 days, mice were exposed to normal lighting (12 hours of light and 12 hours of darkness). After 7 full days, mice were held in constant darkness for an additional 7 days while wheel running was recorded.

Panel B) Separate cohorts of young and old male and female mice were allowed two weeks of acclimation running under normal 12:12 lighting. Beginning on day 14, one hour after lights off at the beginning of the animal’s active period, mice were administered the first of four unique doses (0 [vehicle], 0.001mg/kg, 0.01mg/kg, 0.1mg/kg) of the synthetic cannabinoid CP55940 via intraperitoneal injection. Mice were then left undisturbed for two days. Every 3 days (indicated in green), animals were

administered an additional unique dose, according to a Latin-square experimental design.

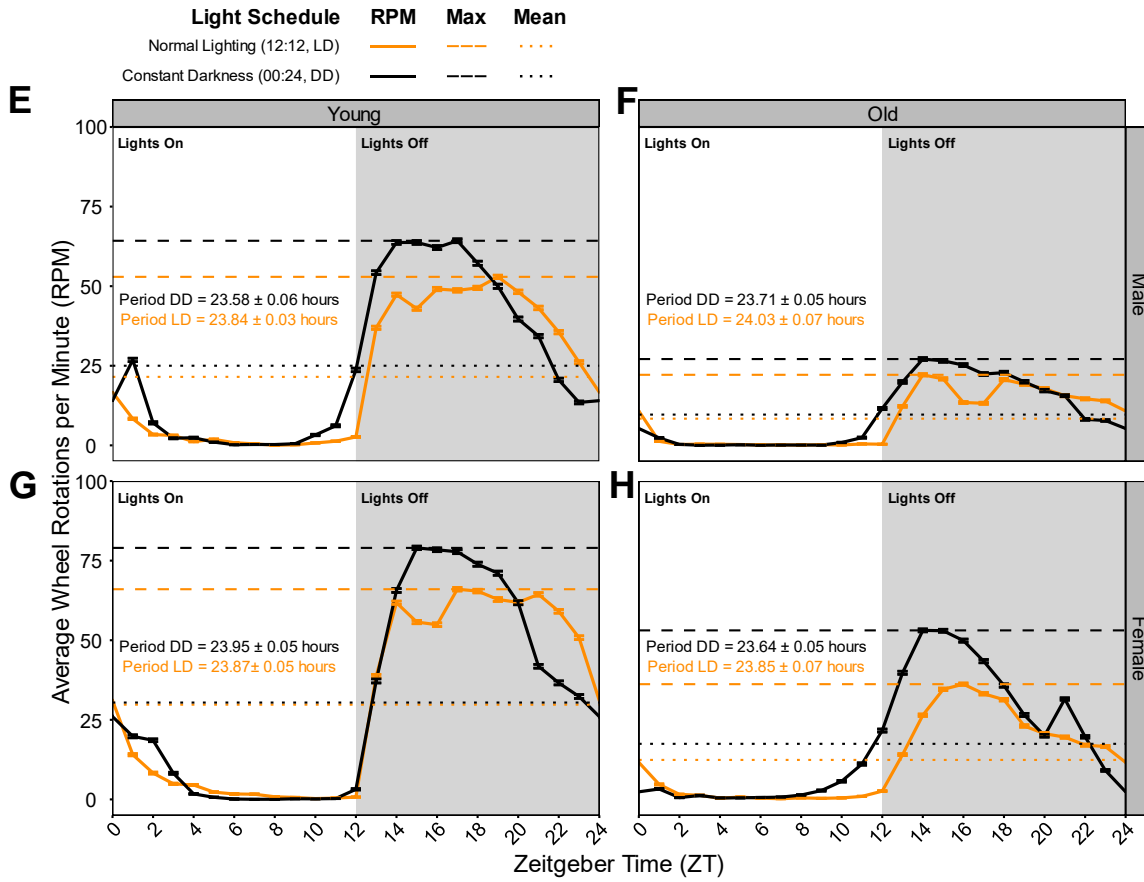
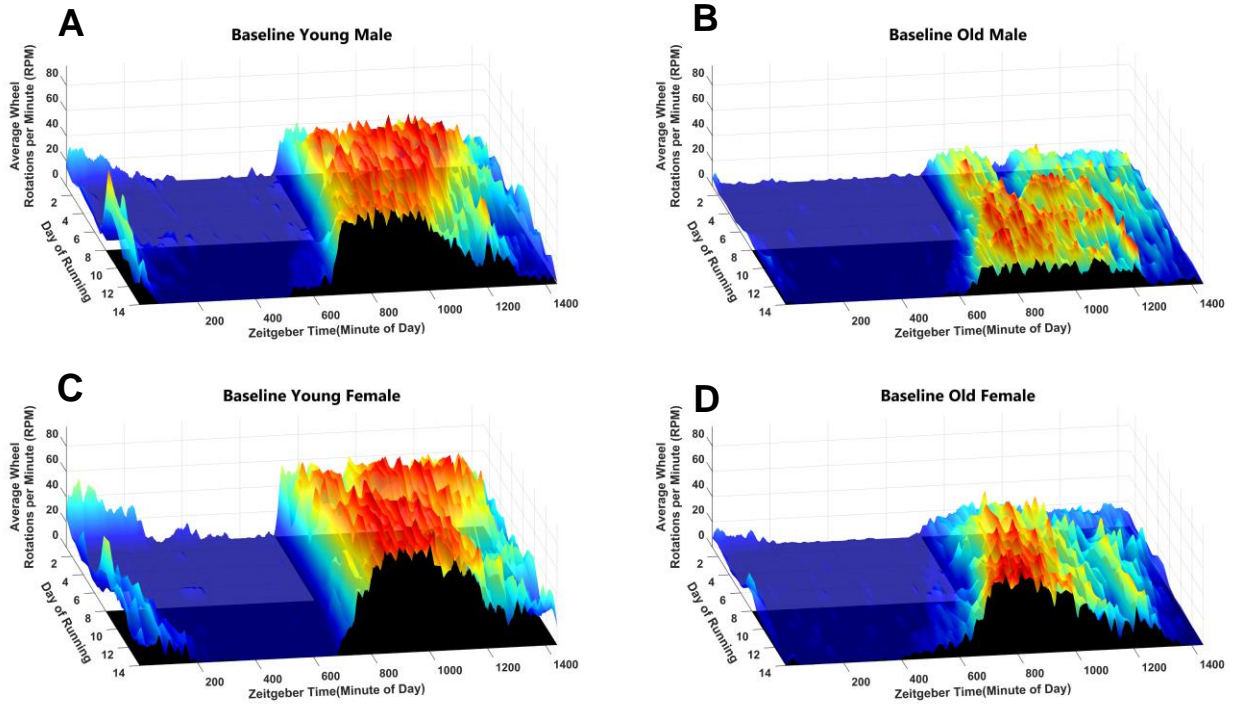


Figure 3.2: Circadian locomotion of C57BL6 mice housed under normal lighting (12:12, LD) and constant darkness (00:24, DD).

Panels A-D) Surface plots of minute-by-minute activity during 7 days of normal (12:12) lighting and 7 days of constant darkness (indicated by the black or white squares under each surface).

Panels E-H) Hour-by-hour average daily means, maxima, and periods of C57BL6 Mice housed under normal lighting and constant darkness. Lights off was defined as Zeitgeber Time (ZT hour 12).

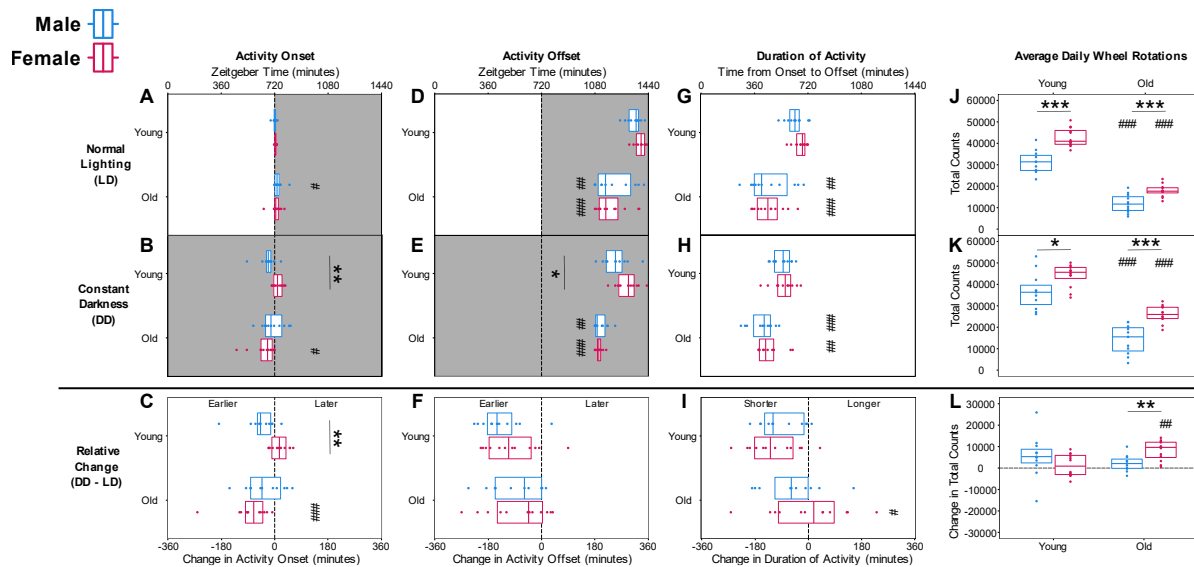


Figure 3.3: Quantification of changes in average activity onset, activity offset, duration of activity, and total activity during normal lighting and constant darkness.

Panels A-B) Average time of activity onset during normal lighting (A) and constant darkness (B).

Panel C) The relative change in timing of activity onset between normal lighting and constant darkness.

Panels D-E) Average time of activity offset during normal lighting (D) and constant darkness (E),

Panel F) The relative change in timing of activity offset between normal lighting and constant darkness.

Panels G-H) Average total minutes of activity during normal lighting (G) and constant darkness (H),

Panel I) The relative change in average duration of activity between normal lighting and constant darkness.

Panels J-K) Average total wheel rotations during normal lighting (J) and constant darkness (K),

Panel L) The relative change in average total wheel rotations during normal lighting and constant darkness. Significant differences ($p < 0.05$) between sexes within an age group are indicated by (*), while significant differences between ages within a sex are indicated by (#).

Age	Sex	n=	Activity Onset				Activity Offset							
			Early	(%)	Consistent	(%)	Late	(%)	Early	(%)	Consistent	(%)	Late	(%)
Young	Male	11	8	(72.7)	2	(18.2)	1	(9.1)	8	(72.7)	2	(18.2)	1	(9.1)
Old	Male	11	6	(54.5)	2	(18.2)	3	(27.3)	6	(54.5)	2	(18.2)	3	(27.3)
Young	Female	12	3	(27.3)	3	(27.3)	6	(54.5)	3	(27.3)	3	(27.3)	6	(54.5)
Old	Female	12	11	(100.0)	1	(9.1)	0	(0.0)	11	(100.0)	1	(9.1)	0	(0.0)

Table 3.1: Proportion of animals whose activity onset and offset shifted greater than 15 minutes from normal lighting to constant darkness.

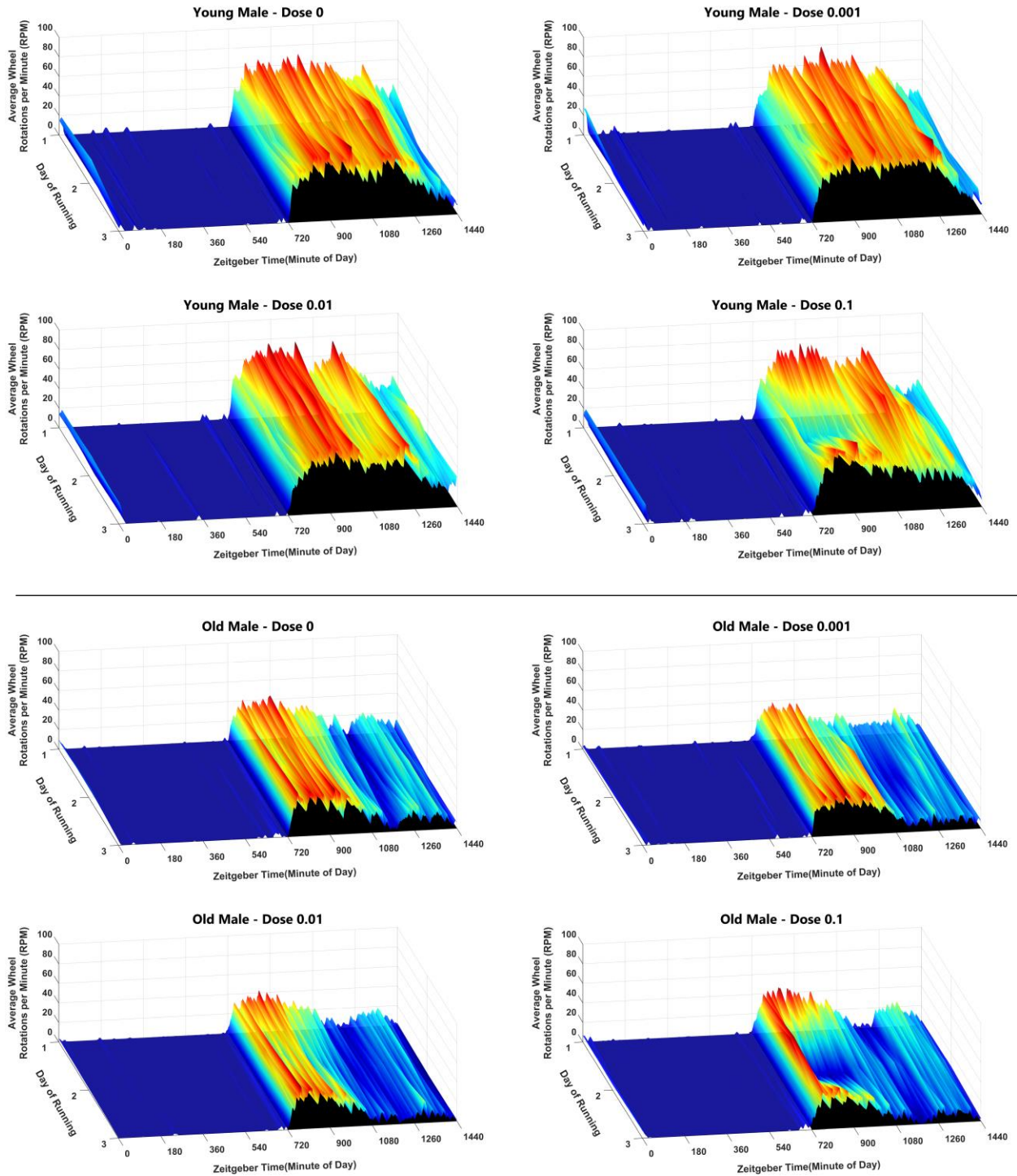


Figure 3.4: Treatment with varying doses of the synthetic cannabinoid CP55940 in young and old male mice.

Average running wheel activity of young (2-4m) and old (18-22m) male mice was quantified the day before (back, day 1), during (middle, day 2), and after injection (front, day 3). Data plotted as Day of Running 2 represent the average group activity following one of four doses of CP55940 (0 [Vehicle], 0.001, 0.01, or 0.1mg/kg, IP). Lights-on was defined as ZT minute 0, and lights-off was defined as ZT minute 720. Each mouse received all 4 doses in a pseudo randomized order. All mice had a 72-hour washout period between subsequent injections.

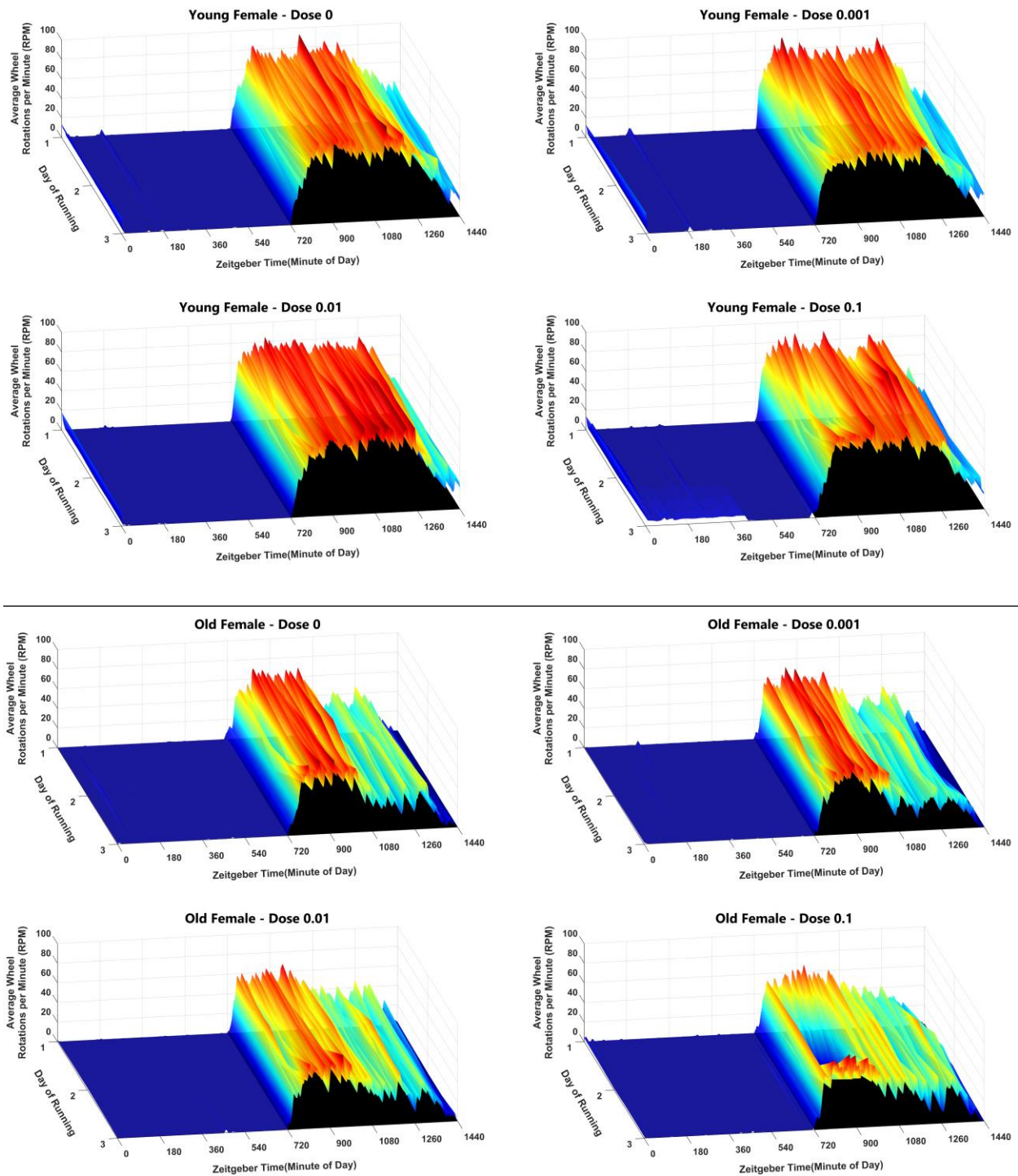


Figure 3.5: Treatment with varying doses of the synthetic cannabinoid CP55940 in young and old female mice.

Average running wheel activity of young (2-4m) and old (18-22m) male mice was quantified the day before (back, day 1), during (middle, day 2), and after injection (front, day 3). Data plotted as Day of Running 2 represent the average group activity following one of four doses of CP55940 (0 [Vehicle], 0.001, 0.01, or 0.1mg/kg, IP). Lights-on was defined as ZT minute 0, and lights-off was defined as ZT minute 720. Each mouse received all 4 doses in a pseudo randomized order. All mice had a 72-hour washout period between subsequent injections.

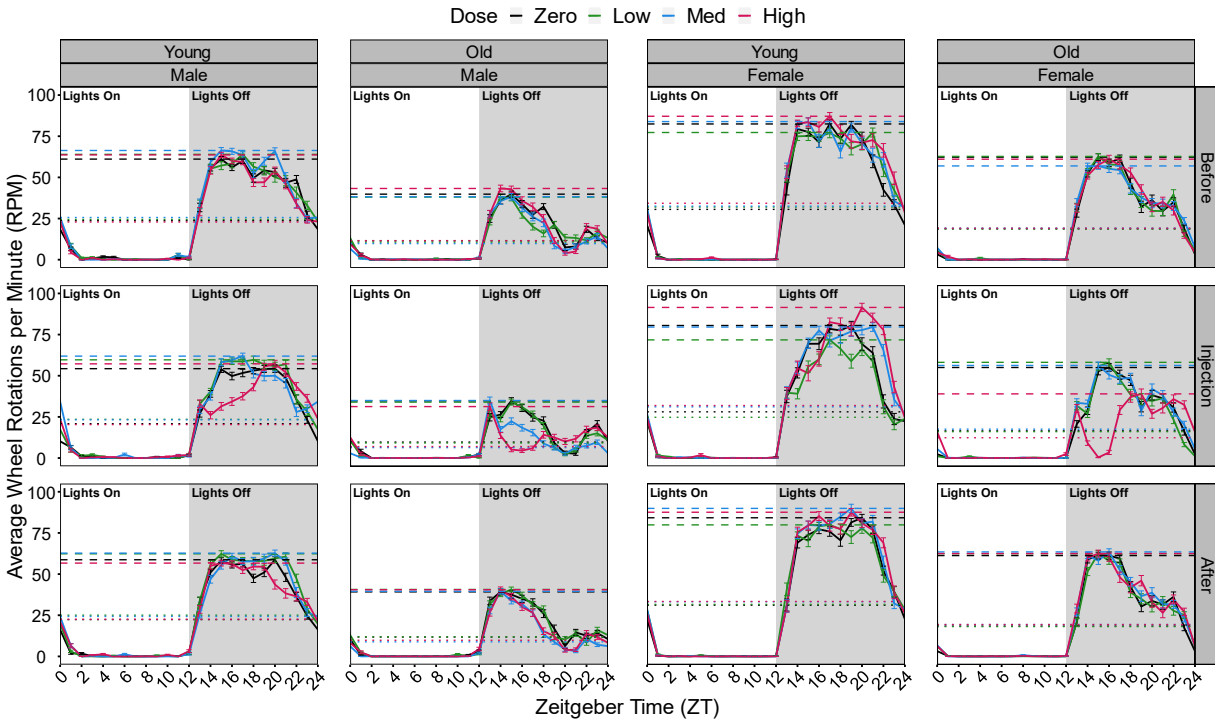
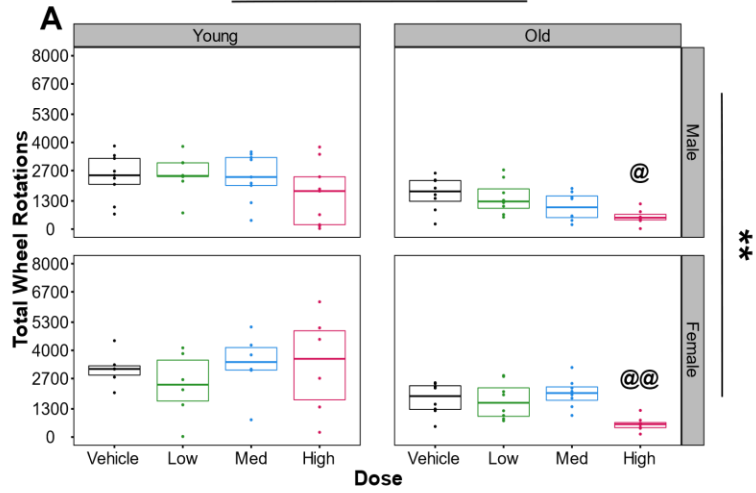


Figure 3.6: Voluntary wheel running of young and old male and female C57BL6 mice on the day before, during, and after injection with varying doses of CP55940.

On the day of injection, 30-60m after lights off (~ZT hour 12.5) mice were administered an intraperitoneal injection of vehicle or varying doses of CP55940 and returned to their running wheels. Doses of CP55940 are (Zero [Vehicle], Low [0.001mg/kg], Med [0.01mg/kg], High [0.1mg/kg]). Lines and error bars represent the average group mean (n=6-9 per dose). Dashed lines indicate maximum rotations per minute (RPM) for a given dose. Dotted lines indicate mean RPM for a given dose.

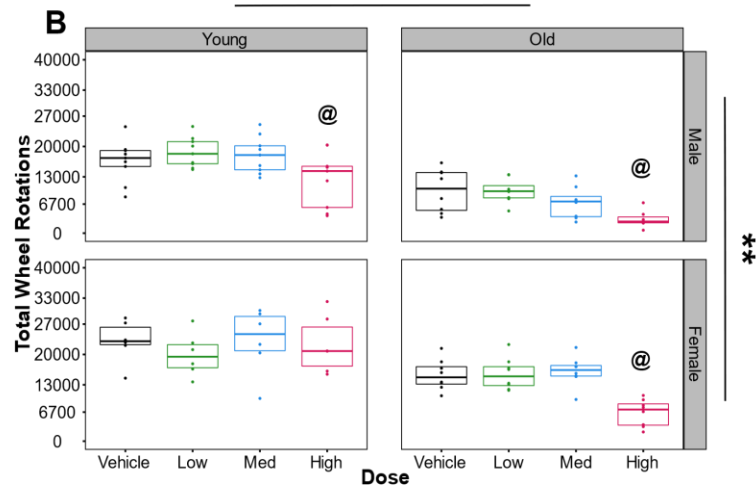
First Hour After Injection

###



1-6 Hours After Injection

###



6-12 Hours After Injection

###

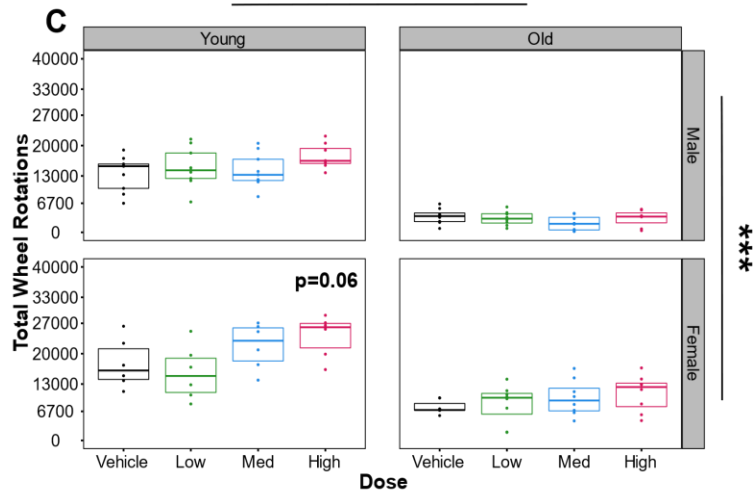


Figure 3.7: Quantification of total wheel running 1, 1-6, and 6-12 hours after injection of the synthetic cannabinoid CP55940.

On the day of injection, 30-60m after lights off (~ZT hour 12.5) mice were administered an intraperitoneal injection of vehicle or varying doses of CP55940 and returned to their running wheels. Doses of CP55940 are (Zero [Vehicle], Low [0.001mg/kg], Med [0.01mg/kg], High [0.1mg/kg]). Total wheel running was quantified by summing the rotations per minute for the given durations listed.

Panel A) Total wheel rotations in the first hour after injection.

Panel B) Total wheel rotations for the first 6 hours after injection.

Panel C) Total wheel rotations 6-12 hours after injection.

Significant differences ($p < 0.05$) between sexes are indicated by (*), while significant differences between ages are indicated by (#). Significant differences between a dose of CP55940 and the vehicle within a sex/age group are indicated by (@).

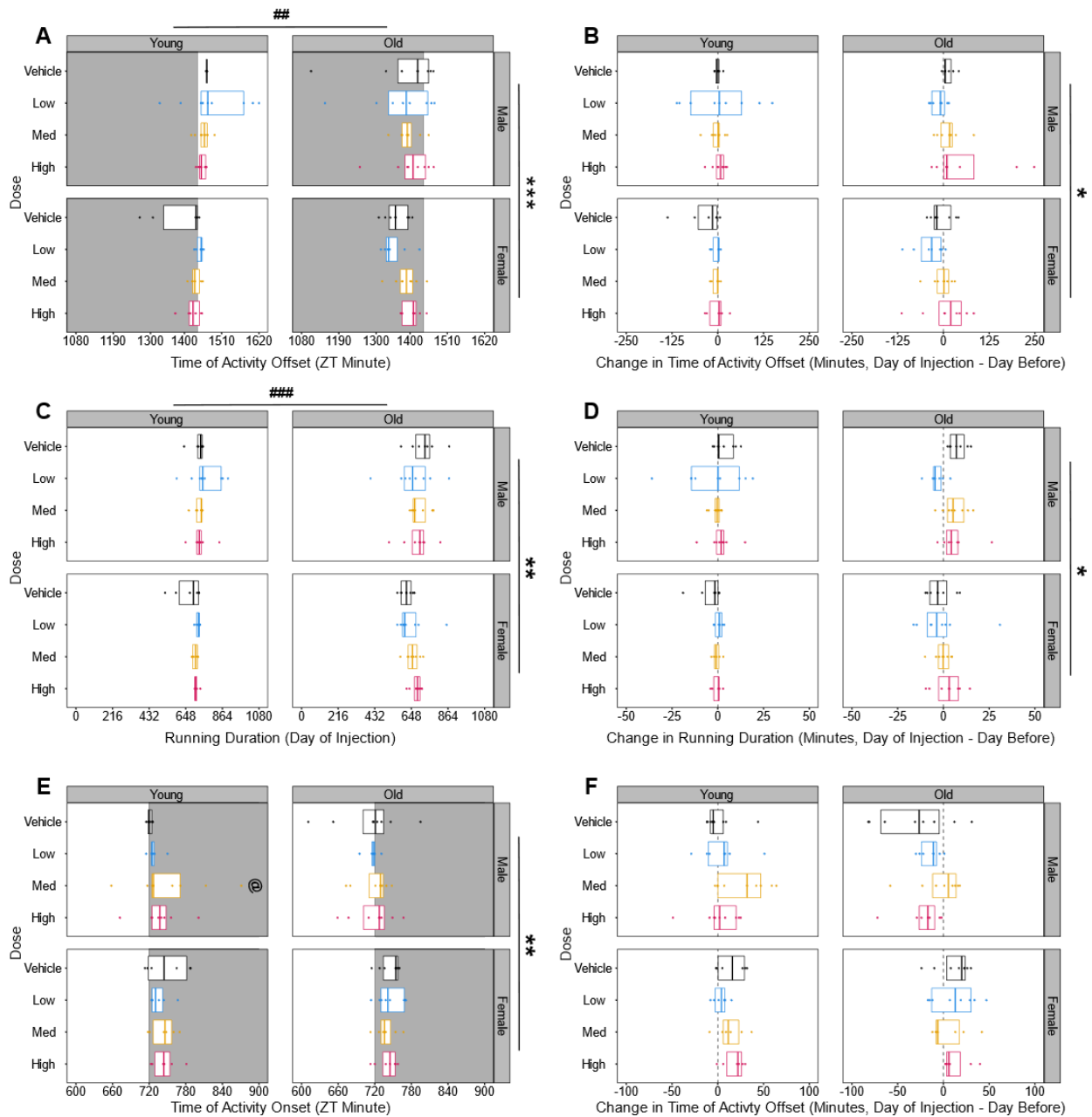


Figure 3.8: Quantification of changes in average activity onset, activity offset, duration of activity following injection of the synthetic cannabinoid CP55940.

On the day of injection, 30-60m after lights off (~ZT hour 12.5) mice were administered an intraperitoneal injection of vehicle or varying doses of CP55940 and returned to their running wheels. Doses of CP55940 are (Zero [Vehicle], Low [0.001mg/kg], Med

[0.01mg/kg], High [0.1mg/kg]). Activity onset and offset were calculated based on the time at which an animal reached 20% of its maximum daily RPM.

Panel A) Average time of activity offset on the day of injection.

Panel B) Change in the time of activity offset from the day before injection.

Panel C) Total minutes spent running at a rate above 20% of each animal's daily maximum RPM on the day of injection.

Panel D) Change in running duration (day of injection - day before injection).

Panel E) Average time of activity onset on the day after injection.

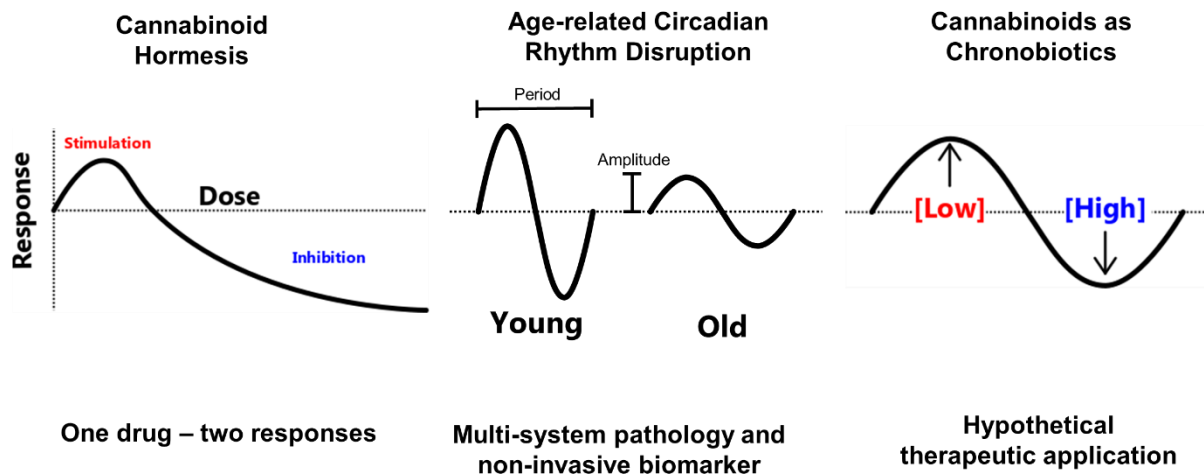
Panel F) Change in the time of activity onset (day after injection - day before injection).

Significant differences ($p < 0.05$) between sexes are indicated by (*), while significant differences between ages are indicated by (#). Significant differences between a dose of CP55940 and the vehicle within a sex/age group are indicated by (@).

CHAPTER 4:

CONCLUSIONS, LIMITATIONS, AND FUTURE DIRECTIONS

GRAPHICAL ABSTRACT:



SUMMARY OF FINDINGS:

Aging Circadian Rhythms and Cannabinoids

While exploring the possibility that circadian rhythms and aging are inextricably linked, it became clear that this idea is not novel. In fact, preliminary literature searches indicated that more publications exist regarding the relationship of aging to circadian rhythms than any other components of this work (**Figure 4.1**). Despite this shared, persistent interest, there are still numerous outstanding questions pertaining to the relationship between circadian rhythms and biological aging. The most glaringly obvious of which is: does the circadian molecular machinery regulate lifespan directly, or is it the collective functional output of these internal clocks? Chapter 1 summarized the findings

from over 150 articles on biological aging, circadian rhythms, and cannabinoid pharmacology and highlighted several theoretical and experimental breakthroughs which have led the field thus far. In particular, the works of Colin Pittendrigh, Jürgen Aschoff, and Arthur Winfree profoundly shaped Chapter 1 and the hypotheses it contains. Collectively, their pioneering work revealed the experimental tractability, pervasiveness, and scale-invariance of biological clocks. The fundamental postulate of Chapter 1 is that circadian rhythms are not only an observable physiological phenomenon throughout the lifespan, but that their manifestation directly influences the rate of biological aging. If we accept the present evidence - that deteriorating circadian rhythms precede the onset of many age-related pathologies - then it stands to reason that the maintenance of the output generated by these molecular clocks may very well stave off pathologies of aging (**Figure 1.5**).

Substantial evidence correlates the molecular and cellular mechanisms of dysregulated circadian rhythms with constituents of the endocannabinoid system. Although much is known about the endocannabinoid system and its regulation of neuronal activity and rodent behavior, there are significant gaps in knowledge regarding endocannabinoid function in advanced age. Limited knowledge about the effects of these compounds in aged subjects coupled with rapidly expanding access to exogenous cannabinoids marketed as therapeutics has placed elderly members of our society at risk for potentially adverse effects. Specifically, these previous gaps in knowledge precluded inferences of cannabinoid-elicited responses in aged animals - which were directly tested in Chapter 2.

Overwhelming evidence of cognitive impairment following high-doses of exogenous cannabinoids has led many to believe that these pharmacological agents lack therapeutic value. Nevertheless, the studies cited in Chapter 1 support the hypothesis that extremely regimented application of CB1 agonists at low doses may benefit certain age-related physiological dysfunctions. Capitalizing on the bidirectional dose-response (hormesis) which was been previously reported in young animals given exogenous cannabinoids, we hypothesized that cannabinoids are capable of both stimulating and suppressing circadian output in a time-dependent manner (**Figure 1.5**). To date, most studies have focused on melatonin for its ability to exhibit this circadian rhythm-modulating chronobiotic effects, though it is highly probable that many other pharmacological agents function in this manner^{59,60}. Since cannabinoid receptors are present in the SCN, and exogenous cannabinoids modulate neuronal activity responsible for thermoregulation and locomotion, the conclusions drawn from this chapter warranted further investigation of these substances in aged subjects and models circadian rhythm disruption.

Cannabinoid Hormesis

The previously hypothesized potential benefits from cannabinoid-based chronotherapeutics are directly proportional to the bidirectional (hormetic) dose-responses they produce. To this end, application of certain cannabinoids at calculated doses would theoretically allow for the rescue of both overactive and underactive biological processes. Such flexibility in a therapeutic agent, at least in theory, would surely be advantageous. Therefore, the work described in Chapter 2 was directly aimed at answering the following questions:

- 1) Do young and old animals differ in their physiological or behavioral responses to exogenous cannabinoids?
- 2) Are exogenous cannabinoids capable of eliciting both stimulation and inhibition of body temperature, locomotion, or nociception in mice?
- 3) Are the stimulatory effects of exogenous cannabinoids restricted to a single time-point in the lifespan?

After testing over 250 young and old mice from 3 independent cohorts and performing 15 iterations of the Tetrad Assay, we concluded that the synthetic cannabinoid CP55940 is both more potent and efficacious in its ability to induce hypolocomotion, hypothermia, and antinociception in aged mice. Additionally, our data indicated that the hormesis-like stimulation induced by low doses of this exogenous cannabinoid were evident and most pronounced in locomotor readouts from young, male mice.

Cannabinoids as Chronobiotics

The stimulation of locomotion by low-doses of CP55940 observed in experiments from Chapter 2 was quite compelling, and supported the hypothesis put forth in Chapter 1. Synthesizing our work and others', it has now been demonstrated that cannabinoids are able to alter neuronal activity, locomotion, and thermoregulation in a bidirectional manner. Therefore, the ability of these compounds to flexibly alter both central and peripheral clock function seems plausible. To experimentally test this we first needed to quantify baseline measures of circadian wheel running, then compare the ability of CP55940 to modulate these measures. The experiments described in Chapter 3 highlight the importance and technical difficulty of experimentally measuring circadian rhythms.

Under baseline normal lighting conditions, female mice produced more wheel rotations than age-matched male mice, although the duration of activity was not different between the sexes (**Fig. 3.3**). These findings agree with previous work reporting that female C57BL6 mice are more active than males^{240,241}. However, we were surprised by the shortening of animals' active periods following transition to constant darkness (**Fig. 3.2**). Despite increased total number of wheel rotations in constant darkness (**Fig. 3.3L**), young male and female mice actually shortened their durations of activity (**Fig. 3.3I**). Furthermore, the resilience of young female mice to circadian disruption in constant darkness, as well as the loss of this resilience with age are significant findings from this study.

To evaluate the potential of CP55940 to alter circadian locomotor rhythms, we chose to administer low to moderate doses of this drug at the beginning of animals' active periods. Although we did not detect significant stimulation of total wheel running in response to low doses of CP55940 (**Fig. 3.7B**), we were intrigued by the temporally biphasic suppression and stimulation of locomotion seen at higher doses. This evening 'rebound' in locomotion may partly explain why previous studies have inconsistently reported locomotor depression and stimulation with modestly low doses of exogenous cannabinoids²⁴². Collectively, the presence of Age:Sex interactions in many of the metrics we reported further solidifies the need to include and transparently report these factors in future studies.

LIMITATIONS AND FUTURE DIRECTIONS:

Existing Data and Tools

It may seem obvious that some aspects of these experiments have been tested previously, however, the lack of freely available well-annotated data have prevented scientists' ability to conduct these vital comparisons post hoc. As modern technology and data repositories seek to remedy these issues, a major benefit of the work described here is the production of a curated, highly annotated, shareable data set. The wealth and density of information present in these data are immeasurable, and it would be foolish to consider the current analysis as 'complete'. Accordingly, future studies utilizing the data produced during vehicle-acclimation described in Chapter 2 or the baseline wheel recordings discussed in Chapter 3 may yield additional insights.

The evaluation of CP55940 as a chronobiotic was technically challenging for numerous reasons, partly because there are no commercial tools currently available to rigorously and efficiently conduct this analysis. Therefore, the success of this entire project directly relied on the ability to generate effective and efficient methods for data collection, curation, and analysis. The primary code and programs written to perform these tasks have been compiled in the **Appendix**. Additionally, the present success of these analytical tools now permits high-throughput testing of the chronobiotic effects of not only cannabinoids but also drugs of abuse and other potential therapeutics.

Mice as a Model for Circadian Rhythm Disruption

The translation of experimental findings from rodents to humans is contentious, to say the least²⁴³. However the value of preclinical rodent models in biological aging research is undeniable^{244,245}. Despite the immense knowledge gained from research on rodent circadian rhythms, the usefulness of these nocturnal animals as a model for

potential chronotherapies in humans remains to be evaluated. From a chronobiology standpoint, rodents (like most other mammals studied thus far) possess homologous core clock molecules²². Nevertheless, mice are nocturnal and exhibit distinct melatonin rhythms compared to diurnal humans. The release of melatonin from the human pineal gland exhibits a robust circadian rhythm whose peak onset corresponds to evening reductions in light. In contrast, mice exhibit a mid-subjective-day spike in melatonin secretion that occurs ~8 hours after the onset of darkness²⁴⁶. This surge in melatonin may be partly responsible for the mid-day ‘siesta’ observed in the baseline recordings presented in Chapter 3 (**Fig. 3.2**). Considering that melatonin is the most well-studied chronobiotic in humans, future studies should compare the temporal release of melatonin in mice treated with novel chronobiotics²⁴⁷.

Mitigation of Circadian Confounds

Another major benefit of the present work over previous studies is that all experimental procedures were performed in the dark, during the animals’ active cycle. The time of day at which a drug is administered profoundly affects its metabolism and efficacy, and the study of these collective time-of-day-effects is known as *chronopharmacology*. Early work with cannabinoids clearly demonstrated that the effects of these compounds are significantly lowered when administered during the animals’ inactive period¹⁸⁹. Therefore, testing animals in the dark while they are active, although technically challenging, is a vital factor to consider when translating these findings to humans.

In addition to these chronopharmacological effects, behavioral endpoints such as locomotion are clearly variable throughout the day (**Fig. 3.2**). Indeed, meta-analysis of

the thermoregulatory responses to vehicle injection were shown to vary depending on the time of injection (**Fig. 4.2**). In the tetrad-based experiments described in Chapter 2, the number of animals which needed to be tested in a single day coupled with a limited number of testing apparatuses necessitated testing animals at varying times during their active period. Although all doses were represented at all time points, we were unable to completely alleviate the potential confound of circadian effects on these physiological and behavioral readouts. Given that the exact time and order of all experiments was included in the annotated data set, it may be possible with future analysis to determine the extent that time-of-administration, and even time of year (**Fig. 4.3**), may have influenced the present findings.

Vehicle, Drug, and Route of Administration

Throughout these studies, great care was taken to mitigate the effects of the injection procedure and vehicle administration. Although the relative concentrations of ethanol and detergent (Kolliphor EL) in the vehicle far exceed the concentration of cannabinoid, the profound effects of CP55940 are observable even at the lowest dose tested (0.001mg/kg, IP). The 1:1:18 (ethanol:Kolliphor:saline) ratio used as a vehicle here was based off of numerous previous reports using this vehicle in studies of THC and CP55940^{139,248,249}. Still, we observed modest but consistent changes in body temperature responses to vehicle injection (**Fig. 4.3**). Evaluation of vehicle specific effects per se was not the intent of these studies, however, future well controlled studies evaluating the continued use of this mixture as a vehicle should be performed.

The intraperitoneal injection of CP55940 is a potential limitation of these studies, as this route of administration does not translate well to human cannabinoid usage.

While the availability of purified phytocannabinoids increases in the United States, many additional studies of the age-, sex-, and dose-dependent effects of isolated phytocannabinoids and cannabis-derived terpenes are now warranted^{126,127,158,160}. Accurately modeling human routes of administration in rodents has traditionally been difficult, though recent advances in electronic vaporization devices may revolutionize models of inhalation¹⁶⁰. In addition to models of cannabinoid inhalation, oral ingestion of cannabinoid-containing products is increasing specifically among elderly patients and should be further investigated.

Experimental Design of Hormesis Study

In order to facilitate the rapid acquisition of multiple behavioral endpoints while mitigating the effects of repeated dosing, it was necessary to perform the behavioral tests in Chapter 2 as a 1.5 hour-long battery. In this experimental design, we first took baseline rectal and IR temperature recordings, weighed the animals, then injected the drug. Thirty minutes later, animals were placed in the open field and allowed to explore for 30 minutes. At the conclusion of open field testing, animals' temperatures were then taken again prior to nociception testing using the hot-plate and tail-withdrawal assays. A major limitation of this approach was discovered when comparing the thermoregulatory responses of vehicle-treatment during acclimation to vehicle-treated animals during the behavioral battery. The most likely explanation for these discrepancies is the stress and increased locomotion resulting from animals being tested in the open field between temperature recordings. Considering that low-dose hyperthermia was intended to be a primary readout of this study, the hyperthermia (likely) induced by open field testing potentially occluded true differences.

The previously mentioned hyperthermia observed following open field testing highlights the importance of choosing, whenever possible, assays with large dynamic range. Since the average body temperature of mice in our study was ~37.5°C, and the maximum rectal temperature recorded was 39°C, it is also conceivable that a 'ceiling effect' occluded potential hyperthermia induced by low-doses of CP55940. Similarly, during hot-water tail withdrawal experiments, vehicle-treated animals withdrew their tails from 48°C water in less than 2 seconds. Such rapid responses by these vehicle-treated mice left little room to detect potentially hyperalgesic effects elicited by low doses of CP55940.

Voluntary Wheel Running

The use of voluntary wheel running to assess circadian locomotion is widespread in rodent research. Yet recent evidence indicates that access to a running wheel and the requisite social isolation both profoundly alter physiology and behavior^{241,250-252}. Furthermore, limitations imposed by the design of currently available commercially-produced running wheels hinders their use in longitudinal studies of aging. Future studies utilizing telemetric systems may greatly improve the quality of this research, as modern technology now permits simultaneous long-term recording from group-housed mice. Additionally, the use of telemetry for chronobiotic studies also presents the additional advantage of simultaneously monitoring body temperature with far greater temporal resolution than is capable with a rectal probe.

BIOLOGICAL AGING AND CIRCADIAN RHYTHMS AS DYNAMICAL SYSTEMS

Though the process biological aging has previously been referred to as a stochastic (random), several lines of research suggest that aging systems are not random - but rather chaotic^{253,254}. In support of this, adaptation of the “two-hit hypothesis” from cancer research to the biology of aging has left open the possibility that the aging systems may actually exhibit features of dynamical systems - that is to say that they are calculable, if the starting conditions are known^{255-257 258}. The biological importance of these high-dimension mathematical properties remains unknown, though the presence or absence of these fractal patterns may correspond to the onset of age-related neuropathology³⁷. Future studies employing these advanced computational analyses are likely to yield valuable insight regarding the onset, progression, and treatment efficacy of age-related diseases.

CONCLUSION

The work contained in this dissertation proposes and tests the novel hypothesis that cannabinoid hormesis can be used to bidirectionally modulate age-related changes in circadian locomotion. Throughout these studies, pronounced age-, sex-, dose-, and time-dependent effects were observed in the physiological and behavioral responses to treatment with exogenous cannabinoids. Testing of this hypothesis required the creation and validation of novel behavioral paradigms, analytical tools, unique technical approaches, and established a framework for evaluating chronobiotic compounds in aging mice. Furthermore, the data collected in these studies has been compiled in a manner that facilitates future analysis and continued usefulness. Collectively, these findings indicate that the exogenous cannabinoid CP55940 possesses hormetic and chronobiotic characteristics in young mice, but the increased sensitivity to this

compound in aged mice suggests that therapeutic applications of cannabinoids in elderly patients must be approached with caution.

FIGURES

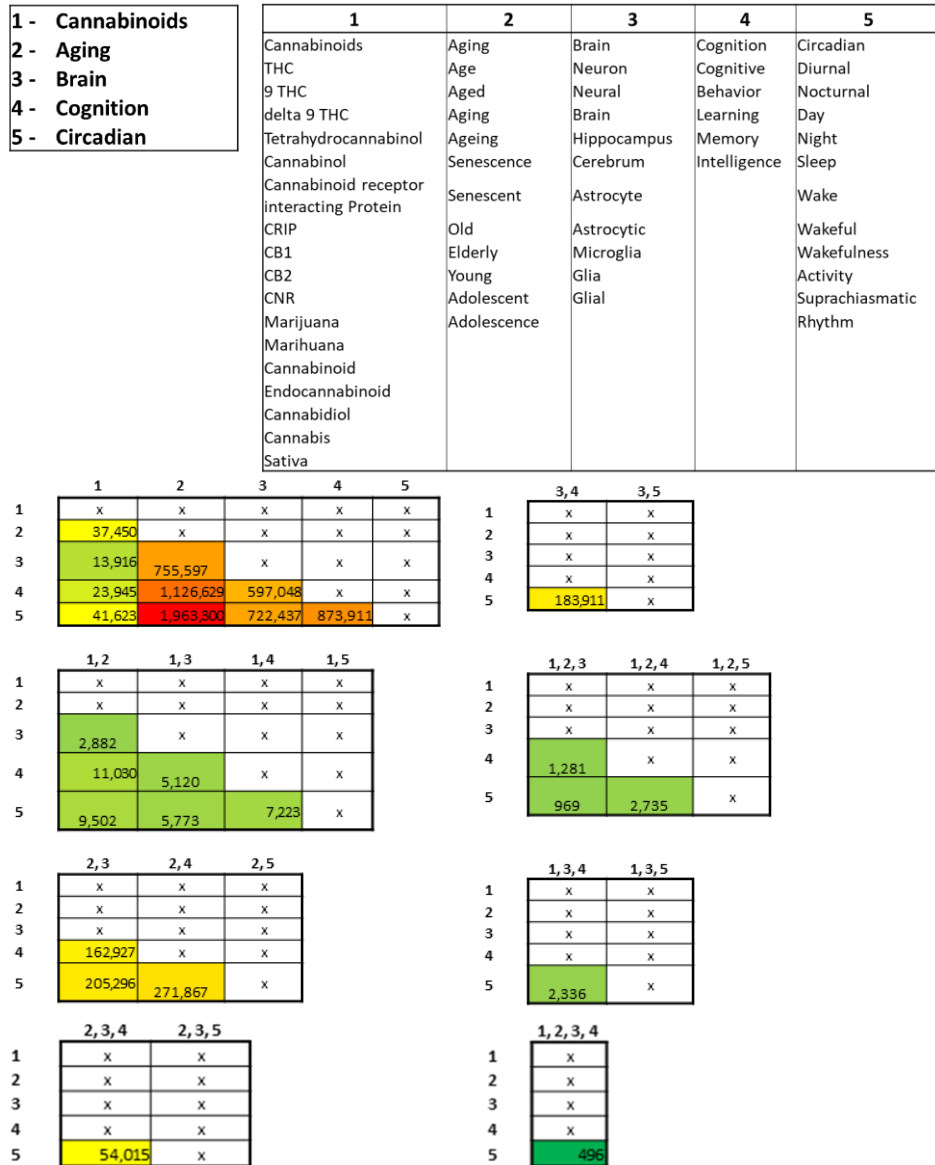


Figure 4.1: Frequency of word-cluster combinations present in a systematic literature search.

Complex clusters of related strings were created to systematically search online databases for relevant literature when writing Chapter 1. The relative number of hits for each combination of word clusters is listed below and coded in a heat map. Search conducted via One Search in November 2018.

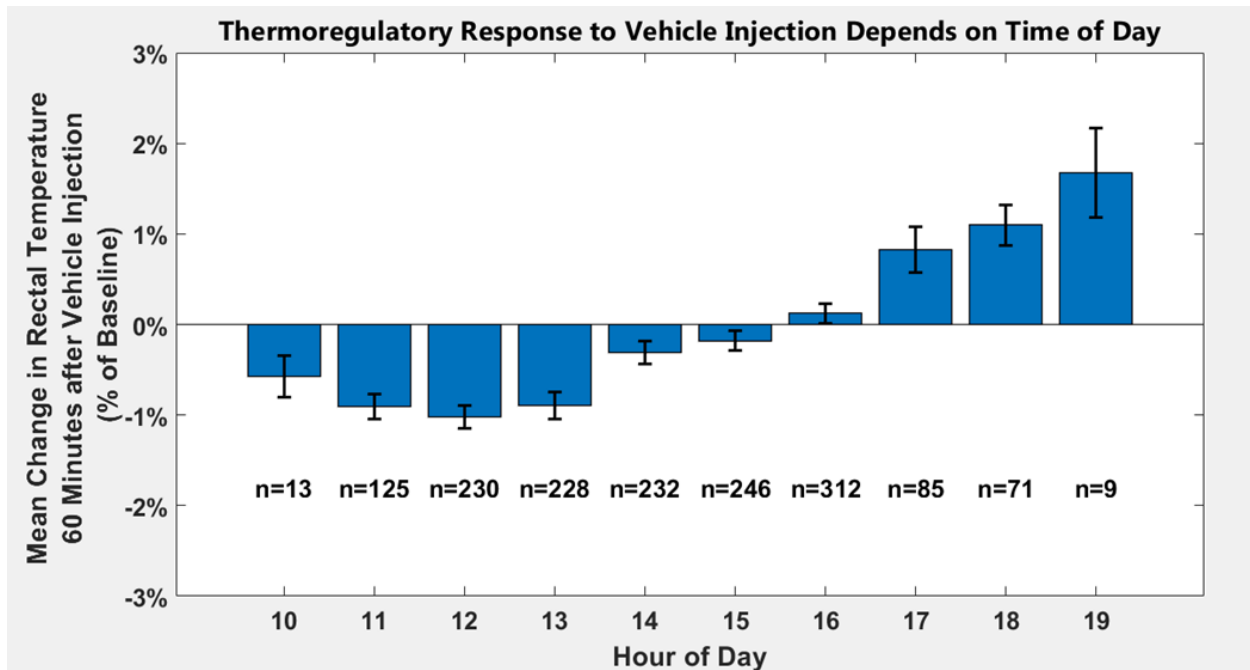


Figure 4.2: Time-of-day effect on thermoregulatory response to vehicle injection during acclimation trials.

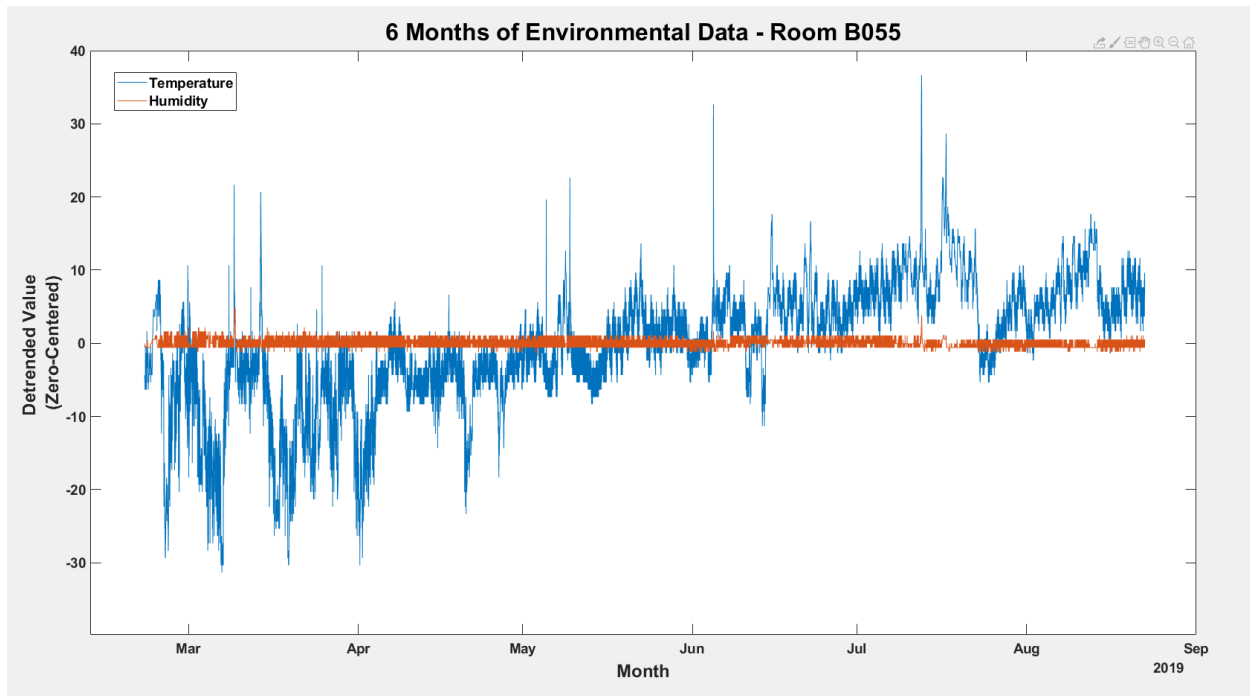


Figure 4.3: Time-of-year effect on housing room humidity.

LIST OF REFERENCES

1. Rowe, J.W. & Kahn, R.L. Successful Aging 2.0: Conceptual Expansions for the 21st Century. *J Gerontol B Psychol Sci Soc Sci* **70**, 593-596 (2015).
2. Hedden, T. & Gabrieli, J.D. Insights into the ageing mind: a view from cognitive neuroscience. *Nature reviews neuroscience* **5**, 87 (2004).
3. Morrison, J.H. & Baxter, M.G. The ageing cortical synapse: hallmarks and implications for cognitive decline. *Nature Reviews Neuroscience* **13**, 240 (2012).
4. Ekdahl, C., Kokaia, Z. & Lindvall, O. Brain inflammation and adult neurogenesis: the dual role of microglia. *Neuroscience* **158**, 1021-1029 (2009).
5. Mariani, E., Polidori, M., Cherubini, A. & Mecocci, P. Oxidative stress in brain aging, neurodegenerative and vascular diseases: an overview. *Journal of Chromatography B* **827**, 65-75 (2005).
6. Li, R.C., *et al.* Exogenous growth hormone attenuates cognitive deficits induced by intermittent hypoxia in rats. *Neuroscience* **196**, 237-250 (2011).
7. Lee, Y.S. & Silva, A.J. The molecular and cellular biology of enhanced cognition. *Nature reviews. Neuroscience* **10**, 126-140 (2009).
8. Cardinali, D.P., *et al.* Therapeutic application of melatonin in mild cognitive impairment. *American journal of neurodegenerative disease* **1**, 280-291 (2012).
9. Benedict, C., *et al.* Intranasal insulin improves memory in humans. *Psychoneuroendocrinology* **29**, 1326-1334 (2004).

10. Lichtenwalner, R.J., *et al.* Intracerebroventricular infusion of insulin-like growth factor-I ameliorates the age-related decline in hippocampal neurogenesis. *Neuroscience* **107**, 603-613 (2001).
11. Musiek, E.S., Xiong, D.D. & Holtzman, D.M. Sleep, circadian rhythms, and the pathogenesis of Alzheimer disease. *Experimental & molecular medicine* **47**, e148 (2015).
12. Rauchs, G., Carrier, J. & Peigneux, P. Sleep and cognition in the elderly. *Frontiers in neurology* **4**, 71 (2013).
13. Bushey, D., Hughes, K.A., Tononi, G. & Cirelli, C. Sleep, aging, and lifespan in *Drosophila*. *BMC Neurosci* **11**, 56 (2010).
14. Stickgold, R. To sleep: perchance to learn. *Nature neuroscience* **15**, 1322-1323 (2012).
15. Harand, C., *et al.* How aging affects sleep-dependent memory consolidation? *Frontiers in neurology* **3**, 8 (2012).
16. Dijk, D.J., Duffy, J.F., Riel, E., Shanahan, T.L. & Czeisler, C.A. Ageing and the circadian and homeostatic regulation of human sleep during forced desynchrony of rest, melatonin and temperature rhythms. *J Physiol* **516 (Pt 2)**, 611-627 (1999).
17. Van Cauter, E., Leproult, R. & Plat, L. Age-related changes in slow wave sleep and REM sleep and relationship with growth hormone and cortisol levels in healthy men. *JAMA* **284**, 861-868 (2000).
18. Herculano-Houzel, S. Neuroscience. Sleep it out. *Science* **342**, 316-317 (2013).

19. Espiritu, J.R. Aging-related sleep changes. *Clinics in geriatric medicine* **24**, 1-14, v (2008).
20. Xie, L., *et al.* Sleep drives metabolite clearance from the adult brain. *Science* **342**, 373-377 (2013).
21. Pittendrigh, C.S. Temporal organization: reflections of a Darwinian clock-watcher. *Annu Rev Physiol* **55**, 16-54 (1993).
22. Refinetti, R. *Circadian physiology*, (CRC press, 2016).
23. Pittendrigh, C.S. Circadian rhythms and the circadian organization of living systems. *Cold Spring Harb Symp Quant Biol* **25**, 159-184 (1960).
24. Aschoff, J. Circadian Rhythms in Man. *Science* **148**, 1427-1432 (1965).
25. Konopka, R.J. & Benzer, S. Clock mutants of *Drosophila melanogaster*. *Proceedings of the National Academy of Sciences of the United States of America* **68**, 2112-2116 (1971).
26. Hardin, P.E., Hall, J.C. & Rosbash, M. Feedback of the *Drosophila* period gene product on circadian cycling of its messenger RNA levels. *Nature* **343**, 536-540 (1990).
27. Liu, C., Weaver, D.R., Strogatz, S.H. & Reppert, S.M. Cellular construction of a circadian clock: period determination in the suprachiasmatic nuclei. *Cell* **91**, 855-860 (1997).
28. Kondratova, A.A. & Kondratov, R.V. The circadian clock and pathology of the ageing brain. *Nature reviews. Neuroscience* **13**, 325-335 (2012).
29. Kress, G.J., *et al.* Regulation of amyloid- β dynamics and pathology by the circadian clock. *Journal of Experimental Medicine*, jem. 20172347 (2018).

30. Pittendrigh, C.S. & Daan, S. Circadian oscillations in rodents: a systematic increase of their frequency with age. *Science* **186**, 548-550 (1974).
31. Nakamura, T.J., Takasu, N.N. & Nakamura, W. The suprachiasmatic nucleus: age-related decline in biological rhythms. *J Physiol Sci* **66**, 367-374 (2016).
32. Nakamura, T.J., *et al.* Age-related decline in circadian output. *The Journal of neuroscience : the official journal of the Society for Neuroscience* **31**, 10201-10205 (2011).
33. Yamazaki, S., *et al.* Effects of aging on central and peripheral mammalian clocks. *Proceedings of the National Academy of Sciences of the United States of America* **99**, 10801-10806 (2002).
34. Nakamura, T.J., *et al.* Age-Related Changes in the Circadian System Unmasked by Constant Conditions(1,2,3). *eNeuro* **2**(2015).
35. Saper, C.B., Cano, G. & Scammell, T.E. Homeostatic, circadian, and emotional regulation of sleep. *The Journal of comparative neurology* **493**, 92-98 (2005).
36. Kramer, A., *et al.* Regulation of daily locomotor activity and sleep by hypothalamic EGF receptor signaling. *Science* **294**, 2511-2515 (2001).
37. Hu, K., Harper, D.G., Shea, S.A., Stopa, E.G. & Scheer, F.A. Noninvasive fractal biomarker of clock neurotransmitter disturbance in humans with dementia. *Sci Rep* **3**, 2229 (2013).
38. Huang, Y.-L., *et al.* Age-associated difference in circadian sleep–wake and rest–activity rhythms. *Physiology & behavior* **76**, 597-603 (2002).

39. Weitzman, E.D., Moline, M.L., Czeisler, C.A. & Zimmerman, J.C. Chronobiology of aging: temperature, sleep-wake rhythms and entrainment. *Neurobiology of aging* **3**, 299-309 (1982).
40. Satinoff, E. Patterns of circadian body temperature rhythms in aged rats. *Clinical and experimental pharmacology and physiology* **25**, 135-140 (1998).
41. Koster-van Hoffen, G., *et al.* Effects of a novel melatonin analog on circadian rhythms of body temperature and activity in young, middle-aged, and old rats. *Neurobiology of aging* **14**, 565-569 (1993).
42. Valentinuzzi, V.S., Scarbrough, K., Takahashi, J.S. & Turek, F.W. Effects of aging on the circadian rhythm of wheel-running activity in C57BL/6 mice. *The American journal of physiology* **273**, R1957-1964 (1997).
43. Michael, S.D., Kaplan, S.B. & Macmillan, B.T. Peripheral plasma concentrations of LH, FSH, prolactin and GH from birth to puberty in male and female mice. *Journal of reproduction and fertility* **59**, 217-222 (1980).
44. Sonntag, W.E., *et al.* Insulin-like growth factor-1 in CNS and cerebrovascular aging. *Frontiers in aging neuroscience* **5**, 27 (2013).
45. Kwapis, J.L., *et al.* Epigenetic regulation of the circadian gene *Per1* contributes to age-related changes in hippocampal memory. *Nature communications* **9**, 3323 (2018).
46. Saper, C.B. The central circadian timing system. *Curr Opin Neurobiol* **23**, 747-751 (2013).

47. Welsh, D.K., Logothetis, D.E., Meister, M. & Reppert, S.M. Individual neurons dissociated from rat suprachiasmatic nucleus express independently phased circadian firing rhythms. *Neuron* **14**, 697-706 (1995).
48. Hastings, M.H., Maywood, E.S. & Brancaccio, M. Generation of circadian rhythms in the suprachiasmatic nucleus. *Nature Reviews Neuroscience*, 1 (2018).
49. Bass, J. & Lazar, M.A. Circadian time signatures of fitness and disease. *Science* **354**, 994-999 (2016).
50. Hastings, M.H., Reddy, A.B. & Maywood, E.S. A clockwork web: circadian timing in brain and periphery, in health and disease. *Nature reviews. Neuroscience* **4**, 649-661 (2003).
51. Menaker, M., Takahashi, J.S. & Eskin, A. The physiology of circadian pacemakers. *Annu Rev Physiol* **40**, 501-526 (1978).
52. Saper, C.B., Scammell, T.E. & Lu, J. Hypothalamic regulation of sleep and circadian rhythms. *Nature* **437**, 1257-1263 (2005).
53. Longo, V.D. & Panda, S. Fasting, Circadian Rhythms, and Time-Restricted Feeding in Healthy Lifespan. *Cell metabolism* **23**, 1048-1059 (2016).
54. Redfern, P., Minors, D. & Waterhouse, J. Circadian rhythms, jet lag, and chronobiotics: an overview. *Chronobiology international* **11**, 253-265 (1994).
55. Hasler, B.P., Smith, L.J., Cousins, J.C. & Bootzin, R.R. Circadian rhythms, sleep, and substance abuse. *Sleep Med Rev* **16**, 67-81 (2012).

56. Whitehurst, L.N., Fogler, K., Hall, K., Hartmann, M. & Dyche, J. The effects of chronic marijuana use on circadian entrainment. *Chronobiology international* **32**, 561-567 (2015).
57. Stein, M.A., Weiss, M. & Hlavaty, L. ADHD treatments, sleep, and sleep problems: complex associations. *Neurotherapeutics : the journal of the American Society for Experimental NeuroTherapeutics* **9**, 509-517 (2012).
58. Burke, T.M., *et al.* Effects of caffeine on the human circadian clock in vivo and in vitro. *Science translational medicine* **7**, 305ra146-305ra146 (2015).
59. Potter, G.D., *et al.* Circadian Rhythm and Sleep Disruption: Causes, Metabolic Consequences, and Countermeasures. *Endocr Rev* **37**, 584-608 (2016).
60. Arendt, J. & Skene, D.J. Melatonin as a chronobiotic. *Sleep Med Rev* **9**, 25-39 (2005).
61. Yamazaki, S., *et al.* Resetting central and peripheral circadian oscillators in transgenic rats. *Science* **288**, 682-685 (2000).
62. Schibler, U., *et al.* Clock-talk: interactions between central and peripheral circadian oscillators in mammals. in *Cold Spring Harbor symposia on quantitative biology*, Vol. 80 223-232 (Cold Spring Harbor Laboratory Press, 2015).
63. Pittendrigh, C.S. & Minis, D.H. The Entrainment of Circadian Oscillations by Light and Their Role as Photoperiodic Clocks. *The American naturalist* **98**, 261-294 (1964).
64. Hattar, S., *et al.* Melanopsin and rod-cone photoreceptive systems account for all major accessory visual functions in mice. *Nature* **424**, 76-81 (2003).

65. Rosenwasser, A.M. & Turek, F.W. Neurobiology of circadian rhythm regulation. *Sleep medicine clinics* **10**, 403-412 (2015).
66. Buhr, E.D., Yoo, S.H. & Takahashi, J.S. Temperature as a universal resetting cue for mammalian circadian oscillators. *Science* **330**, 379-385 (2010).
67. Mohawk, J.A., Green, C.B. & Takahashi, J.S. Central and peripheral circadian clocks in mammals. *Annu Rev Neurosci* **35**, 445-462 (2012).
68. Partch, C.L., Green, C.B. & Takahashi, J.S. Molecular architecture of the mammalian circadian clock. *Trends Cell Biol* **24**, 90-99 (2014).
69. Van Someren, E.J. Thermoregulation and aging. *American journal of physiology. Regulatory, integrative and comparative physiology* **292**, R99-102 (2007).
70. Balmagiya, T. & Rozovski, S.J. Age-related changes in thermoregulation in male albino rats. *Experimental gerontology* **18**, 199-210 (1983).
71. Harper, D.G., *et al.* Disturbance of endogenous circadian rhythm in aging and Alzheimer disease. *Am J Geriatr Psychiatry* **13**, 359-368 (2005).
72. Roozendaal, B., van Gool, W.A., Swaab, D.F., Hoogendijk, J.E. & Mirmiran, M. Changes in vasopressin cells of the rat suprachiasmatic nucleus with aging. *Brain research* **409**, 259-264 (1987).
73. Tsukahara, S., Tanaka, S., Ishida, K., Hoshi, N. & Kitagawa, H. Age-related change and its sex differences in histoarchitecture of the hypothalamic suprachiasmatic nucleus of F344/N rats. *Experimental gerontology* **40**, 147-155 (2005).

74. Farajnia, S., Meijer, J.H. & Michel, S. Age-related changes in large-conductance calcium-activated potassium channels in mammalian circadian clock neurons. *Neurobiology of aging* **36**, 2176-2183 (2015).
75. Farajnia, S., *et al.* Evidence for neuronal desynchrony in the aged suprachiasmatic nucleus clock. *The Journal of neuroscience : the official journal of the Society for Neuroscience* **32**, 5891-5899 (2012).
76. Balsalobre, A., Damiola, F. & Schibler, U. A serum shock induces circadian gene expression in mammalian tissue culture cells. *Cell* **93**, 929-937 (1998).
77. Katewa, S.D., *et al.* Peripheral circadian clocks mediate dietary restriction-dependent changes in lifespan and fat metabolism in *Drosophila*. *Cell metabolism* **23**, 143-154 (2016).
78. Balsalobre, A., *et al.* Resetting of circadian time in peripheral tissues by glucocorticoid signaling. *Science* **289**, 2344-2347 (2000).
79. Sriram, K. & Insel, P.A. G Protein-Coupled Receptors as Targets for Approved Drugs: How Many Targets and How Many Drugs? *Mol Pharmacol* **93**, 251-258 (2018).
80. Howlett, A.C., *et al.* International Union of Pharmacology. XXVII. Classification of cannabinoid receptors. *Pharmacol Rev* **54**, 161-202 (2002).
81. Munro, S., Thomas, K.L. & Abu-Shaar, M. Molecular characterization of a peripheral receptor for cannabinoids. *Nature* **365**, 61-65 (1993).
82. Matsuda, L.A., Lolait, S.J., Brownstein, M.J., Young, A.C. & Bonner, T.I. Structure of a cannabinoid receptor and functional expression of the cloned cDNA. *Nature* **346**, 561-564 (1990).

83. Devane, W.A., Dysarz, F.A., 3rd, Johnson, M.R., Melvin, L.S. & Howlett, A.C. Determination and characterization of a cannabinoid receptor in rat brain. *Mol Pharmacol* **34**, 605-613 (1988).
84. Jarai, Z., *et al.* Cannabinoid-induced mesenteric vasodilation through an endothelial site distinct from CB1 or CB2 receptors. *Proceedings of the National Academy of Sciences of the United States of America* **96**, 14136-14141 (1999).
85. Irving, A., *et al.* Cannabinoid Receptor-Related Orphan G Protein-Coupled Receptors. *Adv Pharmacol* **80**, 223-247 (2017).
86. Console-Bram, L., Brailoiu, E., Brailoiu, G.C., Sharir, H. & Abood, M.E. Activation of GPR18 by cannabinoid compounds: a tale of biased agonism. *British journal of pharmacology* **171**, 3908-3917 (2014).
87. Henstridge, C.M., *et al.* GPR55 ligands promote receptor coupling to multiple signalling pathways. *British journal of pharmacology* **160**, 604-614 (2010).
88. Howlett, A.C. Pharmacology of cannabinoid receptors. *Annu Rev Pharmacol Toxicol* **35**, 607-634 (1995).
89. Herkenham, M., *et al.* Characterization and localization of cannabinoid receptors in rat brain: a quantitative in vitro autoradiographic study. *The Journal of neuroscience : the official journal of the Society for Neuroscience* **11**, 563-583 (1991).
90. Herkenham, M., *et al.* Cannabinoid receptor localization in brain. *Proceedings of the National Academy of Sciences of the United States of America* **87**, 1932-1936 (1990).

91. Wilson, R.I. & Nicoll, R.A. Endocannabinoid signaling in the brain. *Science* **296**, 678-682 (2002).
92. Pertwee, R.G. *Handbook of cannabis*, (Oxford University Press, USA, 2014).
93. Abel, E.L. Marijuana and memory. *Nature* **227**, 1151-1152 (1970).
94. Carlini, E.A., Hamaoui, A., Bieniek, D. & Korte, F. Effects of (–) delta-9-trans-tetrahydrocannabinol and a synthetic derivative on maze performance of rats. *Pharmacology* **4**, 359-368 (1970).
95. Barratt, E.S. & Adams, P.M. Chronic marijuana usage and sleep-wakefulness cycles in cats. *Biol Psychiatry* **6**, 207-214 (1973).
96. Cone, E.J., Johnson, R.E., Paul, B.D., Mell, L.D. & Mitchell, J. Marijuana-laced brownies: behavioral effects, physiologic effects, and urinalysis in humans following ingestion. *J Anal Toxicol* **12**, 169-175 (1988).
97. Bilkei-Gorzo, A. The endocannabinoid system in normal and pathological brain ageing. *Philos Trans R Soc Lond B Biol Sci* **367**, 3326-3341 (2012).
98. Romero, J., *et al.* Time-course of the cannabinoid receptor down-regulation in the adult rat brain caused by repeated exposure to Δ 9-tetrahydrocannabinol. *Synapse* **30**, 298-308 (1998).
99. Canas, P.M., Duarte, J.M., Rodrigues, R.J., Köfalvi, A. & Cunha, R.A. Modification upon aging of the density of presynaptic modulation systems in the hippocampus. *Neurobiology of aging* **30**, 1877-1884 (2009).
100. Mailleux, P. & Vanderhaeghen, J.J. Age-related loss of cannabinoid receptor binding sites and mRNA in the rat striatum. *Neuroscience letters* **147**, 179-181 (1992).

101. Liu, P., Bilkey, D.K., Darlington, C.L. & Smith, P.F. Cannabinoid CB1 receptor protein expression in the rat hippocampus and entorhinal, perirhinal, postrhinal and temporal cortices: regional variations and age-related changes. *Brain research* **979**, 235-239 (2003).
102. Berrendero, F., *et al.* Changes in cannabinoid receptor binding and mRNA levels in several brain regions of aged rats. *Biochimica et Biophysica Acta (BBA)-Molecular Basis of Disease* **1407**, 205-214 (1998).
103. Wang, L., Liu, J., Harvey-White, J., Zimmer, A. & Kunos, G. Endocannabinoid signaling via cannabinoid receptor 1 is involved in ethanol preference and its age-dependent decline in mice. *Proceedings of the National Academy of Sciences* **100**, 1393-1398 (2003).
104. Mato, S. & Pazos, A. Influence of age, postmortem delay and freezing storage period on cannabinoid receptor density and functionality in human brain. *Neuropharmacology* **46**, 716-726 (2004).
105. Westlake, T., Howlett, A., Bonner, T., Matsuda, L. & Herkenham, M. Cannabinoid receptor binding and messenger RNA expression in human brain: an in vitro receptor autoradiography and in situ hybridization histochemistry study of normal aged and Alzheimer's brains. *Neuroscience* **63**, 637-652 (1994).
106. Van Laere, K., *et al.* Gender-dependent increases with healthy aging of the human cerebral cannabinoid-type 1 receptor binding using [18F] MK-9470 PET. *NeuroImage* **39**, 1533-1541 (2008).

107. Piyanova, A., *et al.* Age-related changes in the endocannabinoid system in the mouse hippocampus. *Mechanisms of ageing and development* **150**, 55-64 (2015).
108. Bilkei-Gorzo, A., *et al.* Early age-related cognitive impairment in mice lacking cannabinoid CB1 receptors. *Proceedings of the National Academy of Sciences of the United States of America* **102**, 15670-15675 (2005).
109. Reibaud, M., *et al.* Enhancement of memory in cannabinoid CB1 receptor knock-out mice. *European journal of pharmacology* **379**, R1-2 (1999).
110. Albayram, O., Bilkei-Gorzo, A. & Zimmer, A. Loss of CB1 receptors leads to differential age-related changes in reward-driven learning and memory. *Frontiers in aging neuroscience* **4**, 34 (2012).
111. Sanford, A.E., Castillo, E. & Gannon, R.L. Cannabinoids and hamster circadian activity rhythms. *Brain research* **1222**, 141-148 (2008).
112. Acuna-Goycolea, C., Obrietan, K. & van den Pol, A.N. Cannabinoids excite circadian clock neurons. *The Journal of neuroscience : the official journal of the Society for Neuroscience* **30**, 10061-10066 (2010).
113. Mure, L.S., *et al.* Diurnal transcriptome atlas of a primate across major neural and peripheral tissues. *Science* **359**, eaao0318 (2018).
114. Farnsworth, N.R. Pharmacognosy and chemistry of "cannabis sativa". *J Am Pharm Assoc* **9**, 410-414 passim (1969).
115. Russo, E.B. The pharmacological history of cannabis. *Handbook of cannabis. Oxford University Press, Oxford*, 23-43 (2014).

116. Gaoni, Y. & Mechoulam, R. Isolation, structure, and partial synthesis of an active constituent of hashish. *Journal of the American chemical society* **86**, 1646-1647 (1964).
117. Bow, E.W. & Rimoldi, J.M. The structure–function relationships of classical cannabinoids: CB1/CB2 modulation. *Perspectives in medicinal chemistry* **8**, PMC. S32171 (2016).
118. Russo, E.B. Taming THC: potential cannabis synergy and phytocannabinoid-terpenoid entourage effects. *British journal of pharmacology* **163**, 1344-1364 (2011).
119. Bahi, A., *et al.* β -Caryophyllene, a CB2 receptor agonist produces multiple behavioral changes relevant to anxiety and depression in mice. *Physiology & behavior* **135**, 119-124 (2014).
120. Howlett, A.C. & Abood, M.E. CB1 and CB2 Receptor Pharmacology. *Adv Pharmacol* **80**, 169-206 (2017).
121. Zuardi, A.W. History of cannabis as a medicine: a review. *Rev Bras Psiquiatr* **28**, 153-157 (2006).
122. Zuardi, A.W., *et al.* A critical review of the antipsychotic effects of cannabidiol: 30 years of a translational investigation. *Curr Pharm Des* **18**, 5131-5140 (2012).
123. Soethoudt, M., *et al.* Cannabinoid CB2 receptor ligand profiling reveals biased signalling and off-target activity. *Nature communications* **8**, 13958 (2017).
124. Pertwee, R. The pharmacology of cannabinoid receptors and their ligands: an overview. *International journal of obesity* **30**, S13-S18 (2006).

125. Metna-Laurent, M., Mondesir, M., Grel, A., Vallee, M. & Piazza, P.V. Cannabinoid-Induced Tetrad in Mice. *Curr Protoc Neurosci* **80**, 9 59 51-59 59 10 (2017).
126. Javadi-Paydar, M., *et al.* Effects Of Δ 9-THC And Cannabidiol Vapor Inhalation In Male And Female Rats. *bioRxiv*, 128173 (2017).
127. Hlozek, T., *et al.* Pharmacokinetic and behavioural profile of THC, CBD, and THC+CBD combination after pulmonary, oral, and subcutaneous administration in rats and confirmation of conversion in vivo of CBD to THC. *European neuropsychopharmacology : the journal of the European College of Neuropsychopharmacology* **27**, 1223-1237 (2017).
128. Babson, K.A., Sottile, J. & Morabito, D. Cannabis, Cannabinoids, and Sleep: a Review of the Literature. *Curr Psychiatry Rep* **19**, 23 (2017).
129. Rohleder, C., Muller, J.K., Lange, B. & Leweke, F.M. Cannabidiol as a Potential New Type of an Antipsychotic. A Critical Review of the Evidence. *Front Pharmacol* **7**, 422 (2016).
130. Maldonado, R., Banos, J.E. & Cabanero, D. The endocannabinoid system and neuropathic pain. *Pain* **157 Suppl 1**, S23-32 (2016).
131. Jensen, B., Chen, J., Furnish, T. & Wallace, M. Medical Marijuana and Chronic Pain: a Review of Basic Science and Clinical Evidence. *Curr Pain Headache Rep* **19**, 50 (2015).
132. Long, L.E., *et al.* A behavioural comparison of acute and chronic Delta9-tetrahydrocannabinol and cannabidiol in C57BL/6JArc mice. *Int J Neuropsychopharmacol* **13**, 861-876 (2010).

133. Tai, S., *et al.* Repeated administration of phytocannabinoid Delta(9)-THC or synthetic cannabinoids JWH-018 and JWH-073 induces tolerance to hypothermia but not locomotor suppression in mice, and reduces CB1 receptor expression and function in a brain region-specific manner. *Pharmacological research : the official journal of the Italian Pharmacological Society* **102**, 22-32 (2015).
134. Taffe, M.A. Delta(9)Tetrahydrocannabinol impairs visuo-spatial associative learning and spatial working memory in rhesus macaques. *J Psychopharmacol* **26**, 1299-1306 (2012).
135. Lichtman, A.H., Dimen, K.R. & Martin, B.R. Systemic or intrahippocampal cannabinoid administration impairs spatial memory in rats. *Psychopharmacology (Berl)* **119**, 282-290 (1995).
136. Heyser, C.J., Hampson, R.E. & Deadwyler, S.A. Effects of delta-9-tetrahydrocannabinol on delayed match to sample performance in rats: alterations in short-term memory associated with changes in task specific firing of hippocampal cells. *J Pharmacol Exp Ther* **264**, 294-307 (1993).
137. Nakamura, E.M., da Silva, E.A., Concilio, G.V., Wilkinson, D.A. & Masur, J. Reversible effects of acute and long-term administration of delta-9-tetrahydrocannabinol (THC) on memory in the rat. *Drug Alcohol Depend* **28**, 167-175 (1991).
138. Essman, E.J. Marijuana intoxication in rats: interruption of recent memory and effect on brain concentration of delta 9-tetrahydrocannabinol. *Psychol Rep* **55**, 563-567 (1984).

139. Bilkei-Gorzo, A., *et al.* A chronic low dose of Delta(9)-tetrahydrocannabinol (THC) restores cognitive function in old mice. *Nature medicine* **23**, 782-787 (2017).
140. Fishbein, M., *et al.* Long-term behavioral and biochemical effects of an ultra-low dose of Delta9-tetrahydrocannabinol (THC): neuroprotection and ERK signaling. *Exp Brain Res* **221**, 437-448 (2012).
141. Amal, H., *et al.* Long-term consequences of a single treatment of mice with an ultra-low dose of Delta9-tetrahydrocannabinol (THC). *Behavioural brain research* **206**, 245-253 (2010).
142. Bolla, K.I., Brown, K., Eldreth, D., Tate, K. & Cadet, J.L. Dose-related neurocognitive effects of marijuana use. *Neurology* **59**, 1337-1343 (2002).
143. Suliman, N.A., Taib, C.N.M., Moklas, M.A.M. & Basir, R. Delta-9-Tetrahydrocannabinol ((9)-THC) Induce Neurogenesis and Improve Cognitive Performances of Male Sprague Dawley Rats. *Neurotox Res* (2017).
144. Stark, P. & Dews, P.B. Cannabinoids. I. Behavioral effects. *J Pharmacol Exp Ther* **214**, 124-130 (1980).
145. Morgan, C.J., Schafer, G., Freeman, T.P. & Curran, H.V. Impact of cannabidiol on the acute memory and psychotomimetic effects of smoked cannabis: naturalistic study: naturalistic study [corrected]. *Br J Psychiatry* **197**, 285-290 (2010).
146. Mori, M.A., *et al.* Cannabidiol reduces neuroinflammation and promotes neuroplasticity and functional recovery after brain ischemia. *Prog Neuropsychopharmacol Biol Psychiatry* **75**, 94-105 (2017).

147. McLaughlin, R.J. Toward a Translationally Relevant Preclinical Model of Cannabis Use. *Neuropsychopharmacology* **43**, 213 (2018).
148. Boggs, D.L., Nguyen, J.D., Morgenson, D., Taffe, M.A. & Ranganathan, M. Clinical and Preclinical Evidence for Functional Interactions of Cannabidiol and Delta(9)-Tetrahydrocannabinol. *Neuropsychopharmacology* **43**, 142-154 (2018).
149. McGilveray, I.J. Pharmacokinetics of cannabinoids. *Pain Res Manag* **10 Suppl A**, 15A-22A (2005).
150. Grotenhermen, F. Pharmacokinetics and pharmacodynamics of cannabinoids. *Clin Pharmacokinet* **42**, 327-360 (2003).
151. Martin-Santos, R., *et al.* Acute effects of a single, oral dose of d9-tetrahydrocannabinol (THC) and cannabidiol (CBD) administration in healthy volunteers. *Curr Pharm Des* **18**, 4966-4979 (2012).
152. Ahmed, A.I., *et al.* Safety and pharmacokinetics of oral delta-9-tetrahydrocannabinol in healthy older subjects: a randomized controlled trial. *European neuropsychopharmacology : the journal of the European College of Neuropsychopharmacology* **24**, 1475-1482 (2014).
153. Killestein, J., *et al.* Safety, tolerability, and efficacy of orally administered cannabinoids in MS. *Neurology* **58**, 1404-1407 (2002).
154. Deiana, S., *et al.* Plasma and brain pharmacokinetic profile of cannabidiol (CBD), cannabidivarin (CBDV), Δ 9-tetrahydrocannabivarin (THCV) and cannabigerol (CBG) in rats and mice following oral and intraperitoneal administration and CBD action on obsessive–compulsive behaviour. *Psychopharmacology* **219**, 859-873 (2012).

155. Reagan-Shaw, S., Nihal, M. & Ahmad, N. Dose translation from animal to human studies revisited. *The FASEB journal* **22**, 659-661 (2008).
156. Sarne, Y., Toledano, R., Rachmany, L., Sasson, E. & Doron, R. Reversal of age-related cognitive impairments in mice by an extremely low dose of tetrahydrocannabinol. *Neurobiology of aging* **61**, 177-186 (2018).
157. Grella, C.E., Rodriguez, L. & Kim, T. Patterns of medical marijuana use among individuals sampled from medical marijuana dispensaries in Los Angeles. *Journal of psychoactive drugs* **46**, 263-272 (2014).
158. Vandrey, R., *et al.* Pharmacokinetic Profile of Oral Cannabis in Humans: Blood and Oral Fluid Disposition and Relation to Pharmacodynamic Outcomes. *J Anal Toxicol* **41**, 83-99 (2017).
159. Swortwood, M.J., *et al.* Cannabinoid disposition in oral fluid after controlled smoked, vaporized, and oral cannabis administration. *Drug Test Anal* **9**, 905-915 (2017).
160. Nguyen, J.D., *et al.* Inhaled delivery of Delta(9)-tetrahydrocannabinol (THC) to rats by e-cigarette vapor technology. *Neuropharmacology* **109**, 112-120 (2016).
161. Hart, C.L., *et al.* Comparison of smoked marijuana and oral Delta(9)-tetrahydrocannabinol in humans. *Psychopharmacology (Berl)* **164**, 407-415 (2002).
162. Panee, J., Gerschenson, M. & Chang, L. Associations Between Microbiota, Mitochondrial Function, and Cognition in Chronic Marijuana Users. *Journal of Neuroimmune Pharmacology*, 1-10 (2017).

163. Abel, E.L. Marijuana and memory: acquisition or retrieval? *Science* **173**, 1038-1040 (1971).
164. Abel, E.L. Marijuana, learning, and memory. *Int Rev Neurobiol* **18**, 329-356 (1975).
165. Filbey, F.M., *et al.* Long-term effects of marijuana use on the brain. *Proceedings of the National Academy of Sciences* **111**, 16913-16918 (2014).
166. Long, L.E., *et al.* A behavioural comparison of acute and chronic Δ 9-tetrahydrocannabinol and cannabidiol in C57BL/6JArc mice. *International Journal of Neuropsychopharmacology* **13**, 861-876 (2010).
167. Katsidoni, V., Kastellakis, A. & Panagis, G. Biphasic effects of Δ 9-tetrahydrocannabinol on brain stimulation reward and motor activity. *International journal of neuropsychopharmacology* **16**, 2273-2284 (2013).
168. Rey, A.A., Purrio, M., Viveros, M.-P. & Lutz, B. Biphasic effects of cannabinoids in anxiety responses: CB1 and GABA B receptors in the balance of GABAergic and glutamatergic neurotransmission. *Neuropsychopharmacology* **37**, 2624 (2012).
169. Sulcova, E., Mechoulam, R. & Fride, E. Biphasic effects of anandamide. *Pharmacol Biochem Behav* **59**, 347-352 (1998).
170. Crawley, J.N., *et al.* Anandamide, an endogenous ligand of the cannabinoid receptor, induces hypomotility and hypothermia in vivo in rodents. *Pharmacol Biochem Behav* **46**, 967-972 (1993).

171. Taylor, D.A. & Fennessy, M.R. Biphasic nature of the effects of delta9-tetrahydrocannabinol on body temperature and brain amines of the rat. *European journal of pharmacology* **46**, 93-99 (1977).
172. Grisham, M.G. & Ferraro, D.P. Biphasic effects of 9 -tetrahydrocannabinol on variable interval schedule performance in rats. *Psychopharmacologia* **27**, 163-169 (1972).
173. Sofia, R.D. A paradoxical effect for 1 -tetrahydrocannabinol on rectal temperature in rats. *Res Commun Chem Pathol Pharmacol* **4**, 281-288 (1972).
174. Tselnicker, I., Keren, O., Hefetz, A., Pick, C.G. & Sarne, Y. A single low dose of tetrahydrocannabinol induces long-term cognitive deficits. *Neuroscience letters* **411**, 108-111 (2007).
175. Marchalant, Y., Cerbai, F., Brothers, H.M. & Wenk, G.L. Cannabinoid receptor stimulation is anti-inflammatory and improves memory in old rats. *Neurobiology of aging* **29**, 1894-1901 (2008).
176. Calabrese, E.J. & Rubio-Casillas, A. Biphasic effects of THC in memory and cognition. *European journal of clinical investigation* **48**, e12920 (2018).
177. Calabrese, E.J. & Baldwin, L.A. Defining hormesis. *Human & experimental toxicology* **21**, 91-97 (2002).
178. Calabrese, E.J. Hormetic mechanisms. *Crit Rev Toxicol* **43**, 580-606 (2013).
179. Calabrese, E.J. Hormesis: Path and Progression to Significance. *International journal of molecular sciences* **19**(2018).

180. Sarne, Y., Asaf, F., Fishbein, M., Gafni, M. & Keren, O. The dual neuroprotective–neurotoxic profile of cannabinoid drugs. *British journal of pharmacology* **163**, 1391-1401 (2011).
181. Calabrese, E.J. Preconditioning is hormesis part I: Documentation, dose-response features and mechanistic foundations. *Pharmacological Research* **110**, 242-264 (2016).
182. Sarne, Y. THC for age-related cognitive decline? *Aging* **10**, 3628-3629 (2018).
183. Calabrese, E.J. & Mattson, M.P. How does hormesis impact biology, toxicology, and medicine? *NPJ Aging Mech Dis* **3**, 13 (2017).
184. Gidday, J.M. Extending injury-and disease-resistant CNS phenotypes by repetitive epigenetic conditioning. *Frontiers in neurology* **6**, 42 (2015).
185. Zlebnik, N.E. & Cheer, J.F. Beyond the CB1 Receptor: Is Cannabidiol the Answer for Disorders of Motivation? *Annu Rev Neurosci* **39**, 1-17 (2016).
186. Jenniches, I., *et al.* Anxiety, Stress, and Fear Response in Mice With Reduced Endocannabinoid Levels. *Biol Psychiatry* **79**, 858-868 (2016).
187. Wotjak, C.T. Role of endogenous cannabinoids in cognition and emotionality. *Mini Rev Med Chem* **5**, 659-670 (2005).
188. Witkin, J.M., Tzavara, E.T. & Nomikos, G.G. A role for cannabinoid CB1 receptors in mood and anxiety disorders. *Behav Pharmacol* **16**, 315-331 (2005).
189. Abel, E.L. Chronopharmacology of delta9-tetrahydrocannabinol hypothermia in mice. *Experientia* **29**, 1528-1529 (1973).
190. Pertwee, R.G. & Tavendale, R. EFFECTS OF Δ 9-TETRAHYDROCANNABINOL, 2,4-DINITROPHENOL AND PENTOLINIUM TARTRATE ON BEHAVIOURAL

- THERMOREGULATION IN MICE. *British journal of pharmacology* **66**, 39-50 (1979).
191. Craft, R.M., Marusich, J.A. & Wiley, J.L. Sex differences in cannabinoid pharmacology: a reflection of differences in the endocannabinoid system? *Life sciences* **92**, 476-481 (2013).
192. Makela, P., *et al.* Low doses of Δ -9 tetrahydrocannabinol (THC) have divergent effects on short-term spatial memory in young, healthy adults. *Neuropsychopharmacology* **31**, 462 (2006).
193. Senn, R., Keren, O., Hefetz, A. & Sarne, Y. Long-term cognitive deficits induced by a single, extremely low dose of tetrahydrocannabinol (THC): behavioral, pharmacological and biochemical studies in mice. *Pharmacol Biochem Behav* **88**, 230-237 (2008).
194. Dallmann, R., Brown, S.A. & Gachon, F. Chronopharmacology: new insights and therapeutic implications. *Annual review of pharmacology and toxicology* **54**, 339-361 (2014).
195. Hodges, E.L. & Ashpole, N.M. Aging circadian rhythms and cannabinoids. *Neurobiology of aging* **79**, 110-118 (2019).
196. Martin, B.R., Compton, D.R., Little, P.J., Martin, T.J. & Beardsley, P.M. Pharmacological evaluation of agonistic and antagonistic activity of cannabinoids. *NIDA Res Monogr* **79**, 108-122 (1987).
197. Little, P.J., Compton, D.R., Johnson, M.R., Melvin, L.S. & Martin, B.R. Pharmacology and stereoselectivity of structurally novel cannabinoids in mice. *J Pharmacol Exp Ther* **247**, 1046-1051 (1988).

198. Fan, F., Compton, D.R., Ward, S., Melvin, L. & Martin, B.R. Development of cross-tolerance between delta 9-tetrahydrocannabinol, CP 55,940 and WIN 55,212. *Journal of Pharmacology and Experimental Therapeutics* **271**, 1383-1390 (1994).
199. Brents, L.K., *et al.* Monohydroxylated metabolites of the K2 synthetic cannabinoid JWH-073 retain intermediate to high cannabinoid 1 receptor (CB1R) affinity and exhibit neutral antagonist to partial agonist activity. *Biochemical pharmacology* **83**, 952-961 (2012).
200. Spiller, K.J., *et al.* Cannabinoid CB1 and CB2 receptor mechanisms underlie cannabis reward and aversion in rats. *Br J Pharmacol* **176**, 1268-1281 (2019).
201. Shearman, L., *et al.* Antidepressant-like and anorectic effects of the cannabinoid CB1 receptor inverse agonist AM251 in mice. *Behavioural pharmacology* **14**, 573-582 (2003).
202. Navarrete, F., *et al.* Role of CB2 cannabinoid receptors in the rewarding, reinforcing, and physical effects of nicotine. *Neuropsychopharmacology* **38**, 2515-2524 (2013).
203. Simon, P., Dupuis, R. & Costentin, J. Thigmotaxis as an index of anxiety in mice. Influence of dopaminergic transmissions. *Behavioural brain research* **61**, 59-64 (1994).
204. Pacher, P., Batkai, S. & Kunos, G. Cardiovascular pharmacology of cannabinoids. in *Cannabinoids* 599-625 (Springer, 2005).
205. Friedhoff, A.J. & Miller, J.C. Clinical implications of receptor sensitivity modification. *Annual review of neuroscience* **6**, 121-148 (1983).

206. Howlett, A.C., *et al.* Endocannabinoid tone versus constitutive activity of cannabinoid receptors. *Br J Pharmacol* **163**, 1329-1343 (2011).
207. Christie, S., O'Rielly, R., Li, H., Wittert, G.A. & Page, A.J. Biphasic effects of methanandamide on murine gastric vagal afferent mechanosensitivity. *The Journal of physiology* **598**, 139-150 (2020).
208. Ashpole, N.M., *et al.* IGF-1 has sexually dimorphic, pleiotropic, and time-dependent effects on healthspan, pathology, and lifespan. *Geroscience* **39**, 129-145 (2017).
209. Piotrowska, Z., *et al.* Sex differences in distribution of cannabinoid receptors (CB1 and CB2), S100A6 and CacyBP/SIP in human ageing hearts. *Biol Sex Differ* **9**, 50 (2018).
210. Fattore, L. & Fratta, W. How important are sex differences in cannabinoid action? *Br J Pharmacol* **160**, 544-548 (2010).
211. Farquhar, C.E., *et al.* Sex, THC, and hormones: Effects on density and sensitivity of CB1 cannabinoid receptors in rats. *Drug Alcohol Depend* **194**, 20-27 (2019).
212. Cooper, Z.D. & Haney, M. Sex-dependent effects of cannabis-induced analgesia. *Drug and alcohol dependence* **167**, 112-120 (2016).
213. Wiesenfeld-Hallin, Z. Sex differences in pain perception. *Gender medicine* **2**, 137-145 (2005).
214. Cuttler, C., Mischley, L.K. & Sexton, M. Sex differences in cannabis use and effects: a cross-sectional survey of cannabis users. *Cannabis and cannabinoid research* **1**, 166-175 (2016).

215. Matheson, J., *et al.* Sex differences in the acute effects of smoked cannabis: evidence from a human laboratory study of young adults. *Psychopharmacology*, 1-12 (2019).
216. Schubert, D., *et al.* Efficacy of Cannabinoids in a Pre-Clinical Drug-Screening Platform for Alzheimer's Disease. *Molecular neurobiology* **56**, 7719-7730 (2019).
217. Cristino, L., Bisogno, T. & Di Marzo, V. Cannabinoids and the expanded endocannabinoid system in neurological disorders. *Nature Reviews Neurology*, 1-21 (2019).
218. Bassir Nia, A., Medrano, B., Perkel, C., Galynker, I. & Hurd, Y.L. Psychiatric comorbidity associated with synthetic cannabinoid use compared to cannabis. *Journal of psychopharmacology* **30**, 1321-1330 (2016).
219. McGowan, N.E., Scantlebury, D.M., Maule, A.G. & Marks, N.J. Measuring the emissivity of mammal pelage. *Quantitative InfraRed Thermography Journal* **15**, 214-222 (2018).
220. Faul, F., Erdfelder, E., Lang, A.-G. & Buchner, A. G* Power 3: A flexible statistical power analysis program for the social, behavioral, and biomedical sciences. *Behavior research methods* **39**, 175-191 (2007).
221. Milanović, Z., *et al.* Age-related decrease in physical activity and functional fitness among elderly men and women. *Clinical interventions in aging* **8**, 549 (2013).
222. Emerich, D., *et al.* Locomotion of aged rats: relationship to neurochemical but not morphological changes in nigrostriatal dopaminergic neurons. *Brain research bulletin* **32**, 477-486 (1993).

223. Allen, E., Carlson, K.M., Zigmond, M.J. & Cavanaugh, J.E. L-DOPA reverses motor deficits associated with normal aging in mice. *Neuroscience letters* **489**, 1-4 (2011).
224. Hood, S. & Amir, S. The aging clock: circadian rhythms and later life. *The Journal of clinical investigation* **127**, 437-446 (2017).
225. Deboer, T., Ruijgrok, G. & Meijer, J.H. Short light-dark cycles affect sleep in mice. *The European journal of neuroscience* **26**, 3518-3523 (2007).
226. Tanda, G., Pontieri, F.E. & Di Chiara, G. Cannabinoid and heroin activation of mesolimbic dopamine transmission by a common μ 1 opioid receptor mechanism. *Science* **276**, 2048-2050 (1997).
227. Mangiafico, S. Summary and analysis of extension program evaluation in R, version 1.15. 0. URL <https://rcompanion.org/handbook> (2016).
228. Dinno, A. dunn. test: Dunn's test of multiple comparisons using rank sums. *R package version 1* (2017).
229. Ahlmann-Eltze, C. ggsignif: Significance Brackets for 'ggplot2'. *R package version 0.4. 0* (2017).
230. Auguie, B. gridExtra: miscellaneous functions for "grid" graphics. *R package version 2* (2017).
231. Pohlert, T. PMCMRplus: calculate pairwise multiple comparisons of mean rank sums extended. *R package version 1* (2018).
232. Pohlert, T. The pairwise multiple comparison of mean ranks package (PMCMR). *R package* **27**, 9 (2014).

233. Ogle, D., Wheeler, P. & Dinno, A. FSA: fisheries stock analysis. R package version 0.8. 22. (Recuperado de: <https://github.com/droglenc/FSA>, 2018).
234. Urbanek, S. & Horner, J. Cairo: R graphics device using cairo graphics library for creating high-quality bitmap (PNG, JPEG, TIFF), vector (PDF, SVG, PostScript) and display (X11 and Win32) output [Software]. *R package version*, 1.5-9 (2015).
235. Sievert, C., *et al.* plotly: Create Interactive Web Graphics via 'plotly. js'. *R package version 4*, 110 (2017).
236. Hothorn, T., Bretz, F. & Westfall, P. Simultaneous inference in general parametric models. *Biometrical Journal: Journal of Mathematical Methods in Biosciences* **50**, 346-363 (2008).
237. Kassambara, A. ggpubr: "ggplot2" based publication ready plots. *R package version 0.1 6*(2017).
238. Wickham, H. Tidyverse: Easily install and load the 'tidyverse'. *R package version 1*, 2017 (2017).
239. Team, R. RStudio: integrated development for R. *RStudio, Inc., Boston, MA URL <http://www.rstudio.com>* **42**, 14 (2015).
240. Turner, M.J., Kleeberger, S.R. & Lightfoot, J.T. Influence of genetic background on daily running-wheel activity differs with aging. *Physiological genomics* **22**, 76-85 (2005).
241. Manzanares, G., Brito-da-Silva, G. & Gandra, P. Voluntary wheel running: patterns and physiological effects in mice. *Brazilian Journal of Medical and Biological Research* **52**(2019).

242. McGregor, I.S., Issakidis, C.N. & Prior, G. Aversive effects of the synthetic cannabinoid CP 55,940 in rats. *Pharmacology Biochemistry and Behavior* **53**, 657-664 (1996).
243. Justice, M.J. & Dhillon, P. Using the mouse to model human disease: increasing validity and reproducibility. (The Company of Biologists Ltd, 2016).
244. Sliwinski, M.J., Hofer, S.M., Hall, C., Buschke, H. & Lipton, R.B. Modeling memory decline in older adults: the importance of preclinical dementia, attrition, and chronological age. *Psychology and aging* **18**, 658 (2003).
245. Unnikrishnan, A., Deepa, S.S., Herd, H.R. & Richardson, A. Extension of Life Span in Laboratory Mice. in *Conn's Handbook of Models for Human Aging* 245-270 (Elsevier, 2018).
246. Conti, A. & Maestroni, G.J. HPLC validation of a circadian melatonin rhythm in the pineal gland of inbred mice. *Journal of pineal research* **20**, 138-144 (1996).
247. Stehle, J., Von Gall, C. & Korf, H.W. Melatonin: a clock-output, a clock-input. *Journal of neuroendocrinology* **15**, 383-389 (2003).
248. Martin, B.R., *et al.* Behavioral, biochemical, and molecular modeling evaluations of cannabinoid analogs. *Pharmacol Biochem Behav* **40**, 471-478 (1991).
249. Compton, D.R., *et al.* Cannabinoid structure-activity relationships: correlation of receptor binding and in vivo activities. *J Pharmacol Exp Ther* **265**, 218-226 (1993).
250. Wang, L., *et al.* Enriched physical environment attenuates spatial and social memory impairments of aged socially isolated mice. *International Journal of Neuropsychopharmacology* **21**, 1114-1127 (2018).

251. Leise, T., *et al.* Voluntary exercise can strengthen the circadian system in aged mice. *Age* **35**, 2137-2152 (2013).
252. Yasumoto, Y., Nakao, R. & Oishi, K. Free access to a running-wheel advances the phase of behavioral and physiological circadian rhythms and peripheral molecular clocks in mice. *PLoS one* **10**(2015).
253. Winfree, A.T. Oscillating systems. On emerging coherence. *Science* **298**, 2336-2337 (2002).
254. Savi, M. Chaos and order in biomedical rhythms. *Journal of the Brazilian Society of Mechanical Sciences and Engineering* **27**, 157-169 (2005).
255. Ukai, H. & Ueda, H.R. Systems biology of mammalian circadian clocks. *Annual review of physiology* **72**, 579-603 (2010).
256. Knudson, A.G. Hereditary cancer: two hits revisited. *Journal of cancer research and clinical oncology* **122**, 135-140 (1996).
257. Kelso, J.S. *Dynamic patterns: The self-organization of brain and behavior*, (MIT press, 1995).
258. Kennedy, B.K., *et al.* Geroscience: linking aging to chronic disease. *Cell* **159**, 709-713 (2014).

APPENDIX

MATLAB CODE

Step 1 - Import Merged CSV Counts

```
%%%%%%%%%%%%%%%%%%%%%%%%%%%%%%%%%%%%%%%%%%%%%%%%%%%%%%%%%%%%%%%%%%%%%%%%%
%%
%% Running_wheel_Analysis_MASTER (February 2020) - Erik Hodges
%%
%%%%%%%%%%%%%%%%%%%%%%%%%%%%%%%%%%%%%%%%%%%%%%%%%%%%%%%%%%%%%%%%%%%%%%%%%
%%
% This program takes in exported ClockLab Counts (.csv) which have been
% consolidated using Excel macros stored in the
% "Format_Counts_Master_May.xlsx" file. The goal of this script is to
% reformat the DateTime for Zeitgeber Time (ZT) and save the formatted
file
% as a .mat for future analysis.
%%%%%%%%%%%%%%%%%%%%%%%%%%%%%%%%%%%%%%%%%%%%%%%%%%%%%%%%%%%%%%%%%%%%%%%%%
%%
%%%%%%%%%%%%%%%%%%%%%%%%%%%%%%%%%%%%%%%%%%%%%%%%%%%%%%%%%%%%%%%%%%%%%%%%%
%%

% Clear All Current variables and Console
%
clear all;
close all;
clc
%}

format long;
%%%%%%%%%%%%%%%%%%%%%%%%%%%%%%%%%%%%%%%%%%%%%%%%%%%%%%%%%%%%%%%%%%%%%%%%%
%%
```

Importing

```
Data%%%%%%%%%%%%%%%%%%%%%%%%%%%%%%%%%%%%%%%%%%%%%%%%%%%%%%%%%%%%%%%%%%%%%%%%%
%%%%%%%%%%%%%%%%%%%%%%%%%%%%%%%%%%%%%%%%%%%%%%%%%%%%%%%%%%%%%%%%%%%%%%%%%
```

```
File_Folder = 'C:\Users\erikh\Desktop\Lab Notebook\DATA\Running  
Wheels\Data_Analysis\Data\Input\Merged_Raw_In_Excel**\*.csv';  
CSV_Directory = dir(File_Folder);
```

```
for i = 1:numel(CSV_Directory)  
    CSV_Files(i) = string(CSV_Directory(i).name);  
end
```

```
CSV_Files = CSV_Files(1:end)';
```

```
for q = 1:numel(CSV_Files)
```

```
    % This was added in to specifically remake the  
    % CP_YF_3.mat file after realizing that the original recordings  
hadn't  
    % adjusted for DST and therefore were out of sync with the lights,  
since  
    % the animals were becoming active at 9:00 and 21:00. If working with  
    % this data set in the future, please confirm that CP_YF_3 is  
adjusted  
    % by -1 hours and that ZT is calculated correctly. This is done by  
    % looking through this code and adding back the "if" statements that  
    % target file == "CP_YF_3.csv"  
  
    % if file == "CP_YF_3.csv";  
  
    % file = 'CP_YF_3.csv';  
  
    file = CSV_Files(q);  
    opts = detectImportOptions(file);  
    opts = detectImportOptions(file, 'DatetimeType', 'text');  
  
    ImportedData = readtable(file,opts);  
  
    % For some reason when the data is imported there is a large chunk of
```

empty cells added to the end of the recording

```
ImportedData(ImportedData.Date=="", :) = [];
```

This formats the DateTime as it comes out from ClockLab

```
ImportedData.NewDateTime = strcat(ImportedData.Date, {'
'}, ImportedData.Time);
ImportedData = movevars(ImportedData, 'NewDateTime', 'Before',
'Day');
ImportedData.NewDateTime =
datetime(ImportedData.NewDateTime, 'InputFormat', 'dd-MMM-yy HH:mm');

NewDateTime = ImportedData.NewDateTime;
NewDateTime.Format = 'MMM-dd-yyyy HH:mm:ss';
ImportedData.Date = NewDateTime;
ImportedData.Properties.VariableNames(1) = {'DateTime'};

ImportedData_Columns = ImportedData.Properties.VariableNames'; %save
the header text as a variable

ImportedData.Time = [];
ImportedData.NewDateTime = [];
ImportedData.Day = [];
ImportedData.Hr = [];

if any(ImportedData_Columns() == "Min") > 0
    ImportedData.Min = [];
end

clear('NewDateTime', 'opts');

ImportedData_Columns = ImportedData.Properties.VariableNames'; %save
the header text as a variable

ExpNames = {'Base_YM_1'; 'Base_OM_1'; 'Base_YF_1'; 'Base_OF_1'; ...
'CP_YM_1'; 'CP_YM_2'; 'CP_YM_3'; 'CP_YF_1'; 'CP_YF_2'; 'CP_YF_3'; 'CP_OM_1'; 'CP
_OF_1'; ...
'Pilot_Cipro_1'; 'Pilot_OM_1'};

% This if statement is to adjust for the fact that the computer
```

didn't recognize DST during CP_YF_3

```
%  
if file == "CP_YF_3.csv"  
    ImportedData.DateTime = ImportedData.DateTime - hours(1);  
end  
%}  
  
%}
```

```
%%%%%%%%%%%%%%%%%%%%%%%%%%%%%%%%%%%%%%%%%%%%%%%%%%%%%%%%%%%%  
%%
```

Define Experimental Variables

```
%%%%%%%%%%%%%%%%%%%%%%%%%%%%%%%%%%%%%%%%%%%%%%%%%%%%%%%%%%%%  
%%
```

```
fs = 1/60; % Sample rate, which is set in ClockLab (1 minute =  
1/60sec)  
  
MinutesInDay = 1440;  
  
LightsOffHr = 8; % Input the time that lights turn off  
LightsonHr = 20; % Input the time that lights turn on  
LightsOffMinute = LightsOffHr * 60; % This corresponds to 8:00am  
LightsonMinute = LightsonHr * 60; % This corresponds to 8:00pm  
  
%}
```

ZT Data Padding to BEGINNING of Record

```
% AFTER RUNNING INTO THE PROBLEM WHERE I NEEDED TO PAD THE END OF THE  
% RECORDINGS I DISCOVERED A BETTER WAY TO "ROUND" THE RECORDINGS AND  
% EMPLOYED THIS METHOD TO ROUND THE END OF THE RECORDINGS UP TO  
% 20:00:00, HOWEVER I DID NOT GO BACK AND EMPLOY THIS METHOD TO THE  
% PADDING AT THE BEGINNING OF THE RECORDINGS, BUT I SHOULD DO THIS IN  
% THE FUTURE.
```

```

% New NaN padding to the front of a time series so that ZT can be
% calculated from the moment of LIGHTS ON (20:00:00)

FirstTime = min(ImportedData.DateTime);
NewStart = FirstTime-hours(4); % By doing it this way it does not
adjust for the case when I have to -1 hour for DST

% This if statement is to adjust for the fact that the computer
didn't recognize DST during CP_YF_3
%

if file == "CP_YF_3.csv"
    NewStart = FirstTime-hours(3);
end
%}

TimeDiff = NewStart - FirstTime;

PadTable = ImportedData(1,:);
PadTable(2,:) = PadTable(1,:);
PadTable{2,2:end} = NaN;
Time2Add = FirstTime+TimeDiff; %-'00:01:00'; %might need to add this
extra minute back at some point
PadTable{2,1} = Time2Add;

TTpad = table2timetable(PadTable);
TTadd =
retime(TTpad,'regular','fillwithmissing','TimeStep','00:01:00');
TTadd(end,:) = [];
TTadd = timetable2table(TTadd);
PaddedData = [ImportedData;TTadd];

ImportedData = PaddedData;
ImportedData = sortrows(ImportedData,'DateTime','ascend');

```

ZT Data Padding to END of Record

```

% In this case it is not always clear that it is optimal to 'trim'
the
% final day to end on 20:00:00, therefore I will write a block of

```


code

```
% to pad (round up) the last day to 20:00:00

LastTime = max(ImportedData.DateTime); % Jan-18-2019 15:59:00
NewEnd = LastTime;
NewEnd.Hour = 20 * ceil(NewEnd.Hour/20); % Jan-18-2019 20:59:00
NewEnd.Minute = floor(NewEnd.Minute/60); % Jan-18-2019 20:00:00

EndDiff = NewEnd - LastTime;

PadTable = ImportedData(end,:);
PadTable(2,:) = PadTable(end,:);
PadTable{2,2:end} = NaN;
Time2Add = LastTime+EndDiff; %-'00:01:00'; %might need to add this
extra minute back at some point
PadTable{2,1} = Time2Add;

TTpad = table2timetable(PadTable);
TTadd =
retime(TTpad,'regular','fillwithmissing','TimeStep','00:01:00');
% TTadd(end,:) = []; % I believe I want to keep this last row, so the
recording ends at an even 20:00:00
TTadd = timetable2table(TTadd);
TTadd(1,:) = []; % I introduced a duplicated row and need to get rid
of it before merging with the ImportedData

PaddedData = [ImportedData;TTadd];

ImportedData = PaddedData;
ImportedData = sortrows(ImportedData,'DateTime','ascend');

% This if statement is to adjust for the fact that the computer
didn't recognize DST during CP_YF_3
% This is a terrible way of doing this, but I don't have time to fix
this more elegantly
%
% if file == "CP_YF_3.csv"
%     NewEnd = LastTime-hours(3);
% end
%}
```

```
ImportedData = ImportedData(ImportedData.DateTime<=NewEnd,:);
```

```
%%%%%%%%%%%%%%%%%%%%%%%%%%%%%%%%%%%%%%%%%%%%%%%%%%%%%%%%%%%%%%%%%%%%%%%%  
%%
```

Data Organization and Orientation

```
%%%%%%%%%%%%%%%%%%%%%%%%%%%%%%%%%%%%%%%%%%%%%%%%%%%%%%%%%%%%%%%%%%%%%%%%  
%%
```

Create Timeline Variables for ZT, such as minutes/hours/etc.

```
DataLength = height(ImportedData);  
  
ZTDur = ImportedData.DateTime;  
ZTDur = ZTDur - ZTDur(1);  
  
ImportedData.ZTDuration = ZTDur;  
ImportedData.ZTDay = days(ImportedData.ZTDuration);  
ImportedData.ZTHour = hours(ImportedData.ZTDuration);  
ImportedData.ZTMinute = minutes(ImportedData.ZTDuration);  
ImportedData.ZTDayBin = fix(ImportedData.ZTDay);  
ImportedData.ZTHourBin = fix(ImportedData.ZTHour);  
ImportedData.ZTMinuteBin = fix(ImportedData.ZTMinute);  
  
for i=1>DataLength  
    if ImportedData.ZTDayBin(i) >= 1  
        ImportedData.ZTHourBin(i) = ImportedData.ZTHourBin(i)-  
(24*ImportedData.ZTDayBin(i));  
        ImportedData.ZTMinuteBin(i) = ImportedData.ZTMinuteBin(i)-  
(1440*ImportedData.ZTDayBin(i));  
    end  
end  
  
ImportedData.ClockHourBin = hour(ImportedData.DateTime);  
ImportedData.ClockMinuteOfDay =  
(ImportedData.ClockHourBin*60)+(minute(ImportedData.DateTime));
```

```

    ImportedData = movevars(ImportedData,
{'ZTDuration';'ZTDay';'ZTHour';'ZTMinute';'ZTDayBin';'ZTHourBin';'ZTMinut
eBin';'ClockHourBin';'ClockMinuteOfDay'}, 'After',1);
    %clearvars -except ImportedData Base_YM_1 ExpNames Files

    ImportedData_Columns = ImportedData.Properties.VariableNames'; %save
the header text as a variable

    New_File_Name = strrep(file, '.csv', '.mat');

    assignin('base',strrep(file, '.csv', ''),ImportedData)

    save(New_File_Name,strrep(file, '.csv', ''))

```

end

Step 2 - Add Metadata

```

% Clear All Current Variables and Console
%
clear all;
close all;
clc
%}

format long;

```

Load Files

```

Files = {...
    'Base_YM_1.mat';'Base_YF_1.mat';'Base_OM_1.mat';'Base_OF_1.mat';...

    'CP_YM_1.mat';'CP_YM_2.mat';'CP_YM_3.mat';'CP_YF_1.mat';'CP_YF_2.mat';'CP
_YF_3.mat';'CP_OM_1.mat';'CP_OF_1.mat';...
    'Pilot_Cipro_1.mat';'Pilot_OM_1.mat'};

ExpNames = {...

```

```

    'Base_YM_1'; 'Base_YF_1'; 'Base_OM_1'; 'Base_OF_1'; ...

    'CP_YM_1'; 'CP_YM_2'; 'CP_YM_3'; 'CP_YF_1'; 'CP_YF_2'; 'CP_YF_3'; 'CP_OM_1'; 'CP_
_OF_1'; ...
    'Pilot_Cipro_1'; 'Pilot_OM_1'};

wheelNums =
{'01'; '02'; '03'; '04'; '05'; '06'; '07'; '08'; '09'; '10'; '11'; '12'; '13'; '14'};

wheelNames =
{'wheel_01'; 'wheel_02'; 'wheel_03'; 'wheel_04'; 'wheel_05'; 'wheel_06'; 'wheel_
_07'; ...

'wheel_08'; 'wheel_09'; 'wheel_10'; 'wheel_11'; 'wheel_12'; 'wheel_13'; 'wheel_
14'};

for i = 1: numel(Files)
    load(Files{i});
end

```

Add the MetaData to the 'wide' data files

```

DataStruct = struct(...
    'Base_YM_1', {Base_YM_1, 'Base_YM_1_Metadata.csv', 'Base_YM_1.csv'}, ...
    'Base_YF_1', {Base_YF_1, 'Base_YF_1_Metadata.csv', 'Base_YF_1.csv'}, ...
    'Base_OM_1', {Base_OM_1, 'Base_OM_1_Metadata.csv', 'Base_OM_1.csv'}, ...
    'Base_OF_1', {Base_OF_1, 'Base_OF_1_Metadata.csv', 'Base_OF_1.csv'}, ...
    'CP_YM_1', {CP_YM_1, 'CP_YM_1_Metadata.csv', 'CP_YM_1.csv'}, ...
    'CP_YM_2', {CP_YM_2, 'CP_YM_2_Metadata.csv', 'CP_YM_2.csv'}, ...
    'CP_YM_3', {CP_YM_3, 'CP_YM_3_Metadata.csv', 'CP_YM_3.csv'}, ...
    'CP_YF_1', {CP_YF_1, 'CP_YF_1_Metadata.csv', 'CP_YF_1.csv'}, ...
    'CP_YF_2', {CP_YF_2, 'CP_YF_2_Metadata.csv', 'CP_YF_2.csv'}, ...
    'CP_YF_3', {CP_YF_3, 'CP_YF_3_Metadata.csv', 'CP_YF_3.csv'}, ...
    'CP_OM_1', {CP_OM_1, 'CP_OM_1_Metadata.csv', 'CP_OM_1.csv'}, ...
    'CP_OF_1', {CP_OF_1, 'CP_OF_1_Metadata.csv', 'CP_OF_1.csv'}, ...

    'Pilot_Cipro_1', {Pilot_Cipro_1, 'Pilot_Cipro_1_Metadata.csv', 'Pilot_Cipro_
1.csv'}, ...

    'Pilot_OM_1', {Pilot_OM_1, 'Pilot_OM_1_Metadata.csv', 'Pilot_OM_1.csv'});

NewStruct = DataStruct;

```

```

for i = 1:length(ExpNames)

CurExp = DataStruct(1).(ExpNames{i});

Columns = CurExp.Properties.VariableNames';

opts = detectImportOptions(DataStruct(2).(ExpNames{i}));

opts =
setvartype(opts,{'Experiment';'Cage';'Animal';'DOB';'Age';'Sex';'Cohort';
'Supplier';'wheel';'Lights'},'categorical');

%opts = setvartype(opts,{'DOB'},'datetime');
%opts = setvartype(opts,'DatetimeType','text');

CurMeta = readtable(DataStruct(2).(ExpNames{i}),opts);
CurMeta.DOB =
datetime(string(CurMeta.DOB),'InputFormat','MM/dd/yyyy','Format','MMM-dd-
yyyy');

MetaVars = CurMeta.Properties.VariableNames';

Columns(11:24) = {'wheel_1';'wheel_2';'wheel_3';'wheel_4';...
'wheel_5';'wheel_6';'wheel_7';'wheel_8';'wheel_9';'wheel_10';...
'wheel_11';'wheel_12';'wheel_13';'wheel_14'};

CurExp.Properties.VariableNames = Columns;

Timeline = CurExp(:,1:10);

w01 = [Timeline CurExp(:,11)];
w02 = [Timeline CurExp(:,12)];
w03 = [Timeline CurExp(:,13)];
w04 = [Timeline CurExp(:,14)];
w05 = [Timeline CurExp(:,15)];
w06 = [Timeline CurExp(:,16)];
w07 = [Timeline CurExp(:,17)];
w08 = [Timeline CurExp(:,18)];
w09 = [Timeline CurExp(:,19)];

```

```

w10 = [Timeline CurExp(:,20)];
w11 = [Timeline CurExp(:,21)];
w12 = [Timeline CurExp(:,22)];
w13 = [Timeline CurExp(:,23)];
w14 = [Timeline CurExp(:,24)];

wheels = {w01,w02,w03,w04,w05,w06,w07,w08,w09,w10,w11,w12,w13,w14}';

for k = 1:14
    CurWheel = wheels{k};

    CurWheel.Experiment(:) = CurMeta{k,1};
    CurWheel.Cage(:) = CurMeta{k,2};
    CurWheel.Animal(:) = CurMeta{k,3};
    CurWheel.Age(:) = CurMeta{k,4};
    CurWheel.DOB(:) = CurMeta{k,5};
    CurWheel.Sex(:) = CurMeta{k,6};
    CurWheel.Cohort(:) = CurMeta{k,7};
    CurWheel.Supplier(:) = CurMeta{k,8};
    CurWheel.Wheel(:) = CurMeta{k,9};
    CurWheel.Lights(:) = CurMeta{k,10};

    VarNames = CurWheel.Properties.VariableNames';

    CurWheel = movevars(CurWheel,[12:21],'Before','DateTime');

    CurWheel.Properties.VariableNames(21)={'Counts'};

    wheels{k,2} = CurWheel;

end

FullTable = wheels{1,2};

for m = 2:14
    FullTable = [FullTable;wheels{m,2}];
end

NewStruct(1).(ExpNames{i}) = FullTable;

clear('FullTable','wheels','CurWheel','Timeline','CurExp','CurMeta',...

```

```
'w01', 'w02', 'w03', 'w04', 'w05', 'w06', 'w07', 'w08', 'w09', 'w10', 'w11', 'w12', 'w13', 'w14');
end
```

```
clearvars -except ExpNames NewStruct MetaVars wheelNames wheelNums
```

Stack all individual tables and save as create 'All_Wheel_Data_With_Meta.mat'

```
All_Data = [...
    NewStruct(1).Base_YM_1;...
    NewStruct(1).Base_YF_1;...
    NewStruct(1).Base_OM_1;...
    NewStruct(1).Base_OF_1;...
    NewStruct(1).CP_YM_1;...
    NewStruct(1).CP_YM_2;...
    NewStruct(1).CP_YM_3;...
    NewStruct(1).CP_YF_1;...
    NewStruct(1).CP_YF_2;...
    NewStruct(1).CP_YF_3;...
    NewStruct(1).CP_OM_1;...
    NewStruct(1).CP_OF_1;...
    NewStruct(1).Pilot_Cipro_1;...
    NewStruct(1).Pilot_OM_1];

% save('All_wheel_Data_With_Meta.mat', 'All_Data');

clearvars NewStruct
```

Build The Data Structure from the MegaTable

```
%Files = {'All_wheel_Data_With_Meta.mat'};

%{
for i = 1:numel(Files)
    load(Files{i});
end
%}
```

```

%load('All_wheel_Data_with_Meta.mat');

Noise = table();
Noise.Start = 'Sep-10-2018 12:00:00';
Noise.End = 'Sep-10-2018 12:00:00';
Noise.Type = {''};

Lights = table();
Lights.Regular = 'Sep-10-2018 12:00:00';
Lights.Darkness = 'Sep-10-2018 12:00:00';

All_wheels = table();

wheelInfo = struct(...
    'Has_Data',{''},...
    'Phase',{''}, ...
    'Experiment',{''}, ...
    'Animal',{''},...
    'Cage',{''},...
    'DOB',{''},...
    'Age',{''},...
    'Sex',{''},...
    'Cohort',{''},...
    'Supplier',{''},...
    'Lightschedule',{''},...
    'Lights',{Lights},...
    'RawData',{table()},...
    'Noise',{Noise},...
    'CleanData',{table()},...
    'Notes',{''});

wheelStructure = struct(...
    'wheel_01',wheelInfo,...
    'wheel_02',wheelInfo,...
    'wheel_03',wheelInfo,...
    'wheel_04',wheelInfo,...
    'wheel_05',wheelInfo,...
    'wheel_06',wheelInfo,...
    'wheel_07',wheelInfo,...
    'wheel_08',wheelInfo,...
    'wheel_09',wheelInfo,...
    'wheel_10',wheelInfo,...

```



```

'wheel_11',wheelInfo,...
'wheel_12',wheelInfo,...
'wheel_13',wheelInfo,...
'wheel_14',wheelInfo,...
'All_wheels',All_wheels);

Pilot = struct(...
    'Cipro',wheelStructure,...
    'Old_Male',wheelStructure);

Baseline = struct(...
    'Young_Male',wheelStructure,...
    'Old_Male',wheelStructure,...
    'Young_Female',wheelStructure,...
    'Old_Female',wheelStructure);

CP = struct(...
    'YM_1',wheelStructure,...
    'YM_2',wheelStructure,...
    'YM_3',wheelStructure,...
    'YF_1',wheelStructure,...
    'YF_2',wheelStructure,...
    'YF_3',wheelStructure,...
    'OM_1',wheelStructure,...
    'OF_1',wheelStructure);

Circadian_Study =
struct('Pilot',Pilot,'Baseline',Baseline,'CP',CP,'All_Data',All_Data);

```

Load each experiment from All_Data into the structure

```

Columns = All_Data.Properties.VariableNames';

ExpTitles = unique(All_Data.Experiment);

for i = 1:numel(ExpNames)

    CurTable = All_Data(All_Data.Experiment==ExpNames(i),:);

    if contains(ExpNames(i),'Base_YM_1')==1
        Circadian_Study.Baseline.Young_Male.All_wheels = CurTable;
    else

```

```

end

if contains(ExpNames(i), "Base_OM_1")==1
    Circadian_Study.Baseline.Old_Male.All_wheels = CurTable;
else
end

if contains(ExpNames(i), "Base_YF_1")==1
    Circadian_Study.Baseline.Young_Female.All_wheels = CurTable;
else
end

if contains(ExpNames(i), "Base_OF_1")==1
    Circadian_Study.Baseline.Old_Female.All_wheels = CurTable;
else
end

if contains(ExpNames(i), "CP_YM_1")==1
    Circadian_Study.CP.YM_1.All_wheels = CurTable;
else
end

if contains(ExpNames(i), "CP_YM_2")==1
    Circadian_Study.CP.YM_2.All_wheels = CurTable;
else
end

if contains(ExpNames(i), "CP_YM_3")==1
    Circadian_Study.CP.YM_3.All_wheels = CurTable;
else
end

if contains(ExpNames(i), "CP_YF_1")==1
    Circadian_Study.CP.YF_1.All_wheels = CurTable;
else
end

if contains(ExpNames(i), "CP_YF_2")==1
    Circadian_Study.CP.YF_2.All_wheels = CurTable;
else
end

if contains(ExpNames(i), "CP_YF_3")==1

```

```

        Circadian_Study.CP.YF_3.All_wheels = CurTable;
    else
    end

    if contains(ExpNames(i),"CP_OM_1")==1
        Circadian_Study.CP.OM_1.All_wheels = CurTable;
    else
    end

    if contains(ExpNames(i),"CP_OF_1")==1
        Circadian_Study.CP.OF_1.All_wheels = CurTable;
    else
    end

    if contains(ExpNames(i),"Pilot_Cipro_1")==1
        Circadian_Study.Pilot.Cipro.All_wheels = CurTable;
    else
    end

    if contains(ExpNames(i),"Pilot_OM_1")==1
        Circadian_Study.Pilot.Old_Male.All_wheels = CurTable;
    else
    end

end
%}

```

Load each Wheel's RawData into the structure

```

for i = 1:numel(wheelNames)

    Circadian_Study.Baseline.Young_Male.(wheelNames{i}).RawData = ...

    Circadian_Study.Baseline.Young_Male.All_wheels(Circadian_Study.Baseline.Y
    oung_Male.All_wheels.wheel==wheelNums(i),:);

    Circadian_Study.Baseline.Old_Male.(wheelNames{i}).RawData = ...

    Circadian_Study.Baseline.Old_Male.All_wheels(Circadian_Study.Baseline.Old
    _Male.All_wheels.wheel==wheelNums(i),:);

```

```

Circadian_Study.Baseline.Young_Female.(wheelNames{i}).RawData = ...

Circadian_Study.Baseline.Young_Female.All_wheels(Circadian_Study.Baseline
.Young_Female.All_wheels.wheel==wheelNums(i),:);

Circadian_Study.Baseline.Old_Female.(wheelNames{i}).RawData = ...

Circadian_Study.Baseline.Old_Female.All_wheels(Circadian_Study.Baseline.O
ld_Female.All_wheels.wheel==wheelNums(i),:);

Circadian_Study.CP.YM_1.(wheelNames{i}).RawData = ...

Circadian_Study.CP.YM_1.All_wheels(Circadian_Study.CP.YM_1.All_wheels.whe
el==wheelNums(i),:);

Circadian_Study.CP.YM_2.(wheelNames{i}).RawData = ...

Circadian_Study.CP.YM_2.All_wheels(Circadian_Study.CP.YM_2.All_wheels.whe
el==wheelNums(i),:);

Circadian_Study.CP.YM_3.(wheelNames{i}).RawData = ...

Circadian_Study.CP.YM_3.All_wheels(Circadian_Study.CP.YM_3.All_wheels.whe
el==wheelNums(i),:);

Circadian_Study.CP.YF_1.(wheelNames{i}).RawData = ...

Circadian_Study.CP.YF_1.All_wheels(Circadian_Study.CP.YF_1.All_wheels.whe
el==wheelNums(i),:);

Circadian_Study.CP.YF_2.(wheelNames{i}).RawData = ...

Circadian_Study.CP.YF_2.All_wheels(Circadian_Study.CP.YF_2.All_wheels.whe
el==wheelNums(i),:);

Circadian_Study.CP.YF_3.(wheelNames{i}).RawData = ...

Circadian_Study.CP.YF_3.All_wheels(Circadian_Study.CP.YF_3.All_wheels.whe
el==wheelNums(i),:);

Circadian_Study.CP.OM_1.(wheelNames{i}).RawData = ...

```

```
Circadian_Study.CP.OM_1.All_wheels(Circadian_Study.CP.OM_1.All_wheels.wheel==wheelNums(i),:);
```

```
    Circadian_Study.CP.OF_1.(wheelNames{i}).RawData = ...
```

```
Circadian_Study.CP.OF_1.All_wheels(Circadian_Study.CP.OF_1.All_wheels.wheel==wheelNums(i),:);
```

```
    Circadian_Study.Pilot.Cipro.(wheelNames{i}).RawData = ...
```

```
Circadian_Study.Pilot.Cipro.All_wheels(Circadian_Study.Pilot.Cipro.All_wheels.wheel==wheelNums(i),:);
```

```
    Circadian_Study.Pilot.Old_Male.(wheelNames{i}).RawData = ...
```

```
Circadian_Study.Pilot.Old_Male.All_wheels(Circadian_Study.Pilot.Old_Male.All_wheels.wheel==wheelNums(i),:);
```

```
end
```

```
%}
```

Load the MetaData from each Wheel's RawData into the structure

```
Phases = {'Baseline';'CP';'Pilot'};
```

```
FieldOrder = { ...  
    'Phase'; ...  
    'Experiment'; ...  
    'wheel_Number'; ...  
    'Has_Data'; ...  
    'Animal'; ...  
    'DOB'; ...  
    'Age'; ...  
    'Sex'; ...  
    'Cage'; ...  
    'Cohort'; ...  
    'Supplier'; ...  
    'LightSchedule';...  
    'Lights'; ...  
    'RawData'; ...
```

```

'Noise'; ...
'CleanData'; ...
'Notes'};

for g = 1:numel(Phases)

    if g==1
        MetaDataLocs =
{'Young_Male';'Old_Male';'Young_Female';'Old_Female'};
    elseif g==2
        MetaDataLocs =
{'YM_1';'YM_2';'YM_3';'YF_1';'YF_2';'YF_3';'OM_1';'OF_1'};
    elseif g==3
        MetaDataLocs = {'Cipro';'Old_Male'};
    end

    for h = 1:numel(MetaDataLocs)

        for i = 1:numel(WheelNames)

Circadian_Study.(Phases{g}).(MetaDataLocs{h}).(WheelNames{i}).Wheel_Number
r = ...

char(Circadian_Study.(Phases{g}).(MetaDataLocs{h}).(WheelNames{i}).RawData
a.Wheel(1));

Circadian_Study.(Phases{g}).(MetaDataLocs{h}).(WheelNames{i}).Phase = ...
    Phases{g};

Circadian_Study.(Phases{g}).(MetaDataLocs{h}).(WheelNames{i}).Experiment
= ...

char(Circadian_Study.(Phases{g}).(MetaDataLocs{h}).(WheelNames{i}).RawData
a.Experiment(1));

Circadian_Study.(Phases{g}).(MetaDataLocs{h}).(WheelNames{i}).Animal =
...

char(Circadian_Study.(Phases{g}).(MetaDataLocs{h}).(WheelNames{i}).RawData

```

```

a.Animal(1));

Circadian_Study.(Phases{g}).(MetaDataLocs{h}).(WheelNames{i}).Has_Data =
...

char(Circadian_Study.(Phases{g}).(MetaDataLocs{h}).(WheelNames{i}).RawData.
a.Animal(1));

        if
Circadian_Study.(Phases{g}).(MetaDataLocs{h}).(WheelNames{i}).Has_Data=="
NaN"

Circadian_Study.(Phases{g}).(MetaDataLocs{h}).(WheelNames{i}).Has_Data=false;
        else
Circadian_Study.(Phases{g}).(MetaDataLocs{h}).(WheelNames{i}).Has_Data=true;
        end

Circadian_Study.(Phases{g}).(MetaDataLocs{h}).(WheelNames{i}).Cage = ...

char(Circadian_Study.(Phases{g}).(MetaDataLocs{h}).(WheelNames{i}).RawData.
a.Cage(1));

Circadian_Study.(Phases{g}).(MetaDataLocs{h}).(WheelNames{i}).DOB = ...

char(Circadian_Study.(Phases{g}).(MetaDataLocs{h}).(WheelNames{i}).RawData.
a.DOB(1));

Circadian_Study.(Phases{g}).(MetaDataLocs{h}).(WheelNames{i}).Age = ...

char(Circadian_Study.(Phases{g}).(MetaDataLocs{h}).(WheelNames{i}).RawData.
a.Age(1));

Circadian_Study.(Phases{g}).(MetaDataLocs{h}).(WheelNames{i}).Sex = ...

char(Circadian_Study.(Phases{g}).(MetaDataLocs{h}).(WheelNames{i}).RawData

```

```

a.Sex(1));

Circadian_Study.(Phases{g}).(MetaDataLocs{h}).(WheelNames{i}).Cohort =
...

char(Circadian_Study.(Phases{g}).(MetaDataLocs{h}).(WheelNames{i}).RawData.Cohort(1));

Circadian_Study.(Phases{g}).(MetaDataLocs{h}).(WheelNames{i}).Supplier =
...

char(Circadian_Study.(Phases{g}).(MetaDataLocs{h}).(WheelNames{i}).RawData.Supplier(1));

                Circadian_Study.(Phases{g}).(MetaDataLocs{h}).(WheelNames{i})
= ...

orderfields(Circadian_Study.(Phases{g}).(MetaDataLocs{h}).(WheelNames{i})
,FieldOrder);

        end
    end

end

clearvars -except All_Data Circadian_Study ExpNames;

```

Step 3 - Add Light Schedule

```

% Clear All Current Variables and Console
%
clear all;
close all;
clc
%}

```



```
format long;
```

Load Files (VERY LARGE - TAKES TIME)

```
Files = {...  
    'All_Data_After_Step_2.mat';...  
    'Circadian_Study_Database_After_Step_2.mat'};  
  
ExpNames = string({...  
    'Base_YM_1'; 'Base_YF_1'; 'Base_OM_1'; 'Base_OF_1'; ...  
  
    'CP_YM_1'; 'CP_YM_2'; 'CP_YM_3'; 'CP_YF_1'; 'CP_YF_2'; 'CP_YF_3'; 'CP_OM_1'; 'CP  
_OF_1'; ...  
    'Pilot_Cipro_1'; 'Pilot_OM_1'});  
  
ExpNames = sortrows(ExpNames);  
  
wheelNums =  
{ '01'; '02'; '03'; '04'; '05'; '06'; '07'; '08'; '09'; '10'; '11'; '12'; '13'; '14'};  
  
wheelNames =  
{ 'wheel_01'; 'wheel_02'; 'wheel_03'; 'wheel_04'; 'wheel_05'; 'wheel_06'; 'wheel  
_07'; ...  
  
    'wheel_08'; 'wheel_09'; 'wheel_10'; 'wheel_11'; 'wheel_12'; 'wheel_13'; 'wheel_  
14'};  
  
for i = 1:numel(Files)  
    load(Files{i});  
end
```

Work on One Table At A Time

```
CurData = All_Data;  
%CurData = Circadian_Study.Baseline.Young_Male.All_wheels;  
%CurData = Circadian_Study.Baseline.Old_Male.All_wheels;  
  
clearvars Circadian_Study All_Data
```

```
CurData_ColumnProperties(:,1) = CurData.Properties.VariableNames;
CurData_ColumnProperties(:,2) =
varfun(@class, CurData, 'OutputFormat', 'cell');
```

```
%SideBySide = {};
```

Change the Column Variable Types to Strings from Categorical

```
%{
for i = 1:10
    CurData.(i) = string(table2array(CurData(:,i)));
end
```

```
CurData_ColumnProperties(:,2) =
varfun(@class, CurData, 'OutputFormat', 'cell');
```

```
%{
for i = 1:13
    CurData.(i) = categorical(table2array(CurData(:,i)));
end
%}
%}
```

Experimental Constants

```
fs = 1/60; % Sample rate, which is set in ClockLab (1 minute = 1/60sec)
MinutesInDay = 1440;
LightsOffHr = 8; % Input the time that lights turn off
LightsOnHr = 20; % Input the time that lights turn on
LightsOffMinute = LightsOffHr * 60; % This corresponds to 8:00am
LightsOnMinute = LightsOnHr * 60; % This corresponds to 8:00pm
```

Add HasData, Lights, LightSchedule Columns

```
% Determine if a wheel Record Contains Data

%RowHasData = categorical(1:height(CurData),1)';

CurData.HasData(:) = "1";
```

```

CurData = movevars(CurData, 'HasData', 'Before', 1);
CurData.HasData(CurData.Cage=="NaN") = "0";
CurData.HasData(CurData.Animal=="0000") = "0"; % OM wheel 13 - Didn't run
/ no signal
CurData.HasData(CurData.Animal=="0040") = "0"; % YM wheel 06 - SUPER
noisy

ExpLightSchedule = {};

for i = 1:length(ExpNames)
    ExpLightSchedule{i,1} = string(ExpNames{i});
    ExpLightSchedule{i,2} =
string(min(table2array(CurData(CurData.Experiment==ExpNames(i), 'DateTime'
)))));
    ExpLightSchedule{i,3} =
string(max(table2array(CurData(CurData.Experiment==ExpNames(i), 'DateTime'
)))));
end

% This looks very good now that every experiment begins and ends at
20:00:00

% Converts the ExpLightSchedule to a table, and renames the variables

ExpLightSchedule =
table(ExpLightSchedule(:,1),ExpLightSchedule(:,2),ExpLightSchedule(:,3));

ExpLightSchedule.Properties.VariableNames =
{'Experiment';'Time_Start_Exp';'Time_End_Exp'};

load('ExpDarkness3.mat');

% have to make sure that the ExpLightSchedule experiment names are in the
% same order as the ExpDarkness experiment names *****
% ADDITIONALLY, I NEEDED TO MAKE SURE THAT THE ExpNames LIST WAS ALSO
% SORTED SO THAT A LATER PIECE OF CODE WHICH APPLIES THE 00:24 12:12
VALUES
% WORKS PROPERLY

```

```

ExpLightSchedule.Experiment = string(ExpLightSchedule.Experiment);
ExpLightSchedule = sortrows(ExpLightSchedule,1);

ExpDarkness = sortrows(ExpDarkness,1);

% Not really sure why that was necessary, but I ensured everything was
% sorted correctly before proceeding on 2/6/2020

ExpLightSchedule.Time_Start_Darkness = ExpDarkness(:,2);
ExpLightSchedule.Time_End_Darkness = ExpDarkness(:,3);

% save('ExpLightSchedule_New.mat','ExpLightSchedule'); % This was created
on 2/6/2020

% This initially sets ALL experiments to the default reverse light cycle

CurData.LightSchedule = CurData.Lights;
CurData.LightSchedule(:) = '12:12';
CurData =
movevars(CurData,{'LightSchedule';'Lights'},'Before','DateTime');

% Extract Light and Dark Rows
RowsDark = CurData.ClockHourBin>=LightsOffHr &
CurData.ClockHourBin<LightsOnHr;
RowsLight = CurData.ClockHourBin<LightsOffHr |
CurData.ClockHourBin>=LightsOnHr;

% Set .Lights value to binary: 0 = off , 1 = on
CurData.Lights(RowsDark) = 'off';
CurData.Lights(RowsLight) = 'on';

%ExpDarkness(1:6,2:3) = datetime(ExpDarkness(1:6,2:3),'InputFormat','MMM-
dd-yyyy HH:mm:ss');

for i = 1:length(ExpNames)
    if ~strcmp(ExpDarkness(i,2),"NaN")

CurData.LightSchedule((CurData.Experiment==ExpNames(i))&(CurData.DateTime
>=ExpDarkness(i,2))&(CurData.DateTime<=ExpDarkness(i,3))) = "00:24";

```

```

end
end

CurData.Lights_Normal = CurData.Lights;
CurData = movevars(CurData,{'Lights_Normal'},'After','LightSchedule');

CurData.Lights(CurData.LightSchedule=="00:24")="Off";

% ConstantDarkness = CurData(CurData.LightSchedule=="00:24",:);

All_Data = CurData;

%clearvars -except All_Data ExpNames Circadian_Study

All_Data.ColumnProperties(:,1) = All_Data.Properties.VariableNames;
All_Data.ColumnProperties(:,2) =
varfun(@class,All_Data,'OutputFormat','cell');

Phases = ["Baseline","CP","Pilot"];

All_Data.Phase(:) = "Filler";
All_Data = movevars(All_Data,'Phase','After','HasData');

for g = 1:length(Phases)

    if g==1
        NewPhase = {'Base_YM_1';'Base_OM_1';'Base_YF_1';'Base_OF_1'};

    elseif g==2
        NewPhase =
{'CP_YM_1';'CP_YM_2';'CP_YM_3';'CP_YF_1';'CP_YF_2';'CP_YF_3';'CP_OM_1';'C
P_OF_1'};

    elseif g==3
        NewPhase = {'Pilot_Cipro_1';'Pilot_OM_1'};
    end

    for i = 1:length(NewPhase)
        All_Data.Phase(All_Data.Experiment==NewPhase(i)) = Phases{g};
    end
end

```

```
end
```

Change Values for Lights On and Off

```
%All_Data.LightSchedule(All_Data.LightSchedule=="Reverse")= "12:12";  
%All_Data.LightSchedule(All_Data.LightSchedule=="Darkness")= "00:24";  
  
%All_Data.Lights_Normal(All_Data.Lights_Normal=="0")= "off";  
%All_Data.Lights_Normal(All_Data.Lights_Normal=="1")= "on";  
  
%All_Data.Lights(All_Data.Lights=="0")= "off";  
%All_Data.Lights(All_Data.Lights=="1")= "on";
```

Save Output

```
% save('All_Data_After_Step_3.mat', 'All_Data'); % This was created on  
2/6/2020
```

Step 4 - Mark Noise and Cleanup Data

```
% Clear All Current Variables and Console  
%  
clear all;  
close all;  
clc  
%}  
  
format long;
```

Load Files (VERY LARGE - TAKES TIME)

```
Files = {...  
    'All_Data_After_Step_3.mat'};
```

```

ExpNames = string({...
    'Base_YM_1'; 'Base_YF_1'; 'Base_OM_1'; 'Base_OF_1'; ...

    'CP_YM_1'; 'CP_YM_2'; 'CP_YM_3'; 'CP_YF_1'; 'CP_YF_2'; 'CP_YF_3'; 'CP_OM_1'; 'CP
_OF_1'; ...
    'Pilot_Cipro_1'; 'Pilot_OM_1'});

ExpNames = sortrows(ExpNames);

wheelNums =
{'01'; '02'; '03'; '04'; '05'; '06'; '07'; '08'; '09'; '10'; '11'; '12'; '13'; '14'};

wheelNames =
{'wheel_01'; 'wheel_02'; 'wheel_03'; 'wheel_04'; 'wheel_05'; 'wheel_06'; 'wheel
_07'; ...

'wheel_08'; 'wheel_09'; 'wheel_10'; 'wheel_11'; 'wheel_12'; 'wheel_13'; 'wheel_
14'};

for i = 1:numel(Files)
    load(Files{i});
end

All_Data_Columns(:,1) = All_Data.Properties.VariableNames;
All_Data_Columns(:,2) = varfun(@class, All_Data, 'OutputFormat', 'cell');

%%%%%%%%%%%%%%%%%%%%%%%%%%%%%%%%%%%%%%%%%%%%%%%%%%%%%%%%%%%%%%%%%%%%%%%%
%%

```

Data Cleanup (Spurious Data)

```

%%%%%%%%%%%%%%%%%%%%%%%%%%%%%%%%%%%%%%%%%%%%%%%%%%%%%%%%%%%%%%%%%%%%%%%%
%%

% Moving Average** Filter for Spurious Data
% Sets noise = average of DAY BEFORE activity (3 point moving average)
%

% CURRENTLY, THIS FILTER IS SET UP TO PASS THROUGH THE DATA TWICE,

```

```

% ACCORDING TO THE LOOP COUNTER 'N', A SECOND PASS WAS NEEDED TO CORRECT
% RESIDUAL BACKGROUND NOISE IN WHEEL 6 OF THE OLD FEMALES. THE UNFILTERED
% FILE USED FOR THIS WAS 'Baseline_Data_Cleaned_9_23_19.mat', AND WAS
% SAVED
% AS 'Baseline_Data_Twice_Filtered_9_26

%load('Baseline_Data_Cleaned_9_23_19.mat');

%load('All_Data_BEFORE_NOISE_CLEANUP.mat');

% load('All_Data_Before_Clean_Oct_3.mat') % This was originally
% uncommented when I began working on 2-6-2020

%{
load('Noise_Notes4.mat'); % Noise_Notes 4 includes a filter for the one
minute of missing OM data on 10-17-2018

% Create a blank template with unique Experiment and Wheel combinations
so
% that I can go record by record in ClockLab and determine which chunks
of
% time need to be filtered...

Noise_Notes_5 = unique(All_Data(:,{'Experiment';'Wheel'}));
Noise_Notes_5.Experiment = string(Noise_Notes_5.Experiment);
Noise_Notes_5.Wheel = string(Noise_Notes_5.Wheel);
Noise_Notes_5.Noise_Start(:) = "";
Noise_Notes_5.Noise_End(:) = "";
Noise_Notes_5.Noise_Type(:) = "";

% Create a new blank template to manually look at each recording and list
% the times that need to be cleaned

Noise_Notes_6 = vertcat(Noise_Notes,Noise_Notes_5);
Injection_Times = Noise_Notes_6;
Noise_Notes_5 = Noise_Notes_6;

%{
TableToWrite = Injection_Times;
FileName = 'Injection_Times_New.csv';
writetable(TableToWrite,FileName);
%}
%}

```



```

file = 'Noise_Notes_5.csv';

opts = delimitedTextImportOptions('NumVariables',6,...

'VariableNames',{'Experiment','wheel','Noise_Start','Noise_End','Noise_Type','Discard_After'},...

'VariableTypes',{'categorical','double','string','string','string','string'},...
    'DataLines',[2 inf]);

Noise_Notes_5 = readtable(file,opts);

Noise_Notes_5.wheel = arrayfun(@(x)
sprintf('%02d',x),Noise_Notes_5.wheel,'un',0);
Noise_Notes_5.wheel = categorical(Noise_Notes_5.wheel);

Noise_Notes_5.Noise_Start =
datetime(Noise_Notes_5.Noise_Start,'InputFormat','MMM-dd-yyyy HH:mm:ss');
Noise_Notes_5.Noise_Start.Format = 'MMM-dd-yyyy HH:mm:ss';

Noise_Notes_5.Noise_End =
datetime(Noise_Notes_5.Noise_End,'InputFormat','MMM-dd-yyyy HH:mm:ss');
Noise_Notes_5.Noise_End.Format = 'MMM-dd-yyyy HH:mm:ss';

Noise_Notes_5.Discard_After =
datetime(Noise_Notes_5.Discard_After,'InputFormat','MMM-dd-yyyy
HH:mm:ss');
Noise_Notes_5.Discard_After.Format = 'MMM-dd-yyyy HH:mm:ss';

% THIS LINE ADJUSTS THE NOISE_NOTES TO MATCH THE CORRECTED TIMES FOR
CP_YF_3
Noise_Notes_5{Noise_Notes_5.Experiment=="CP_YF_3",{'Noise_Start','Noise_End'}} = ...

Noise_Notes_5{Noise_Notes_5.Experiment=="CP_YF_3",{'Noise_Start','Noise_End'}}-hours(1);

Noise_Notes_ColumnProperties(:,1) =

```

```

Noise_Notes_5.Properties.VariableNames;
Noise_Notes_ColumnProperties(:,2) =
varfun(@class,Noise_Notes_5,'OutputFormat','cell');

%Noise_Notes_5 = fillmissing(Noise_Notes_5,'constant','');

Discard =
unique(Noise_Notes_5(:,{'Experiment';'Wheel';'Discard_After'}));

Discard = Discard(~isnan(Discard.Discard_After),:);

Noise_Notes_5 = Noise_Notes_5(:,1:5);
Noise_Notes_5 = Noise_Notes_5(~isnan(Noise_Notes_5.Noise_Start),:);

%Injection_Times =
unique(Noise_Notes_5(:,{'Experiment';'Discard_After'}));
%Injection_Times = unique(All_Data(:,{'Experiment','Wheel'}));

```

Add Injection_Times

```

All_Data.Dose(:) = "NaN";
All_Data.Injection_Number(:) = NaN;
All_Data.Injection_Day(:) = NaN;

All_Data = movevars(All_Data, 'Dose', 'Before', 'DateTime');
All_Data = movevars(All_Data, 'Injection_Number', 'Before', 'DateTime');
All_Data = movevars(All_Data, 'Injection_Day', 'Before', 'DateTime');

file = 'Injection_Times_1.csv';

opts = delimitedTextImportOptions('NumVariables',6,...

'VariableNames',{'Experiment','Wheel','Injection_Number','Injection_DateT
ime','Dose'},...

'VariableTypes',{'categorical','double','double','string','categorical'},
...

```

```

'DataLines',[2 inf]);

Injection_Times = readtable(file,opts);

Injection_Times.wheel = arrayfun(@(x)
sprintf('%02d',x),Injection_Times.wheel,'un',0);
Injection_Times.wheel = categorical(Injection_Times.wheel);

Injection_Times.Injection_DateTime =
datetime(Injection_Times.Injection_DateTime,'InputFormat','MMM-dd-yyyy
HH:mm:ss');
Injection_Times.Injection_DateTime.Format = 'MMM-dd-yyyy HH:mm:ss';
Injection_Times.Injection_DateTime.Format = 'MMM-dd-yyyy';

Injection_Columns(:,1) = Injection_Times.Properties.VariableNames;
Injection_Columns(:,2) =
varfun(@class,Injection_Times,'OutputFormat','cell');

[All_YMD(:,1) All_YMD(:,2) All_YMD(:,3)] = ymd(All_Data.DateTime);

for i = 1:height(Injection_Times)

    % Set the injection day
    [Cur_YMD(:,1) Cur_YMD(:,2) Cur_YMD(:,3)] =
ymd(Injection_Times{i},'Injection_DateTime');
    Cur_Locations = All_YMD(:, :) == Cur_YMD(1, :);
    Cur_Index = double(Cur_Locations);
    Cur_Index(:,4) = Cur_Index(:,1)+Cur_Index(:,2)+Cur_Index(:,3);

    All_Data{((All_Data.Experiment == Injection_Times{i},'Experiment')
&...
    All_Data.wheel == Injection_Times{i},'wheel')) &...
    Cur_Index(:,4)==3),'Injection_Day'} = 0;

    All_Data{((All_Data.Experiment == Injection_Times{i},'Experiment')
&...
    All_Data.wheel == Injection_Times{i},'wheel')) &...
    Cur_Index(:,4)==3),'Dose'} = Injection_Times{i},'Dose'};

    All_Data{((All_Data.Experiment == Injection_Times{i},'Experiment')
&...

```

```

All_Data.wheel == Injection_Times{i,'wheel'}) &...
Cur_Index(:,4)==3), 'Injection_Number'} = ...
Injection_Times{i, 'Injection_Number'};

if Injection_Times{i, 'Experiment'}=="CP_YM_3" ||...
    Injection_Times{i, 'Experiment'}=="CP_YF_3" ||...
    Injection_Times{i, 'Experiment'}=="CP_OM_1" ||...
    Injection_Times{i, 'Experiment'}=="CP_OF_1"

% Set the PRE-injection day **** NOTE THIS WILL NOT WORK IF
INJECTIONS
% WERE MADE ON SEQUENTIAL DAYS
[Pre_YMD(:,1) Pre_YMD(:,2) Pre_YMD(:,3)] =
ymd((Injection_Times{i, 'Injection_DateTime'})-days(1));
Pre_Locations = All_YMD(:, :) == Pre_YMD(1, :);
Pre_Index = double(Pre_Locations);
Pre_Index(:,4) = Pre_Index(:,1)+Pre_Index(:,2)+Pre_Index(:,3);

All_Data{((All_Data.Experiment == Injection_Times{i, 'Experiment'})
&...
    All_Data.wheel == Injection_Times{i, 'wheel'}) &...
    Pre_Index(:,4)==3), 'Injection_Day'} = -1; % This signifies one
day BEFORE injection

All_Data{((All_Data.Experiment == Injection_Times{i, 'Experiment'})
&...
    All_Data.wheel == Injection_Times{i, 'wheel'}) &...
    Pre_Index(:,4)==3), 'Dose'} = Injection_Times{i, 'Dose'};

All_Data{((All_Data.Experiment == Injection_Times{i, 'Experiment'})
&...
    All_Data.wheel == Injection_Times{i, 'wheel'}) &...
    Pre_Index(:,4)==3), 'Injection_Number'} = ...
Injection_Times{i, 'Injection_Number'};

% Set the POST-injection day **** NOTE THIS WILL NOT WORK IF
INJECTIONS
% WERE MADE ON SEQUENTIAL DAYS
[Post_YMD(:,1) Post_YMD(:,2) Post_YMD(:,3)] =
ymd((Injection_Times{i, 'Injection_DateTime'})+days(1));
Post_Locations = All_YMD(:, :) == Post_YMD(1, :);
Post_Index = double(Post_Locations);

```

```

Post_Index(:,4) = Post_Index(:,1)+Post_Index(:,2)+Post_Index(:,3);

All_Data{((All_Data.Experiment == Injection_Times{i,'Experiment'}
&...
    All_Data.wheel == Injection_Times{i,'wheel'}) &...
    Post_Index(:,4)==3), 'Injection_Day'} = 1; % This signifies one
day AFTER injection

All_Data{((All_Data.Experiment == Injection_Times{i,'Experiment'}
&...
    All_Data.wheel == Injection_Times{i,'wheel'}) &...
    Post_Index(:,4)==3), 'Dose'} = Injection_Times{i,'Dose'};

All_Data{((All_Data.Experiment == Injection_Times{i,'Experiment'}
&...
    All_Data.wheel == Injection_Times{i,'wheel'}) &...
    Post_Index(:,4)==3), 'Injection_Number'} = ...
    Injection_Times{i,'Injection_Number'};
else
end

end

%Low_Dose = All_Data(All_Data.Dose=="0.001",:);
%Low_Dose = sortrows(Low_Dose,'DateTime');

%unique(Low_Dose(:,{'Experiment','wheel'}));

```

Discard Data

```

Only_Data = All_Data(All_Data.HasData=="1",:);
No_Data = All_Data(All_Data.HasData=="0",:);

for i = 1:height(Discard)
    All_Data{(All_Data.Experiment == Discard{i,'Experiment'} &...
        All_Data.wheel == Discard{i,'wheel'}) &...
        All_Data.DateTime >= Discard{i,'Discard_After'}, 'HasData'} = "0";
end

No_Data_After = All_Data(All_Data.HasData=="0",:);

```

```
All_Data = All_Data(All_Data.HasData=="1", :);
```

Try with the whole data set...

```
workingData = All_Data;
%workingData = All_Data(All_Data.Experiment=="CP_YM_3", :);

%workingData = All_Data(All_Data.HasData=="1", :);

Noise_Notes = Noise_Notes_5;

workingData.Counts_Cleaned = workingData.Counts;

DataHeight = length(workingData.Counts);
Noise_Height = height(Noise_Notes);

%TemporaryData = [workingData.Counts_Cleaned, double(workingData.wheel)];
NoisyFiles = unique(Noise_Notes(:, {'Experiment'; 'wheel'}));

Errors=table();
Errors2=table();
Errors3=table();

for i = 1:height(NoisyFiles)
    FilterSet =
workingData((workingData.Experiment==NoisyFiles{i, 'Experiment'} &
workingData.wheel==NoisyFiles{i, 'wheel'}), {'Experiment'; 'wheel'; 'DateTIme
'; 'Counts'});
    FilterSet.Counts_Cleaned(:) = NaN;
    FilterSet.Has_Noise(:) = logical(false);
    FilterSet.Plus_2(:) = NaN;
    FilterSet.Minus_2(:) = NaN;
    FilterSet.Plus_1(:) = NaN;
    FilterSet.Minus_1(:) = NaN;
    FilterHeight = height(FilterSet);

    CurNoise =
Noise_Notes(Noise_Notes.Experiment==NoisyFiles{i, 'Experiment'}&
Noise_Notes.wheel==NoisyFiles{i, 'wheel'}, :);
```

```

if height(FilterSet)>0
    for j = 1:height(CurNoise)

FilterSet.Has_Noise(FilterSet.DateTime>=CurNoise.Noise_Start(j) &
FilterSet.DateTime<=CurNoise.Noise_End(j)) = 1;

    end

    N = 1;

    while N <= 2

        for k = 1:height(FilterSet)
            if FilterSet.Has_Noise(k)>0

                % Check +2 days
                if ((k+2880<=FilterHeight) &&
FilterSet.Has_Noise(k+2880)==0 && isnan(FilterSet.Counts(k+2880))==0)==1
                    FilterSet.Plus_2(k) = FilterSet.Counts(k+2880);
                end

                % Check -2 days
                if ((k-2880>0) && FilterSet.Has_Noise(k-2880)==0 &&
isnan(FilterSet.Counts(k-2880))==0)==1
                    FilterSet.Minus_2(k) = FilterSet.Counts(k-2880);
                end

                % Check +1 days
                if ((k+1440<=FilterHeight) &&
FilterSet.Has_Noise(k+1440)==0 && isnan(FilterSet.Counts(k+1440))==0)==1
                    FilterSet.Plus_1(k) = FilterSet.Counts(k+1440);
                end

                % Check -1 days
                if ((k-1440>0) && FilterSet.Has_Noise(k-1440)==0 &&
isnan(FilterSet.Counts(k-1440))==0)==1
                    FilterSet.Minus_1(k) = FilterSet.Counts(k-1440);
                end
            end
        end
    end
end

```

```

FilterValues = table2array(FilterSet(k,[7 8 9 10]));
FilterLocs = find(~isnan(FilterValues));
FilterSize = length(FilterLocs);

%%%%%%%%%%%%%%%%%%%%%%%%%%%%%%%%%%%%%%%%%%%%%%%%%%%%%%%%%%%%%%%%%%%%%%%%
% Weighting factors to favor the day before or after

%%%%%%%%%%%%%%%%%%%%%%%%%%%%%%%%%%%%%%%%%%%%%%%%%%%%%%%%%%%%%%%%%%%%%%%%
% NOTE - THIS MAY NEED TO BE MODIFIED IF TWO DAY 2
VALUES ARE
% COMBINED WITH A SINGLE DAY 1 VALUE

%%%%%%%%%%%%%%%%%%%%%%%%%%%%%%%%%%%%%%%%%%%%%%%%%%%%%%%%%%%%%%%%%%%%%%%%
if (any(~isnan(FilterValues([1 2])))==1 &
any(isnan(FilterValues([3 4])))==1)==1
    FilterValues([1 2]) = FilterValues([1 2])*0.5;
    FilterValues([3 4]) = FilterValues([3 4])*1.5;
end

if FilterSize>0
    FilterSet.Counts_Cleaned(k) =
(sum(FilterValues(FilterLocs)))/FilterSize;

    % what is this shit????
    %{
if (CurNoise.Experiment(1)=="Base_OF_1" &
CurNoise.wheel(1)=="06")==1
    FilterSet.Has_Noise(FilterSet.Has_Noise==1) = 1;
else
    FilterSet.Has_Noise(k) = FilterSet.Has_Noise(k)-
1;
end
    %}
else
if N==1
    Errors = [Errors;FilterSet(k,:)];
else
end
if N==2
    Errors2 = [Errors2;FilterSet(k,:)];
else

```



```

        end

        if N==3
            Errors3 = [Errors3;FilterSet(k,:)];
        else
            end

        end

    else
        %FilterSet.Counts_Cleaned(k) = FilterSet.Counts(k);

    end

end

N=N+1;

end

FilterSet.Counts_Cleaned(isnan(FilterSet.Counts_Cleaned)) =
FilterSet.Counts(isnan(FilterSet.Counts_Cleaned));

WorkingData.Counts_Cleaned((WorkingData.Experiment==NoisyFiles{i, 'Experiment'} & workingData.wheel==NoisyFiles{i, 'wheel'})) =
FilterSet.Counts_Cleaned;
    else
    end
end

%All_Data = workingData;

%{
%{

%{
figure(12)
hold on;
Sub1 = subplot(3,1,1);
P1 = plot(WorkingData.Counts);
P1(1).Color = [0 0 0 1];

```

```

Sub2 = subplot(3,1,2)
P2 = plot(workingData.Counts_Cleaned);
P2(1).Color = [0 1 0 1];

Sub3 = subplot(3,1,3)
P3 = plot([workingData.Counts, workingData.Counts_Cleaned]);
P3(1).Color = [0 0 0 1];
P3(2).Color = [0 1 0 1];

hold off;
linkaxes([Sub1,Sub2,Sub3], 'xy');

plot(workingData.DateTime, [workingData.Counts
workingData.Counts_Cleaned]);
plot(workingData.DateTime, [workingData.Counts_Cleaned]);

Baseline_Data = workingData;

%}

%}
LessTen = workingData(workingData.ZTDayBin<=10,:);

workingData = All_Data;

%}

```

Step 5 - Select and Splice Data

```

clear all
close all
clc

```

```

load('All_Data_After_Step_4.mat');

Baseline_Data = All_Data(All_Data.Phase=="Baseline",:);
clearvars All_Data

ExpNames = string({...
    'Base_YM_1'; 'Base_OM_1'; 'Base_YF_1'; 'Base_OF_1'});
%ExpNames = sortrows(ExpNames);

TimeScale = 1440;

if TimeScale == 1440
    TimeVariable = 'ZTMinuteBin';
elseif TimeScale == 24
    TimeVariable = 'ZTHourBin';
end

% This section removes the single timepoint at the end of each experiment
for i = 1:length(ExpNames)
    LastDay =
    round(max(Baseline_Data.ZTDay(Baseline_Data.Experiment==ExpNames(i))));

    Baseline_Data((Baseline_Data.Experiment==ExpNames(i)&Baseline_Data.ZTDay=
    =LastDay),:) = [];
end

%{
% This section removes the entire LAST ZTDayBin
for i = 1:length(ExpNames)
    LastDay =
    max(Baseline_Data.ZTDayBin(Baseline_Data.Experiment==ExpNames(i)));

    Baseline_Data((Baseline_Data.Experiment==ExpNames(i)&Baseline_Data.ZTDayB
    in==LastDay),:) = [];
end

% This section removes the entire FIRST ZTDayBin
for i = 1:length(ExpNames)
    FirstDay =
    min(Baseline_Data.ZTDayBin(Baseline_Data.Experiment==ExpNames(i)));

    Baseline_Data((Baseline_Data.Experiment==ExpNames(i)&Baseline_Data.ZTDayB
    in==FirstDay),:) = [];
}

```

```

end
%}

Start_12_12 = 1;
End_12_12 = 8; %this value is used with a '<' sign
Start_0_24 = 8; %this value is used with a '<=' sign

NumberOfDarkDays = 9;

%Baseline_Data = Baseline_Data(Baseline_Data.ZTDay>=1,:);

Data_LD = Baseline_Data(Baseline_Data.LightSchedule=="12:12",:);

```

The sorting issue stems from not including NaN's at the end of the ReverseData

```

Data_LD = Data_LD(Data_LD.ZTDay>=Start_12_12,:);
Data_LD = Data_LD(Data_LD.ZTDay<End_12_12,:);

Data_LD = sortrows(Data_LD, 'Animal', 'ascend');
%ReverseData = ReverseData((ReverseData.ZTDay>=Start_12_12) &
(ReverseData.ZTDay<End_12_12),:);

Data_DD = Baseline_Data(Baseline_Data.LightSchedule=="00:24",:);
Data_DD = sortrows(Data_DD, 'Animal', 'ascend');

YM_Dark = Data_DD(Data_DD.Experiment=="Base_YM_1",:);
YM_Dark_Days = unique(YM_Dark.ZTDayBin);
YM_Dark_Days(:,2) = 1:1:length(YM_Dark_Days);
YM_Dark = YM_Dark(YM_Dark.ZTDayBin<=(YM_Dark_Days(NumberOfDarkDays)),:);

for i = 1:length(YM_Dark_Days)

YM_Dark{YM_Dark.ZTDayBin==YM_Dark_Days(i,1), 'ZTDayBin'}=YM_Dark_Days(i,2)
;
end

OM_Dark = Data_DD(Data_DD.Experiment=="Base_OM_1",:);
OM_Dark_Days = unique(OM_Dark.ZTDayBin);
OM_Dark_Days(:,2) = 1:1:length(OM_Dark_Days);
OM_Dark = OM_Dark(OM_Dark.ZTDayBin<=(OM_Dark_Days(NumberOfDarkDays)),:);

```

```

for i = 1:length(OM_Dark_Days)

OM_Dark{OM_Dark.ZTDayBin==OM_Dark_Days(i), 'ZTDayBin'}=OM_Dark_Days(i,2);
end

YF_Dark = Data_DD(Data_DD.Experiment=="Base_YF_1",:);
YF_Dark_Days = unique(YF_Dark.ZTDayBin);
YF_Dark_Days(:,2) = 1:1:length(YF_Dark_Days);
YF_Dark = YF_Dark(YF_Dark.ZTDayBin<=(YF_Dark_Days(NumberOfDarkDays)),:);

for i = 1:length(YF_Dark_Days)

YF_Dark{YF_Dark.ZTDayBin==YF_Dark_Days(i), 'ZTDayBin'}=YF_Dark_Days(i,2);
end

OF_Dark = Data_DD(Data_DD.Experiment=="Base_OF_1",:);
OF_Dark_Days = unique(OF_Dark.ZTDayBin);
OF_Dark_Days(:,2) = 1:1:length(OF_Dark_Days);
OF_Dark = OF_Dark(OF_Dark.ZTDayBin<=(OF_Dark_Days(NumberOfDarkDays)),:);

for i = 1:length(OF_Dark_Days)

OF_Dark{OF_Dark.ZTDayBin==OF_Dark_Days(i), 'ZTDayBin'}=OF_Dark_Days(i,2);
end

DarknessData_09Days = [YM_Dark;OM_Dark;YF_Dark;OF_Dark];

DarknessData_09Days.ZTDayBin = DarknessData_09Days.ZTDayBin+(End_12_12-
Start_12_12);

Fused_Light_Dark_Days = [Data_LD;DarknessData_09Days];

Fused_Light_Dark_Days.ZTDayMinuteBin =
Fused_Light_Dark_Days.ZTDayBin+(Fused_Light_Dark_Days.ZTMinuteBin/1440);
Fused_Light_Dark_Days.ZTDayHourBin =
Fused_Light_Dark_Days.ZTDayBin+(Fused_Light_Dark_Days.ZTHourBin/24);

%Fused_YM =
Fused_Light_Dark_Days(Fused_Light_Dark_Days.Experiment=="Base_YM_1",:);
%Fused_YM_0035 = Fused_YM(Fused_YM.Animal=="0035",:);

```

Step 6 - Create Surface Plots

```
clear all
close all
clc

%load('All_Data_After_Step_4.mat');

%load('Fused_Light_Dark_Days_Feb_26.mat');

%load('Fused_Light_Dark_Days_March_25_7LD_7DD.mat');

% for baseline
load('Fused_Light_Dark_Days_March_25_7LD_7DD.mat');
All_Data = Fused_Light_Dark_Days;
clearvars Fused_Light_Dark_Days

ExpNames = string({...
    'Base_YM_1'; 'Base_OM_1'; 'Base_YF_1'; 'Base_OF_1'});

wheelNums = string({...
    '01'; '02'; '03'; '04'; '05'; '06'; '08'; '09'; '10'; '11'; '12'; '13'; '14'});

% for the chronobiotic records
%load('A:\Data_Analysis\Data\Input\MATLAB_Step_4_Mark_Noise_Info_Clean\All
Data_After_Step_4.mat')
%All_Data = All_Data(All_Data.Phase=="CP",:);
```

Moving Mean on each wheel of each experiment

```
movmean_window = 10;
All_Data.Mov_Mean = All_Data.Counts_Cleaned;

i=1;
k=1;

for i = 1:length(ExpNames)
    for k = 1:length(wheelNums)

        cur_wheel_Name = strcat('wheel_',wheelNums(k));
```

```

        if numel(All_Data((All_Data.Experiment==ExpNames(i) &
All_Data.wheel==wheelNums(k)),:)) ~= 0

            % Replace the mean_Counts_Cleaned column with a moving mean
            average
            All_Data.Mov_Mean((All_Data.Experiment==ExpNames(i) &
All_Data.wheel==wheelNums(k))) = ...

movmean(All_Data.Mov_Mean((All_Data.Experiment==ExpNames(i) &
All_Data.wheel==wheelNums(k))), movmean_window);

        end
    end
end

All_Data.Counts_Cleaned = All_Data.Mov_Mean;
All_Data.Mov_Mean = [];

```

If using normalized data to show 'percentage of daily activity'

```

%load('Baseline_Normalized_Percent_Daily_Counts.mat');
%All_Data = Data_Normalized;

```

Calculate Average Activity of the Groups

```

clearvars Data_Normalized Fused_Light_Dark_Days

Baseline_Data = All_Data(All_Data.Phase=="Baseline",:);
clearvars All_Data Fused_Light_Dark_Days

ExpNames = string({...
    'Base_YM_1'; 'Base_OM_1'; 'Base_YF_1'; 'Base_OF_1'});
%ExpNames = sortrows(ExpNames);

Timescale = 1440;

if Timescale == 1440

```

```

    TimeVariable = 'ZTMinuteBin';
elseif Timescale == 24
    TimeVariable = 'ZTHourBin';
end

Early_Risers = 0;

%{
% This section removes the single timepoint at the end of each experiment
for i = 1:length(ExpNames)
    LastDay =
round(max(Baseline_Data.ZTDay(Baseline_Data.Experiment==ExpNames(i)))));

Baseline_Data((Baseline_Data.Experiment==ExpNames(i)&Baseline_Data.ZTDay=
=LastDay),:) = [];
end

%}

LD_DD = unique(Baseline_Data(:,{'LightSchedule';'ZTDayBin'}));

% This section removes the entire LAST ZTDayBin
% On 3-25-2020 I ran this section twice using the file
% 'Fused_Light_Dark_Days_Feb_26.mat' to produce a file containing 7 days
of
% LD and 7 days of DD, this new file is saved as both .csv and .mat,

% The csv is 'Fused_Light_Dark_Days_March_25_7LD_7DD.csv'
% The .mat is 'Fused_Light_Dark_Days_March_25_7LD_7DD.mat'

%{
% Fused_Light_Dark_Days = Baseline_Data;
% LD_DD_Sevens =
unique(Fused_Light_Dark_Days(:,{'LightSchedule';'ZTDayBin'}));
%
writetable(Fused_Light_Dark_Days,'Fused_Light_Dark_Days_March_25.csv','De
limiter','');
%}

%{
i=1;
for i = 1:length(ExpNames)
    LastDay =

```



```

max(Baseline_Data.ZTDayBin(Baseline_Data.Experiment==ExpNames(i)));

Baseline_Data((Baseline_Data.Experiment==ExpNames(i)&Baseline_Data.ZTDayB
in==LastDay),:) = [];
end
LD_DD = unique(Baseline_Data(:,{'LightSchedule';'ZTDayBin'}));
%}

%{
k=1;
while k<=3 %This is a counter to remove the first 3 days

    % This section removes the entire FIRST ZTDayBin
    for i = 1:length(ExpNames)
        FirstDay =
min(Baseline_Data.ZTDayBin(Baseline_Data.Experiment==ExpNames(i)));

Baseline_Data((Baseline_Data.Experiment==ExpNames(i)&Baseline_Data.ZTDayB
in==FirstDay),:) = [];
        end
        k = k+1;
    end
%}

GroupingFactors =
{'Experiment','ZTDay','ZTDayBin','ZTHourBin','ZTMinuteBin','LightSchedule
','Lights','Lights_Normal'};
Measurements = {'Counts_Cleaned'};
Stats = {'mean'};
Averages =
grpstats(Baseline_Data,GroupingFactors,Stats,'DataVars',Measurements);
Averages.Properties.VariableNames(Averages.Properties.VariableNames=="mea
n_Counts_Cleaned") = "Counts_Cleaned";
Averages.GroupCount = [];

clearvars Baseline_Data

```

Normalization of Daily Activity (SLOW)

```

%{
GroupingFactors = {'Experiment';'ZTDayBin'};

```

```

Measurements = {'Counts_Cleaned'};
Stats = {'sum'};

Table2Norm = Averages;

Norm_StatsTable =
grpstats(Table2Norm,GroupingFactors,Stats,'DataVars',Measurements);

Norm_StatsTableVariables = Norm_StatsTable.Properties.VariableNames;
Norm_StatsTableVariables = strrep(Norm_StatsTableVariables,"sum_","");
Norm_StatsTable.Properties.VariableNames = Norm_StatsTableVariables;

Exp_Names = unique(Norm_StatsTable.Experiment);
ZTDayBins = unique(Norm_StatsTable.ZTDayBin);

Data_Normalized = Table2Norm;

ZTMinuteBin = unique(Data_Normalized.ZTMinuteBin);

Columns_Norm_StatsTable = [Norm_StatsTable.Properties.VariableNames'
varfun(@class,Norm_StatsTable,'OutputFormat','cell')'];
Columns_NormData = [Data_Normalized.Properties.VariableNames'
varfun(@class,Data_Normalized,'OutputFormat','cell')'];

h=1;
i=1;
j=1;
k=2;

for h = 1:length(Measurements)
    for i = 1:length(Exp_Names)
        for k = 1:length(ZTDayBins)
            for m = 1:length(ZTMinuteBin)

                Data_Normalized{(Data_Normalized.Experiment ==
Exp_Names(i) & ...
                Data_Normalized.ZTDayBin == ZTDayBins(k) & ...
                Data_Normalized.ZTMinuteBin == ZTMinuteBin(m)), ...
                Measurements(h)} = ...
                Data_Normalized{(Data_Normalized.Experiment ==
Exp_Names(i) & ...
                Data_Normalized.ZTDayBin == ZTDayBins(k) & ...

```

```

        Data_Normalized.ZTMinuteBin == ZTMinuteBin(m)), ...
        Measurements(h)} ./
(Norm_StatsTable{(Norm_StatsTable.Experiment == Exp_Names(i) & ...
        Norm_StatsTable.ZTDayBin == ZTDayBins(k)),
Measurements(h)})*100;...

        end
    end
end
end

Averages = Data_Normalized;
%}

```

Creating the Surface Plots

```

Plots = struct();
for i = 1:length(ExpNames)
    Plots.(ExpNames(i)).Surf_Off = [];
    Plots.(ExpNames(i)).Surf_All = [];
    Plots.(ExpNames(i)).ax1 = [];
    Plots.(ExpNames(i)).ax2 = [];
    Plots.(ExpNames(i)).All_Axes = [];
    Plots.(ExpNames(i)).AxisLink = [];
end

for j = 1:length(ExpNames)
    Cur_Data = Averages(Averages.Experiment==ExpNames(j), ...

{'Experiment', 'ZTDay', 'ZTDayBin', 'ZTHourBin', 'ZTMinuteBin', 'LightSchedule
', 'Lights', 'Lights_Normal', 'Counts_Cleaned'});

    %Cur_Data = Cur_Data(Cur_Data.ZTDay<=5, :);

    Exp_Start = min(Cur_Data.ZTDayBin);
    Exp_End = max(Cur_Data.ZTDayBin);
    Exp_Length = length(unique(Cur_Data.ZTDayBin));

    ZTDay = Cur_Data.ZTDay;
    ZTDayBin = Cur_Data.ZTDayBin;

```

```

ZTHourBin = Cur_Data.ZTHourBin;
ZTMinuteBin = Cur_Data.ZTMinuteBin;

Counts_Cleaned = Cur_Data.Counts_Cleaned;

LightSchedule = Cur_Data.LightSchedule;
Lights = Cur_Data.Lights;
Lights_Normal = Cur_Data.Lights_Normal;

Lights_On = find(Lights=="On");
Lights_Off = find(Lights=="Off");

Signal = Counts_Cleaned;

Signal_Lights_On = Signal-NaN;
Signal_Lights_On(Lights_On) = Signal(Lights_On);

Signal_Lights_Off = Signal-NaN;
Signal_Lights_Off(Lights_Off) = Signal(Lights_Off);

if Exp_Start>0
    Length_Day(1:Exp_Length) = TimeScale;
elseif Exp_Start == 0
    Length_Day(1:(Exp_Length+1)) = TimeScale;
end

RR(1:max(ZTDayBin)+1) = TimeScale; % this was functional

%RR = ExpLength;

% Exp_Length = length(Length_Day);

Days_Used = unique(Averages.ZTDayBin);

%Stack=zeros(TimeScale,M)+NaN; %from spiral plot
Stack = zeros(TimeScale,Exp_Length)+NaN;
Stack_Lights_On = Stack;
Stack_Lights_Off = Stack;
for i = 1:Exp_Length
    %Stack(:,i) = Signal((Cur_Data.ZTDay>=i & Cur_Data.ZTDay<i+1));
    Stack(:,i) = Signal((Cur_Data.ZTDayBin>=Days_Used(i)) &
Cur_Data.ZTDayBin<Days_Used(i)+1); % Note that (i,:) is reversed from
before

```

```

        Stack_Lights_On(:,i) =
Signal_Lights_On((Cur_Data.ZTDayBin>=Days_Used(i) &
Cur_Data.ZTDayBin<Days_Used(i)+1)); % Note that (i,:) is reversed from
before
        Stack_Lights_Off(:,i) =
Signal_Lights_Off((Cur_Data.ZTDayBin>=Days_Used(i) &
Cur_Data.ZTDayBin<Days_Used(i)+1)); % Note that (i,:) is reversed from
before
    end

    % Stack_Lights_On = Stack_Lights_On + 0.01;
    Stack_Lights_Off = Stack_Lights_Off*0;

    %Stack_Lights_On = Stack_Lights_On(Lights_On);
    %Stack_Lights_Off = Stack_Lights_Off(Lights_Off);

    %ZTDayBin_Lights_On = ZTDayBin_Lights_On(Lights_On);
    %ZTDayBin_Lights_Off = ZTDayBin_Lights_Off(Lights_Off);

    GraphTitle = ExpNames(j);
    GraphTitle = strrep(GraphTitle, "_1", "");
    GraphTitle = strrep(GraphTitle, "_", " ");
    GraphTitle = strrep(GraphTitle, "Base", "Baseline");
    GraphTitle = strrep(GraphTitle, "Y", "Young ");
    GraphTitle = strrep(GraphTitle, "O", "Old ");
    GraphTitle = strrep(GraphTitle, "M", "Male");
    GraphTitle = strrep(GraphTitle, "F", "Female");

    %figure('NumberTitle','off','Name',GraphTitle,'Tag',GraphTitle)
    if j==1
        figure('Position',[0 0 1 1]);
        set(gcf, 'Units', 'Normalized', 'OuterPosition', [0 0 1 1]);
        set(gcf, 'color', 'white')
    end

    end

    Plots.(ExpNames(j)).ax1 = subplot(2,2,j);
    [X1,Y1] = meshgrid(1:Exp_Length,1:TimeScale);
    Plots.(ExpNames(j)).Surf_Off = surf(X1,Y1,Stack_Lights_Off);
    hold(Plots.(ExpNames(j)).ax1, 'on')

    grid on;
    Plots.(ExpNames(j)).ax1.ActivePositionProperty = 'position';

```

```

Plots.(ExpNames(j)).Surf_Off.CDataMapping = 'scaled'; %'direct';
Plots.(ExpNames(j)).ax1.Colormap(:) = 0;
shading interp
lighting gouraud
%Plots.(ExpNames(j)).Surf_Off.FaceAlpha = 0.8;
Plots.(ExpNames(j)).Surf_Off.FaceAlpha = 1;
axis off

Cur_Sub_Pos = Plots.(ExpNames(j)).ax1.Position;
Plots.(ExpNames(j)).ax2 = axes('Position',Cur_Sub_Pos);

%Plots.(ExpNames(j)).ax2 = axes;
Plots.(ExpNames(j)).Surf_All = surf(X1,Y1,Stack);
Plots.(ExpNames(j)).Surf_All.CDataMapping = 'scaled'; %'direct';
Plots.(ExpNames(j)).ax2.ActivePositionProperty = 'position';

c = jet;
%c = parula;

Plots.(ExpNames(j)).ax2.Colormap = c;
shading interp
lighting gouraud
%Plots.(ExpNames(j)).Surf_All.FaceAlpha = 0.6;
Plots.(ExpNames(j)).Surf_All.FaceAlpha = 0.8;
%plot3(1:M,qrs(:,1),qrs(:,2)+offset,'go-','MarkerFaceColor','g') %
need to make this plot the daily peaks or something
axis off

title(GraphTitle,'FontName','Gadugi','FontSize',16,'FontWeight','bold');
Plots.(ExpNames(j)).ax1.Visible = 'on';

Plots.(ExpNames(j)).ax2.YLim = [0 Timescale];
Plots.(ExpNames(j)).ax2.YTick = linspace(0,1440,9);
Plots.(ExpNames(j)).ax2.XLim = [1 Exp_Length];

Plots.(ExpNames(j)).ax2.ZLim = [0 max(Averages.Counts_Cleaned)];

Plots.(ExpNames(j)).ax2.ZLim = [0 100];

Plots.(ExpNames(j)).ax1.ZLim = Plots.(ExpNames(j)).ax2.ZLim;

Plots.(ExpNames(j)).ax1.YLim = Plots.(ExpNames(j)).ax2.YLim;
Plots.(ExpNames(j)).ax1.XLim = Plots.(ExpNames(j)).ax2.XLim;
%}

```

```

Plots.(ExpNames(j)).ax1.view = [80, 45];
Plots.(ExpNames(j)).ax2.view = [80, 45];

%{
Axes = findobj(gcf,'type', 'axes');

%Plots.(ExpNames(j)).All_Axes = Axes;
Plots.(ExpNames(j)).AxisLink =
linkprop(Axes,{'view','XLim','YLim','ZLim'});
%}

%Plots.(ExpNames(j)).AxisLink = linkprop(Axes,{'CameraUpVector',...
%   'CameraPosition','CameraTarget','CameraViewAngle','view'});
% 'CameraViewAngle' % makes the graph small, but appropriately scaled
% 'CameraTarget' % Doesn't do much...
% 'CameraPosition' % Doesn't do much...
% 'CameraUpVector' % Doesn't do much...

%Axes = findobj('type', 'axes');
%Plots.AxisLink = linkprop(Axes,{'view','XLim','YLim','ZLim'});
%setappdata(gcf, 'StoreTheLink', Plots.AxisLink);

%

Plots.(ExpNames(j)).ax1.FontName = 'Arial';
Plots.(ExpNames(j)).ax1.FontWeight = 'bold';
Plots.(ExpNames(j)).ax1.FontSize = 11;

Plots.(ExpNames(j)).ax1.XLabel.String = 'Day of Running';
Plots.(ExpNames(j)).ax1.XLabel.FontName = 'Arial';
Plots.(ExpNames(j)).ax1.XLabel.FontWeight = 'bold';
Plots.(ExpNames(j)).ax1.XLabel.FontSize = 12;
Plots.(ExpNames(j)).ax1.XLabel.Rotation = 300;
Plots.(ExpNames(j)).ax1.XLabel.Position =
Plots.(ExpNames(j)).ax1.XLabel.Position + [0 40 0];

Plots.(ExpNames(j)).ax1.ZLabel.String = ['Average wheel' newline
'Rotations per Minute (RPM)'];
Plots.(ExpNames(j)).ax1.XLabel.FontName = 'Arial';
Plots.(ExpNames(j)).ax1.XLabel.FontWeight = 'bold';

```

```

Plots.(ExpNames(j)).ax1.XLabel.FontSize = 12;
% Plots.(ExpNames(j)).ax1.ZLabel.Rotation = 0;

if TimeVariable=='ZTMinuteBin'
    Plots.(ExpNames(j)).ax1.YLabel.String = 'Zeitgeber Time(Minute of
Day)';
elseif TimeVariable=='ZTHourBin'
    Plots.(ExpNames(j)).ax1.YLabel.String = 'Zeitgeber Time(Hour of
Day)';
end

Plots.(ExpNames(j)).ax1.XLabel.FontName = 'Arial';

Plots.(ExpNames(j)).ax1.YTick = linspace(0,1440,9);
Plots.(ExpNames(j)).ax1.YLabel.FontWeight = 'bold';
Plots.(ExpNames(j)).ax1.YLabel.FontSize = 12;
Plots.(ExpNames(j)).ax1.YLabel.Rotation = 2;
Plots.(ExpNames(j)).ax1.YLabel.Position =
Plots.(ExpNames(j)).ax1.YLabel.Position - 2;

end

Axes = findobj('type', 'axes');
Plots.AxisLink = linkprop(Axes,{'View','XLim','YLim','ZLim'});
setappdata(gcf, 'StoreTheLink', Plots.AxisLink);

```


CURRICULUM VITAE

Erik L. Hodges, Ph.D.

EDUCATION

- 2017-present **Ph.D., Pharmaceutical Sciences**
University of Mississippi
Mentor: Nicole M. Ashpole, Ph.D.
- 2012-2015 **M.Sc., Behavioral Neuroscience**
University of Oklahoma - Health Sciences Center
Mentor: William E. Sonntag, Ph.D.
- 2008-2012 **B.Sc., Chemistry**
Northwestern Oklahoma State University
Mentor: Jason Wickham, Ph.D.

RESEARCH EXPERIENCE

- 2017-present Graduate Research Assistant, Ashpole Lab
Dissertation: *Aging, Circadian Rhythms, and Cannabinoids*
University of Mississippi
- 2012-2015 Graduate Research Assistant, Sonntag Lab
Thesis: *Insulin/IGF-1 in the Aging Brain*
University of Oklahoma - Health Sciences Center
- 2012 Data Analyst and Method Engineer
International Environmental Corporation
- 2011 Undergraduate Research Assistant, Curtis Lab
Oklahoma State University - Center for Health Sciences
- 2010-2012 Undergraduate Research Assistant, Wickham Lab
Northwestern Oklahoma State University
- 2010-2011 Laboratory Intern
Arysta Life Science Technology

TECHNIQUES

Molecular and *In vitro*

- Primary neuron culture
- Time-lapse microscopy
- Immunohistochemistry
- Brain histopathology

In vivo

- Transgenic rodent models
- Stereotactic survival surgery
 - Hippocampal injection
- Quantification of behavior
 - Cognition
 - Circadian rhythms

Data Analysis

- Non-parametric statistics
- Big data processing
- Coding
 - MATLAB
 - R

PUBLICATIONS

1. **Hodges, E.L.** and Ashpole, N.M., 2019. Aging circadian rhythms and cannabinoids. *Neurobiology of aging*.
2. Ashpole, N.M., Logan, S., Yabluchanskiy, A., Mitschelen, M.C., Yan, H., Farley, J.A., **Hodges, E.L.**, Ungvari, Z., Csiszar, A., Chen, S. and Georgescu, C., 2017. IGF-1 has sexually dimorphic, pleiotropic, and time-dependent effects on healthspan, pathology, and lifespan. *Geroscience*, 39(2), p.129-145.
3. Ashpole, N.M., Herron, J.C., Estep, P.N., Logan, S., **Hodges, E.L.**, Yabluchanskiy, A., Humphrey, M.B. and Sonntag, W.E., 2016. Differential effects of IGF-1 deficiency during the life span on structural and biomechanical properties in the tibia of aged mice. *Age*, 38(2), p.38.
4. Ashpole, N.M., Herron, J.C., Mitschelen, M.C., Farley, J.A., Logan, S., Yan, H., Ungvari, Z., **Hodges, E.L.**, Csiszar, A., Ikeno, Y. and Humphrey, M.B., 2016. IGF-1 regulates vertebral bone aging through sex-specific and time-dependent mechanisms. *Journal of Bone and Mineral Research*, 31(2), p.443-454.
5. Tarantini, S., Hertelendy, P., Tucsek, Z., Valcarcel-Ares, M.N., Smith, N., Menyhart, A., Farkas, E., **Hodges, E.L.**, Towner, R., Deak, F. and Sonntag, W.E., 2015. Pharmacologically-induced neurovascular uncoupling is associated with cognitive impairment in mice. *Journal of Cerebral Blood Flow & Metabolism*, 35(11), p.1871-1881.
6. de Souza, P.C., Smith, N., Pody, R., He, T., Njoku, C., Silasi-Mansat, R., Lupu, F., Meek, B., Chen, H., Dong, Y. Saunders, D., Orock, A., **Hodges, E.L.**, and Towner, R., 2015. OKN-007 decreases VEGFR-2 levels in a preclinical GL261 mouse glioma model. *American journal of nuclear medicine and molecular imaging*, 5(4), p.363.
7. Ashpole, N.M., Sanders, J.E., **Hodges, E.L.**, Yan, H. and Sonntag, W.E., 2015. Growth hormone, insulin-like growth factor-1 and the aging brain. *Experimental gerontology*, 68, p.76-81.
8. Yan, H., Mitschelen, M., Toth, P., Ashpole, N.M., Farley, J.A., **Hodges, E.L.**, Warrington, J.P., Han, S., Fung, K.M., Csiszar, A. and Ungvari, Z., 2014. Endothelin-1-induced focal cerebral ischemia in the growth hormone/IGF-1 deficient Lewis Dwarf rat. *Journals of Gerontology Series A: Biomedical Sciences and Medical Sciences*, 69(11), p.1353-1362.

MANUSCRIPTS IN PREPARATION

1. Hodges, E.L. and Ashpole, N.M., 2019. Age-specific bidirectional effects of the synthetic cannabinoid CP55940. (Submitted August 2019).
2. Hodges, E.L. and Ashpole, N.M., Cannabinoids as chronobiotics for age-related circadian rhythm disorder. (In preparation).

PRESENTATIONS

- 2019 Society for Neuroscience Annual Meeting
Poster: Aging Circadian Rhythms and Cannabinoids.
Hodges E.L., Ashpole N.M.
- 2019 Youth Movement Against Alzheimer's - Univ. Mississippi Chapter
Invited Talk: The Aging Brain and Neurodegenerative Diseases.
- 2019 University of Mississippi Research Day
Poster: Aging Circadian Rhythms and Cannabinoids.
Hodges E.L., Ashpole N.M.
- 2019 University of Mississippi Neuroscience Research Showcase
Poster: Aging Circadian Rhythms and Cannabinoids.
Hodges E.L., Ashpole N.M.
- 2015 Society for Neuroscience Annual Meeting
Poster: Early Life IGF-1 Deficiency Results in Age-Related
Cognitive Impairment. **Hodges E.L.**, Ashpole N.M., Sonntag W.E.
- 2015 American Aging Association Annual Meeting
Poster: The Influence of IGF-1 Deficiency on Lifespan and Bone
Health is Sex-Specific and Age-of-Onset Dependent. Ashpole N.M.,
Herron J.C., Mitschelen M.C., Farley J.A., **Hodges E.L.**, Logan S., Yan H.
Ungvari Z., Csiszar A., Ikeno Y., Humphrey M.B., Sonntag W.E.
- 2015 Northwestern Oklahoma State University - Dept. of Life Sciences
Invited Talk: Growth Hormone and IGF-1 in the Aging Brain.
- 2015 Oklahoma Center for Neuroscience - Neuro Night
Invited Talk: Age-related Cognitive Decline
- 2014 American Aging Association Annual Meeting
Poster: Lifespan and Pathological Effects of Circulating IGF-1 Are
Dependent on Both Sex and Age-of-Onset: An Interim Report.
Sonntag W.E., Mitschelen M.C., Farley J., Ashpole N.M., Yan H., Siefers
N., **Hodges E.L.**, Landoll J., Richardson A., van Remmen H., Ikeno Y.
- 2011 Oklahoma Undergraduate Research Exhibition
Poster: Sex and Salt Stress - The Effects of Ovarian Hormones on
Behavioral Responses to Physiological Stressors. **Hodges E.L.**, Jones
A., Fan L., Curtis K.S.

HONORS AND AWARDS

- 2019 Edith Pritchard Graduate Student in Pharmacology Award
University of Mississippi, Department of BioMolecular Sciences.

- 2019 Poster Presentation Award
University of Mississippi Research Day
- 2019 Poster Presentation Award
University of Mississippi Neuroscience Research Showcase
- 2018 Virginia Dolores Cantú Fellowship for Ethical Animal Research
University of Mississippi Office of Research
- 2011 Oklahoma BioMedical Research Experience Fellowship
Oklahoma Medical Research Foundation
- 2010 Joe Melton Scholarship
Northwestern Oklahoma State University, Department of Chemistry
- 2008-2011 Regional University Baccalaureate Scholarship
Oklahoma State Regents for Higher Education

TEACHING EXPERIENCE

- 2018-present Teaching Assistant
University of Mississippi - Department of BioMolecular Sciences
Courses: Toxicology, Pathophysiology, Neuropharmacology
- 2015 Laboratory Teaching Assistant, Rose State College

LEADERSHIP POSITIONS

- 2018-2019 Founding President, UM-SOP BioMolecular Sciences Student Advocates
- 2018-2019 Senator, University of Mississippi Graduate Student Council
- 2015 Founding President, American Aging Association - Graduate Chapter
- 2009-2012 President, NWOSU Chemistry Club

PROFESSIONAL AFFILIATIONS

- 2013-present Student Member, Society for Neuroscience
- 2013-2016 Student Member, American Aging Association
- 2009-2012 Student Member, American Chemical Society

INTRAMURAL AND EXTRAMURAL SERVICE

- | | |
|-----------|--|
| 2019 | Volunteer, No-cost health screening event for Spanish speaking residents in Lafayette County, MS. |
| 2019 | Coordinator, BioMolecular Sciences Distinguished Guest Lectureship
Speaker: Allyn Howlett, Ph.D. |
| 2018-2019 | Coordinator, Bimonthly Graduate Student Professional Skills Workshops for graduate students in the University of Mississippi School of Pharmacy. |
| 2018-2019 | Coordinator, Bimonthly Journal Club/Discussion Panels for graduate students in the University of Mississippi School of Pharmacy. |
| 2018 | Volunteer, Oxford community cleanup project. |